Dissertation

Ca^{2+} homeostasis in human vascular endothelial cells

submitted by:

M.Sc. Shamim NAGHDI

for the Academic Degree of

Doctor of Philosophy

(Ph.D.)

at the

Medical University of Graz

Institute for Molecular Biology and Biochemistry

under Supervision of:

Prof. Wolfgang F. Graier

2010

Publication

1. Naghdi, S., Waldeck-Weiermair, M., Fertschai, I., Poteser, M., Graier, W.F., Malli, R. 2010. Mitochondrial Ca^{2+} uptake and not mitochondrial motility is required for STIM1-Orai1-dependent store-operated. J. Cell Sci. In press.

2. Bondarenko, A., Waldeck-Weiermair, M., Naghdi, S., Poteser M., Malli, R., Graier, W.F. G-protein coupled receptor 55-dependent and -independent ion signaling in response to lysophosphatidylinositol in endothelial cells. British J. Phrmacology. In press.

3. Waldeck-Weiermair, M., Malli, R., Naghdi, S., Trenker, M., Kahn, M.J., Graier, W.F. 2010.The contribution of UCP2 and UCP3 to mitochondrial Ca^{2+} uptake is differentially determined by the source of supplied Ca^{2+}.Cell Calcium 47,433-440.

4. Malli, R., Naghdi, S., Romanin, C., Graier W.F. 2008. Cytosolic Ca^{2+} prevents the subplasmalemmal clustering of STIM1: an intrinsic mechanism to avoid Ca^{2+} overload. J. Cell. Sci. 121, 3133-3139.

Acknowledgments

I would like to appreciate my supervisor Prof. Wolfgang F. Graier for all his support for my studies in his laboratory, for his availability, enthusiast, nice discussions and advices for research in last years.I thank him for all his advices, comments and discussions that helped me in promoting my career.

I would like to thank Dr. Roland Malli for his great companionship in my research, his unique ideas and discussions regarding my project that helped me to learn alot. I thank him for his enthusiast for science, his patience and his availability.

I would like to thank my colleagues in the lab, Markus, Anna, Muhammad, Ismene, Sasha, Rizi, Stephan and Ian.

I would like to thank mom and dad for their unbelievable support and love, for all their efforts in keeping me happy and motivated to continue my career.

I would like to thank my lovely sister, Asal, for her great heart, for the time we shared, for her friendship that made my life much easier and made me stronger in dealing with problems.

Table of contents

Abbreviation

ACLSM	array confocal laser scanning microscopy
ADP	adenosine-5-diphosphate
Amp	ampicllin
ATP	adenosine-5-triphosphate
BHQ	2,5-di-tert-butylhydroquinone
BSA	bovine serum albumin
$[Ca^{2+}]$	Ca^{2+} concentration
$[Ca^{2+}]_{cyto}$	cytosolic Ca^{2+} concentration
$[Ca^{2+}]_{mito}$	mitochondrial Ca^{2+} concentration
$[Ca^{2+}]_{ER}$	endoplasmic reticulum Ca^{2+} concentration
CCE	capacitative Ca^{2+} entry
cDNA	complementary DNA
CFP	cyan fluorescent protein
CGP 35157	7-chloro-5-(2-chlorophenyl)-1, 5-dihydro-4, 1- benzothiazepin-2(3H)-one
CICR	calcium- induced calcium release
$\Delta\psi_m$	mitochondrial membrane potential
DAG	diacylglycerol
ddH_2O	double distilled water
DMEM	Dulbecco's modified eagles medium
DMSO	dimethylsulfoxide
DNA	desoxyribonucleic acid
DNase	desoxyribonuclease
dNTP	didesoxyribonucleotide: dATP, dGTP, dCTP, dTTP
EC	endothelial cell
EDTA	Ethylenedinitrilo-tetraacetic acid
EGTA	ethylene glycol tetraacetic acid
ER	endoplasmic reticulum

EtOH	ethanol
FCCP	carbonylcyanide-4 (trifluoromethoxy) phenylhydrazone
FCS	fetal calf serum
FP	fluorescent protein
FRET	Forster resonance energy transfer
g	gram
GFP	green fluorescent protein
h	hour
HCl	hydrochloric acid
HEPES	N-2-hydroxyethylpiperazine-N'-2-ethasulfonic acid
IMM	inner mitochondrial membrane
l	liter
I_{CRAC}	Ca^{2+} release activated Ca^{2+} current
IP_3	inositol-1,4, 5, triphosphate
IP_3 receptor	inositol-1,4, 5, triphosphate recptor
Kan	kanamycin
kDa	kilo Dalton
µ	micro (10^{-6})
m	mili (10^{-3})
MCU	mitochondrial Ca^{2+} uniporter
min	minute
min.	minimum
mRNA	messenger RNA
mtDsRed	mitochondria- targeted DsRed
MW	molecular weight
NaOH	natrium hydroxide
NCX_{pm}	plasma membrane Na^+/Ca^{2+} exchanger
NCX_{mito}	mitochondrial Na^+/Ca^{2+} exchanger
NCLX	Na^+/Ca^{2+} /Li^+ exchanger
N-TRPC	N-dominant negative mutant of TRPC
OD	optical density

OMM	outer mitochondria membrane
PCR	polymerase chain reaction
PIP_2	phosphatydilinositol -4,5-bisphosphate
PKC	protein kinase C
PLC	phospholipase C
PM	plasma membrane
PMCA	plasma membrane Ca^{2+} ATPase
RaM	rapid uptake mode
ROS	reactive oxygen species
RNA	ribonucleic acid
RNAi	RNA interference
RNase	ribonuclease
rpm	rotation per minute
RPmt	mitochondria- targeted ratiometric pericam
sec	seconds
SERCA	sarco/endoplasmic reticulum Ca^{2+} ATPase
siRNA	small interfering RNA
SOC	store-operated channel
STIM1	stromal interacting molecule 1
TEMED	N, N, N', N'-tetramethyl-ethylendiamine
Tris	Tris-hydroxymethyl- aminomethane
UCP	uncoupling protein
VDAC	voltage dependent anion channel
VOC	voltage-operated channel
Vol	volume
YFP	yellow fluorescent protein

Abstract

Ca^{2+} entry upon store depletion or SOCE (Store-operated Ca^{2+} entry) has a role in diverse range of cell function such as exocytosis, enzymatic activity, muscle contraction, gene transcription, cell cycle and apoptosis. On the other hand, mitochondrial Ca^{2+} handling has been proposed as an essential phenomenon in shaping temporal and spatial pattern of cytosolic Ca^{2+} in eukaryotic cells. Applications of pharmacological tools, which disrupt mitochondrial Ca^{2+} signaling, have an inhibitory effect in the extent of SOCE. Molecular components of SOCE have been identified very recently. Upon ER Ca^{2+} depletion, the ER located Stromal interacting molecule 1 (STIM1) clusters and subplasmalemmal clusters interact with the plasma membrane Ca^{2+} channel Orai1 that , in turn, gets activated, resulting in Ca^{2+} entry. Nevertheless, mitochondrial Ca^{2+} sequestering effect on this specific pathway has not been investigated so far. The aim of this research was to study the effect of mitochondrial function (uptake/buffering) and motility on STIM1/Orai1- mediated SOCE. To achieve this aim, global and organelle Ca^{2+} signaling were recorded on high-resolution fluorescence microscopes using either fura-2/am or genetically encoded Ca^{2+} sensors that were targeted in the respective organelle (e.g. ratiometric pericam-mt, $D1_{ER}$). Array confocal laser scanning microscopy was used for high-resolution imaging and 3D- reconstruction was achieved after deconvolution (Huygens) using Imaris software. SOCE in cells expressing STIM1 and Orai1, exhibited less sensitivity to FCCP/oligomycine in comparison with control cells. In agreement, using different concentration of extracellular Ca^{2+} (0.5, 2, 10 and 20 mM) in nontransfected cells, revealed a reduced sensitivity of SOCE to mitochondrial poisoning at high concentration of extracellular Ca^{2+} concentration. It was found that application of the inhibitor of NCX_{mito}, CGP 37157, blocked the FCCP-insensitive signal. Accordingly, upon large SOCE (STIM1/Orai1 overexpressing or high extra cellular Ca^{2+} concentration) and under depolarizing condition (FCCP/oligomycin), mitochondrial Ca^{2+} accumulation was found to be sensitive to the NCX_{mito} inhibitor, CGP 37157. In contrast, mitochondrial Ca^{2+} uptake was insensitive to inhibition of NCX_{mito} under control condition (i.e. in the absence of FCCP/oligomycin). Immobilization of mitochondria using mAKAP-RFP-CAAX expression decreased mitochondrial Ca^{2+} uptake. However, it did not have any effect on SOCE-mediated Ca^{2+} entry. Depolarization of immobilized mitochondria in

cells expressing mAKAP-RFP-CAAX, using FCCP/oligomycin had an inhibitory effect on SOCE mediated Ca^{2+} entry. This result indicate that mitochondrial Ca^{2+} is necessary for SOCE process in cells expressing STIM1 and Orai1, however, proximity, motility as well as the amount of local Ca^{2+} buffering of this organelle does not seem to play a role.

Abstract (In German)

Der Speicher operierende Ca^{2+} Einstrom (SOCE = Store-operated Ca^{2+} entry) spielt eine wichtige Rolle in einer Reihe von zellulären Funktionen wie Exocytose, enzymatische Aktivitäten, Muskelkontraktion, Gentranskription, Zellzyklus und Apoptose. Auf der anderen Seite wird das Mitochondrium für die Gestaltung der räumlichen und zeitlichen Muster des cytosolischen Ca^{2+} in einer eukaryotischen Zelle als essentiell angesehen. Pharmaka, die gezielt das mitochondriale Ca^{2+} Signal unterbrechen, haben einen inhibitorischen Effekt auf das Ausmaß des SOCE.

Nach Entleerung des ER Ca^{2+} kommt es zu einer Bildung von subplasmalemalen STIM1 Cluster, welche mit dem plasmamembran-gebundenen Ca^{2+} Kanal Orai1 interagieren. Dieser wird so aktiviert und führt zu einem Ca^{2+} Einstrom. Dennoch ist bisher der Einfluss der mitochondrialen Pufferung / Funktion auf diesem spezifischen Signalweg nicht untersucht. Das Ziel dieser Arbeit war es, die Wirkung der mitochondrialen Funktion (ausgenommen Pufferung) und der mitochondrialen Motilität auf den STIM1/Orai1 vermittelten SOCE zu untersuchen.

Um dieses Ziel zu erreichen wurden die globalen und die organellspezifischen Ca^{2+} Signale, mit Hilfe eines hochauflösenden Fluoreszenzmikroskops aufgezeichnet. Hierfür wurde einerseits fura-2/am verwendet, oder es wurden rekombinante Ca^{2+} Sensoren eingesetzt, die gezielt in den entsprechenden Organellen exprimieren (wie z.B. ratiometric pericam-mt, $D1_{ER}$). Die konfokale Laser-Scanning-Mikroskopie wurde für hochauflösende Bildgebung verwendet und nach einer Dekonvolution mit hilfe der Imaris Software konnte eine 3D-Rekonstruktion erzielt werden. In Zellen, die STIM1 und Orai1 überexprimieren, zeigte SOCE eine geringere Empfindlichkeit zu FCCP/Oligomycin im Vergleich zu Kontrollzellen. Bekräftigt wurde dies dadurch, dass bei untransfektierten Zellen, die hohen extrazellulären Ca^{2+} Konzentrationen ausgesetzt wurden, zu einer verminderten Empfindlichkeit des SOCE gegenüber mitochondrialen Toxinen führte.

Die Anwendung des Hemmstoffs von NCX_{mito}, CGP 35157 blockierte das FCCP - unempfindliche Signal. Dementsprechend zeigte sich, dass durch eine erhöhte SOCE (STIM1/Orai1 Überexpression oder hohe extrazelluläre Ca^{2+} Konzentration) und unter depolarisierenden Bedingungen, die mitochondriale Ca^{2+} Akkumulation gegenüber den NCX_{mito} Inhibitor, CGP 35157 empfindlich war. Im Gegensatz dazu war die

mitochondriale Ca^{2+} Aufnahme gegen die Hemmung durch NCX_{mito} unter Kontrollbedingungen unempfindlich (in Abwesenheit von FCCP/oligomycine) Nach Immobilisierung der Mitochondrien durch mAKAP-RFP-CAAX Expression wurde die mitochondriale Ca^{2+} Aufnahme herabgesetzt. Allerdings hatte diese Immobilisierung keinen Einfluss auf den SOCE vermittelten Ca^{2+} Einstrom. Dieses Ergebnis zeigt, dass das mitochondriale Ca^{2+} für den SOCE Prozess in Zellen, die STIM1 und Orai1 exprimieren, erforderlich ist. Jedoch scheinen hierbei die Nähe, die Motilität und die Menge der lokalen Ca^{2+} Pufferung von Mitochondrien keine Rolle zu spielen.

1. Introduction

1.1. Endothelial cells and Ca^{2+} homeostasis in this cell type

The inner layer of vessels walls is covered by the cells that are called endothelial cells. They were initially proposed as a passive physical barrier between blood flow and tissues. Later this barrier has been noticed as a dynamic organ, which has specific regulatory role in blood pressure by releasing of factors, which are important in tuning of this pressure. They are also known to control gas and metabolites exchange between cells tissues and blood cells. They are also Involved in angiogenesis, and healing the wounds (Cines *et al.,* 1998).

In this cell type, Ca^{2+} is one of the most essential ions, which has a regulatory effect on several versatile cellular processes. Fast responses involving contraction, exocytosis of factors like NO and PGI2), cell motility and long-term response involving gene transcription, proliferation, division, energy metabolism and programmed cell death are the most prominent processes that Ca^{2+} plays a role (Nilius and Droogmans, 2001).

While Ca^{2+} is necessary, overloading of this ion is threatening for the cell vitality. High concentration of Ca^{2+} induces caspase activity and it may leads to Ca^{2+} elevation in mitochondria, which is followed by transition pore opening and apoptotic factor release. Therefore, cell controls Ca^{2+} concentration precisely (cytosolic Ca^{2+} concentration is 100 nM versus extracellular which is about mM), by extruding this ion to extracellular space, subcellular compartments or using the proteins which bind to Ca^{2+} and buffer it (Clapham, 2007).

1.1.1. Ca^{2+} extrusion from eukaryotic cell

The first strategy of cells to modulate Ca^{2+} ion concentration is simply extruding the ions to the extracellular space. There are at least two Ca^{2+} extrusion pathways from eukaryotic cells, plasma membrane Ca^{2+} ATPase (PMCA) and Na^{+}/Ca^{2+} exchanger (NCX) (Prasad *et al*., 2004; Monteith and Roufogalis, 1995; Carafoli, 1994).

1.1.1.1. Plasma membrane Ca^{2+} ATPase (PMCA)

Plasma membrane Ca^{2+} ATPase or PMCA pump has ten transembrane spanning parts and four cytosolic domains. This pump is electrogenic and exchanges one Ca^{2+} ion with one H^+ with the expense of one ATP molecule (Hao *et al*., 1994; Di Leva *et al*. 2008).
Four genes are transcribed for different isoforms of this pump and splice in different ways depending on the cell type and its Ca^{2+} handling pattern. Some of the isoforms have higher kinetics in Ca^{2+} extrusion comparing with others, therefore while it expresses in most of eukaryotic cells the isoforms in excitable cells which deals with higher amount of Ca^{2+} are faster than non-excitable ones (e.g. PMCA2a versus PMCA4b) (Caride, 2001; Berridge et *al.,* 2003).
PMCA can bind very strongly to Ca^{2+} (high affinity (nM)), meaning that in resting condition this pump is able to help cells in dealing with small changes in cellular Ca^{2+} concentration (Carafoli ,1994). Calmodulin (Sedova *et al*., 1999), phospholipids, and two protein kinases including phospho kinase A, Src kinases (Wan *et al.*, 2003; Dean *et al*., 1997) have modulating effect on the conformation of PMCA. These elements change the pump shape into an active form. Upon activation of the channel, the K_d of PMCA for Ca^{2+} reduces dramatically (to nM) (Di Leva *et al*. 2008).
In addition PMCA is able to have regulatory role on other pathways (Shuh *et al.*, 2001; Oceandy *et al.,* 2007; Shuh *et al*., 2003). Very recently, it has been found that this pump has a negative regulatory effect on nitric oxide synthase (eNOS) in endothelium via its association with this enzyme (Holton *et al*. 2010).

1.1.1.2. Plasma membrane Na^+/Ca^{2+} exchanger

Na^+/Ca^{2+} exchanger (NCX) is an ion carrier in plasma membrane that extrudes 1 Ca^{2+} and imports 3 Na^+ in forward mode and conversely in reverse mode. Therefore, this exchanger is important in cellular Na^+ and Ca^{2+} homeostasis. Up to now, three NCX (1, 2, and 3) from three different genes have been recognized. Role of this exchanger is more dominant in excitable cells like heart and β-cells (Brini *et al*., 2002).

The relative contribution of these two extrusion pathways in different tissues varies. In excitable cells, NCX is the main pathway for Ca^{2+} extrusion, while in non-excitable cells, PMCA plays the role (Blatter *et al.,* 1999).

In nonexcitable cells, PMCA with higher affinity and lower capacity (lower rate of extrusion), extrudes Ca^{2+} under resting condition. However, under stimulatory condition and sudden elevation of Ca^{2+} concentration, NCX with low affinity and high capacity, extrudes Ca^{2+} outside the cell (Blatter *et al*., 1999; Clapham, 2007).

In agreement with this information, in endothelial cells it has been proved that upon stimulation the cells with an agonist, bradykinin, NCX_{pm} plays the main role in Ca^{2+} extrusion (Paltauf-Doburzynska *et al*., 1998). However, under high loading of Na^{+} in these cells NCX_{pm} functions in reverse mode (Paltauf-Doburzynska *et al*., 2000).

1.1.2. Compartmentalization

The second mechanism applied by cells to control cytosolic Ca^{2+} concentration is to transfer Ca^{2+} ions to the intracellular organelles e.g. endoplasmic reticulum and mitochondria.

Endoplasmic reticulum has been known as the biggest intracellular organelle that stores Ca^{2+} ions. Free Ca^{2+} ion concentration of ER is between 100 to 500 μM (Berridge, 2002). Ca^{2+} ions enter to the lumen of ER via Sarco/Endoplasmic Reticulum Ca^{2+}-ATPase (SERCA) pump.

1.1.2.1. Sarco/Endoplasmic Reticulum Ca^{2+}-ATPase (SERCA) pump

SERCA is an ATPase - Ca^{2+} pump. Three genes code for this pump and depend on the tissues, they spliced differently. SERCA transfers one Ca^{2+} in exchange of two H^{+} from cytosol to endoplasmic reticulum using one molecule ATP. Similar to PMCA, SERCA has a slow rate of transfer with high affinity thus under basal condition, this pump is active and acts against constant leak from endoplasmic reticulum (Brini and Carafoli, 2009). Inhibition of SERCA unmasks a passive leak of Ca^{2+} from endoplasmic reticulum (Malli *et al.* 2003a). Thapsigargin, Cyclopiazonic acid and 2, 5-di-t-butylhydroquinone (BHQ) are specific inhibitors for SERCA.

In endothelial (EA.hy926) cells, the dominant isoform of SERCA is SERCA2b, however upon chronicle treatment with histamine, SERCA 3 protein level increases (Hadri *et al*., 2006).

1.1.2.2. Mitochondrial Ca^{2+} uptake by uniporter

Mitochondrion had been recognized for its role as a power plant for the cell but later researcher recognized it as an extremely important organelle in cellular Ca^{2+} homeostasis and in shaping the spatial and temporal pattern of Ca^{2+} signal in eukaryotic cells. For more details about the uptake of Ca^{2+} by mitochondria, see: Mitochondrial Ca^{2+} uniporter.

1.1.3. Ca^{2+} buffering proteins

The third tactics of most of the cells to control cytosolic Ca^{2+} concentration is using proteins with a high range of affinity for Ca^{2+} (from nM to mM). These proteins bind to Ca^{2+}, chelate it and consequently reduce free Ca^{2+} concentration. These buffering proteins may bind to other signal pathways proteins and activate or deactivate pathways (Berridge *et al.*, 2003). Depend on the cell demand for Ca^{2+}, the expression pattern of these proteins is very specific. Consequently, buffering capacity of the cells is different which result in the unique spatial and temporal pattern of Ca^{2+} in each cell type (Berridge *et al*., 2003; Parekh, 2008). The most common characteristics of these proteins is an EF hand, a conserved helix – loop - helix motif which binds to Ca^{2+} using negative charge of oxygen and carboxyl of amino acids in the loop of the motif. Usually EF hand is pair and depends on the amino acids in side chain and structure of the protein, the affinity of EF hands are different (Nakayama and Kretsinger, 1994). Calreticulin, Calbindin and S100 protein family are some examples of Ca^{2+} chelators, which have EF hand and are involved in Ca^{2+} buffering.

There is another Ca^{2+}-binding domain called C2 domain. This domain originally was found in an isoforms of protein kinase C. But later it has identified in many proteins which are mainly bounded to membrane and are involved in a various signaling

pathways like membrane trafficking. It seems that many of the C2 domain regulated by Ca^{2+} (Nalefski and Falke 1996; Clapham 2007).

1.2. Ca^{2+} microdomains

There is some evidence showing that Ca^{2+} concentration in the cell is not homogenous. In cellular microenvironments the concentration of Ca^{2+} might be different from global Ca^{2+} measured by imaging techniques (Rizzuto *et al.*, 2000). These so-called microdomains have different amplitude and extension comparing with global concentration of Ca^{2+} (Parekh, 2008; Berridge, 2006; Malli *et al.*, 2003a). These microdomains are transient in the time and space (Alonso *et al.*, 2006). The space that the microdomains occupy could range from a single hot spot to a significant portion of cytosol (Parekh, 2008). Concentration of Ca^{2+} in microdomain has a reverse relation with distance from the mouth of the channel. In all kinds of the channels the concentration of Ca^{2+} close to the channels is much higher than global Ca^{2+} in cytosol and it decreases as the distance increase from the mouth of channels (Parekh, 2008). The amplitude of Ca^{2+} ion concentration in the microdomains depends on the channels' conductivity, electrochemical gradient of Ca^{2+}, membrane potential (Rizzuto and Pozzan, 2006) and buffer capacity (Neher, 1998; Parekh, 2008; Rizzuto and Pozzan, 2006) of the cell.

The presence of any effectors in the exact range of microdomains leads to specific regulation of some signaling pathways (Berridge *et al.,* 2003).

Also, colocalization or physical interaction of entrance channel with targets shows that the target is regulated by local effect (Parekh, 2008).

In addition, if Ca^{2+} concentration required for a reaction is much higher than maximum increase in cytosolic Ca^{2+}, it should be regulate by a local high concentration of Ca^{2+}.

Interestingly, Malli *et al*. showed that in endothelial cells, subplasmalemmal mitochondria and ER are able to provide different local microdomains (with different gradients) for Ca^{2+} ions which result in activation or deactivation of Ca^{2+} related channels (Malli *et al*., 2003a).

Effect of microdomains can be especially on the final target, which exposed to high Ca^{2+} concentration in microdomain, or can be through some modulators that located in

microdomain space. These modulators may diffuse to other part of the cell and join in other cellular pathways, which are not necessarily in close vicinity to channel. Gene expression (Dolmetsch *et al*., 2001), Exocytosis (Rizzuto and Pozzan, 2006), Adenylyl cyclase (Willoughby *et al*., 2010), PMCA (Bautista and Lewis, 2004), NO synthase (Lin *et al.,* 2000), TRPC7 (Lemonnier *et al.*, 2006) are some of the examples which known so far to be regulated by local effect of Ca^{2+}.

1.3. Ca^{2+} signaling

Ca^{2+} signaling is a process involving regulated changes in spatial and temporal pattern of Ca^{2+} ion in the cytosol and other organelle in the cell (Putney *et al.*, 2001).
Cellular Ca^{2+} can be provided from two different sources, intracellular organelles mainly endoplasmic reticulum and extracellualr space. In non-excitable cells, Ca^{2+} signaling is a biphasic process. It starts when a transmitter, hormone, growth factor or an agonist reacts with its receptor in the plasma membrane and phospholipase C is activated. Phospholipase C hydrolizes phosphoinositol 4, 5- phosphate (PIP_2) to inositol 1, 4, 5- triphosphate (IP_3) and diacyleglycerol (DAG). Interaction between IP_3 and its receptor in the membrane of Endoplasmic reticulum or Golgi leads to release of Ca^{2+} into the cytosol (see the following parts). In the second phase of Ca^{2+} signaling, depletion of the stores, activate SOCE in the plasma membrane, which result in Ca^{2+} entrance into the cell (Malli *et al*., 2005; Putney, 1986; Putney, 2009; Laude and Simpson, 2009).
It needs to be mentioned that, diacylglycerol (produced from phospholipase C activity) is capable to activate channels like some types of TRP family (see the following part), which in turn are responsible in Ca^{2+} entrance into the cytosol (Nilius *et al.,* 2007).

1.3.1. Ca^{2+} release

Endoplasmic reticulum, Golgi apparatus, nuclear envelope and secretary vesicules considered as Ca^{2+} store organelle. Second messengers like IP_3, cyclic ADP ribose (cADPR) and sphingosin-1-phosphate (S1P) mediate Ca^{2+} release from these organelles (Young *et al.,* 2000). The most well known target for these ligands is IP_3 and Ryanodine receptors (Laude and Simpson, 2008). These receptors are intracellular

ligand - gated channels encoded from three genes (which are almost conserved with 70 % identities in animals). Each channel composed of four homo or hetero subunits. Each subunit composed of six transmembrane domains near C -terminal, which stabilizes the channel in ER membrane and an IP_3 - binding domain in N - terminal part. IP_3, Ca^{2+}, ATP, phosphorylation of the subunits and proteins that may bind to the channel, are the main modulators of IP_3 receptor (Rizzuto and Pozzan, 2006). IP_3 regulates the receptor in a positively cooperative manner, thus binding more subunits to IP_3 (all four) increases the activity of the channels. Ca^{2+} is also a regulator of this channel but the interplay between Ca^{2+} and IP_3 as regulators is not cleared yet. It assumed that IP_3 binding will change the conformation of the receptor and facilitates Ca^{2+} binding to stimulatory site rather than inhibitory site of the receptor. Binding of Ca^{2+} to stimulatory site of the receptor leads to more release of Ca^{2+} from the channels (this phenomenon called Ca^{2+} induced Ca^{2+} release (CICR)). It means that IP_3 receptor is capable to be regulated by the function of other near IP_3 receptors and is able to affect other IP_3 receptors (Taylor *et al.* 2004; Foskett *et al*., 2007; Rizzuto and Pozzan, 2006).

In different cell type and depend on the metabolic signaling pathways in the cells, various Ca^{2+} signaling patterns take place. Different subtypes of IP_3 receptor, spatial localization of IP_3 receptors, expression level of buffering proteins and the amount of Ca^{2+} uptake into ER or other organelles (e.g. mitochondria) are the causes which shape Ca^{2+} signals in different cell types (Laude and Simpson, 2009).

Also, there are some proteins which are reported to bind to IP_3 recptor (e.g. Bcl_2 (Rong *et al*., 2007), cytochrome C (Boehning *et al*., 2003)) and have a modulatory role on the function of this receptor (Rong *et al.*, 2009; Rizzuto and Pozzan, 2006).

1.3.2. Ca^{2+} entry

There are a large number of different channels involve in Ca^{2+} influx into the cell (Parekh and Putney 2005; Berridge *et al.,* 2003):

1.3.2.1. Voltage operated channel (VOCs)

These channels are commonly expressed in excitable cells (neurons and muscles) and get activated upon depolarization of the plasma membrane. These channels include L-

type (Benitah *et al*., 2009), P/Q-type (Zhang *et al*., 2008), N-type (Jarvis and Zamponi, 2001) R-type and T-type (Perez-Reyes, 2003).

1.3.2.2. Receptor operated channels (ROCs)

These channels activate upon binding a ligand from extracellular space to the channel. NMDA (*N*-methyl *D*-aspartate) receptor that is ionotropic L-glutamate neurotransmitter receptor is an example of these channels. These channels are, mostly in excitable cells like neurons (Stephenson *et al*., 2008).

1.3.2.3. Second-messenger-operated channels (SMOCs)

These channels modulate by a cytosolic second messenger. They include arachidonat-regulated Ca^{2+} channel (Shuttleworth, 2009), cyclic nucleotide - gated channel (CNGs) (Biel and Michalakis, 2009) and inositol phosphate channels, which can be activated by arachidonic acid, cGMP and inositol phosphates, respectively.

1.3.2.4. Store operated Ca^{2+} entry (SOCE)

One of the most prevalent entry pathways is store-operated channel (SOC), which has been explained in details in following part. Putney (Putney, 1986) proposed the concept of capacitative Ca^{2+} entry for the first time in 1986. This concept expresses that intracellular filling state, control Ca^{2+} entry channels in plasma membrane similar to an electrical circuit of capacitator and resistant in series mode. Charging and discharging of capacitator (endoplasmic reticulum) control the current that is passing through resistant (channels). The preliminary evidence came from the experiments showing there is a relation between the level of refilling of the intracellular organelle and the amount of Ca^{2+}, which enters the cell, separate from agonist activating of the receptors (Putney, 1986; Putney, 2009). Further, this idea, renamed store-operated Ca^{2+} entry (SOCE) which looks more accurate on the base of depletion of the store in the cell. SOCE was verified using thapsigargin that depletes the store without any effect on PLC activity, however, under physiological condition any stimulator that increases IP_3 in the cell can deplete intracellular Ca^{2+} store and activate SOCE. The typical current detected in Ca^{2+} entrance upon store depletion is I_{CRAC} (for Ca^{2+} release–activated Ca^{2+} current) in mast

cells. This current is non-voltage activated Ca^{2+} specific, and inwardly rectifying (Hoth and Penner 1992). Nevertheless, there are some evidence showing that, it is slightly dependent on membrane potential (Hogan *et al.*, 2007).

Trivalent cations like Gd^{3+} and La^{3+} in low concentration are specific blockers of SOCE current, which are so far known (Weiss, 1974; Kwan *et al.,* 1990*;* Putney, 2001; Parekh and Putney, 2005).

In endothelial cells, Ca^{2+} entry upon stimulation of the cells using an agonist, involves SOCE–dependent and independent pathways. SOCE-independent pathways are mainly assumed to be activated by second messengers (like diacyleglycerol (Hofmann *et al*., 1999)) or Ca^{2+} (Kamouchi *et al*., 1999). These entry pathways can be nonselective channels like TRPs which are highly expressed in endothelial cells or NCX that in severe Na^{+} loading functions in reverse mode (Girardin *et al*., 2010).

1.3.2.4.1. Models for SOCE activation

1.3.2.4.1.1. Diffusible Messenger

Definition of SOCE and the evidence that Ca^{2+} first enters the cytosole and then to endoplasmic reticulum shows there should be a mechanism to convey a signal from a depleted endoplasmic reticulum to plasma membrane. Diffusible messenger model proposes that depletion of the store triggers production of a diffusible messenger which release from endoplasmic reticulum, migrate to plasma membrane and activates store operated Ca^{2+} entry. So far, cyclic GMP (Pandol and Schoeffield-Payne 1990; Xu et al., 1994), arachidonic acid (Gaily 1998; Rzigalinski *et al*. 1999), cytochrome P450 mono-oxygenase derivatives (Cytp450 MO) (Hoebl *et al.* 1997; Graier *et al*. 1995; Watanabe *et al*., 2003), Ca^{2+} influx factor (CIF) (Randriamampita and Tsien 1993; Thomas and Hanley 1995; Bolotina and Csutora, 2005) has been recognized as the messengers that can activate SOCE. Nevertheless, the structure of the CIF is not known so far, and the research about this molecule continues by indirect measurements of CIF biological activity (Csutora *et al*., 2008).

1.3.2.4.1.2 Concept of conformational coupling

This model originated from the research showing there is an interaction between L-type channels and sarcoplasmic reticulum ryanodine receptors in skeletal muscle cells (Sencer *et al.*, 2001). In addition, there are data showing IP_3 receptor can make interaction with some of TRP channels (Yuan *et al.,* 2003). According to this model, IP_3R has a sensory role and upon store depletion, conformation of this receptor alters and binds to SOCE channels (Juan, 2005). However, the slow activation of SOCE in comparison with protein-protein interaction that occurs in less than a millisecond modifies this hypothesis to secretion-like coupling model. This model proposes that upon depletion of store, conformation of the IP_3 receptors alters, the peripheral part of the ER get close to the plasma membrane and then IP_3R attach to SOC channels (Patterson et al., 1999; Parekh and Putney, 2005).

1.3.2.4.1.3 Vesicular fusion

This hypothesis, suggest that SOCE channels are not originally in plasma membrane but in the vesicles and upon depletion of the stores, the vesicles carry the channels to plasma membrane. This evidence has been recorded for some other carriers like glucose transporter GLUT4 in adyposites, which moves to plasma membrane upon stimulation with insulin (Bryant *et al.* 2002). While it is not clear by which mechanism depleting of store can direct vesicles to membrane, the strongest evidence for molecular mechanism is regarding to two protein families STIM (Stromal interacting molecule) and Orai (CRACM1) and their interactions. Data from these proteins has been reproducible by many laboratories and with different cell lines (in both excitable and non-excitable) (Orci *et al.*, 2009).

1.3.2.4.2. Coupling of STIM and Orai Protein

1.3.2.4.2.1. STIM1

Stromal interacting molecule 1 a protein originally was founded in plasma membrane using biotynilation assay, not for its role in Ca^{2+} signaling but for its involvement as a recessive tumor suppressor and mediator for interaction between hematopoetic and stromal cells. Function-based RNAi screening, clarified STIM in Drosophila S2 (Sobollof

et al., 2006; Roos *et al*., 2005) and in Hela cell line (Liou *et al*., 2005) as an important component for SOCE activation. 30 % of STIM in drosophila and mammalian STIM1 are equal and 60 % are similar. STIM1 protein mostly located in the membrane of endoplasmic reticulum (Wu *et al.* 2006). N-terminal part of this protein is in the lumen of endoplasmic reticulum and C-terminal is in cytosol. It made up of a single EF-hand and a SAM (sterile alpha motif) with two glycosyaltion site in N-terminal part. A transmembrane helix anchors this protein in ER membrane. In addition, an ERM (ezrin-radixin-moesin) like domain, a glutamate-, a serin/proline- a serin/threonin and a lysine-rich domain are in cytosolic part of STIM1 (Dziadek and Johnstone 2007; Sobollof *et al*., 2006; Lewis 2007; Cahalan, 2009).

STIM2 is a homologue of STIM1 (with 60 % homology) and localized in endoplasmic reticulum membrane (Williams *et al*., 2001). This protein also has an EF-hand, which is in N terminal and in the luminal side of endoplasmic reticulum. There is some evidence showing that STIM2 interacts with STIM1 and regulates SOCE by blocking of STIM1-mediated Ca^{2+} Entry (Spassova *et al.*, 2006; Soboloff *et al.*, 2006; Zheng *et al*., 2008). Also, it has been suggested STIM2 has a regulatory effect on basal Ca^{2+} concentration (Brandman *et al*., 2007).

1.3.2.4.2.2. Orai1

Intense effort for finding CRAC (Ca^{2+} release - activated Ca^{2+}) channel, applying whole genome RNAi screening leads to Orai protein (CRACM) finding in Drosophila S2 cell line and mammalian cells. Also, point mutation in the Orai gene (R91W8) leads to deficient CRAC channels activity and thus, a severe and lethal immunodeficiency disease named SCID. Orai is in plasma membrane, has four transmembrane domains and both N and C terminal part of the protein located in cytosol. There are three homologues for Orai gene in human (1, 2 and three) (Vig *et al*., 2006; Feske *et al.*, 2006; Zhang et al., 2006; Thompson *et al.*, 2009). Over expression of Orai1 and STIM1 raise the current with the same biophysical and pharmacological characteristics of I_{CRAC} (Zhang *et al*., 2006; Peinelt *et al*., 2006; Soboloff *et al*., 2006; Mercer *et al*., 2006). Moreover, mutation in this protein, changes the Ca^{2+} specificity of CRAC channels, therefore it has been speculated that Orai is the pore forming unit of CRAC channel (Prakriya *et al*., 2006;

Putney, 2009; Cahalan, 2009). This protein is in dimer form in resting condition and turn into tetramer upon activation (Penna *et al*., 2008; Deng *et al*., 2009).

1.3.2.4.3. Molecular mechanism of STIM1/Orai1 function

Blocking of STIM1 EF-hand interaction site with Ca^{2+} by mutation leads to continues SOCE activity, therefore it has been suggested that EF-hand in STIM1 performs as a sensor for Ca^{2+} in the lumen of endoplasmic reticulum (Liou *et al*., 2007; Lewis, 2007). After depletion of the store, Ca^{2+} ions dissociate form EF hands. STIM1 proteins, which are dimer under resting condition, rearrange very quickly as oligomers (through SAM domain) and translocate to the pre-existing junction of endoplasmic reticulum and plasma membrane very quickly. STIM1 oligomers couple with Orai oligomers and trigger store operated Ca^{2+} entry (Liou *et al*., 2007; Smyth *et al*., 2008; Mullins *et al*., 2009; Malli *et al*., 2004). Drug-induced oligomerization of STIM1 proved that oligomerization is a necessary process for translocation of the protein to puncta (Luik *et al*., 2008).

Co-immunopercipitation and deletion analysis show there is a direct interaction between STIM1 and Orai1 protein. The interactions take places between a small segment of C terminal and 100bp in coiled-coil part in STIM1 protein, which activates Orai1 protein (Yeromin *et al*., 2006). Other than protein-protein interaction between STIM and Orai (direct or indirect), there is another hypothesis for store operated Ca^{2+} entry activation. This hypothesis expresses that STIM1 induces producing of calcium influx factor (CIF). This factor diffuses and activates PLA2β, which in turn will transduce the message to CRAC channel and thus, activates Orai dependent SOCE (Bolotina, 2008).

Intense studies in finding other functional or structural partners for STIM1-Orai1 coupling and the role of other probable compartment, propose SERCA2 (Sampieri *et al*., 2009), TRPC channels (Yuan *et al*., 2007; Sours-Brothers *et al.,* 2009; Liao *et al.,* 2007), different Orai family members (Mercer *et al.,* 2006), and iLPA2β (Bolotina, 2008) as important candidate in this regard.

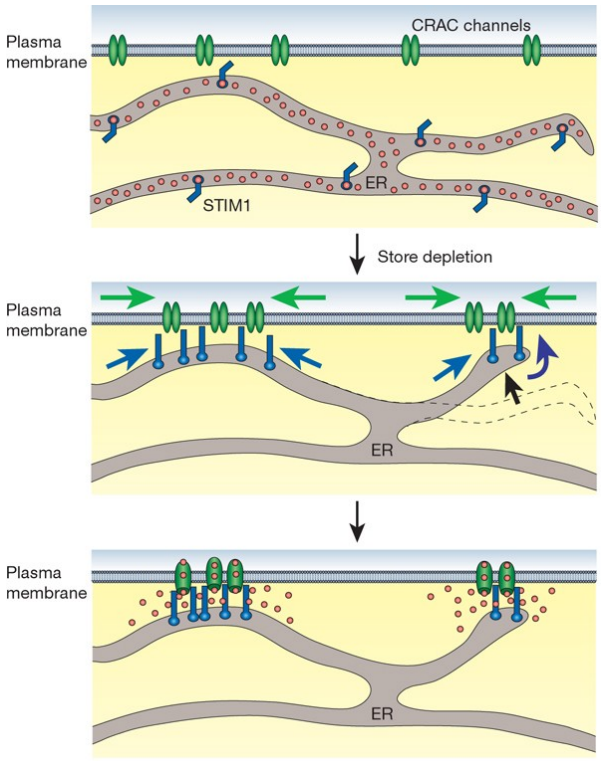

Figure 1.1. Schematic view of STIM1 and Orai1 proteins interaction (Lewis 2007). For details refer to the text.

1.3.2.4.4. TRP family

Transient receptor potential channels (TRPs) are a big super family, which express in almost all species. These channels mostly are in plasma membrane, and composed of 6 transmembrane spaning motifs, a pore forming domain with both C and N terminal in the cytosol. TRP channels mostly form homo or hetertetramers. In mammalian cells, on the base of amino acid homology, they are mainly divided in 6 groups includes: TRPC (canonical), TRPV (vanilloid), TRPM (melastatin) TRPP (polycistin) TRPML (mucolipin) and TRPA (ankyrin). These channels contribute in ion homeostasis and have affinity for both Na^{+} and Ca^{2+} ions. Many of stimulators including mechanical, temperature and osmotic stress can activate these channels (Nilius *et al*., 2007).

Evidence showed that some members of TRPC (TRPC3, TRPC6, TRPC7) family are dependent on phospholipase C (PLC) activity and involved in receptor-dependent Ca^{2+}

influx. Diacylglycerol (DAG) is known to be one of the modulator of some of TRPC channels (Soboloff *et al*., 2007; Hardie *et al.*, 2007).

Very recently, co-immunopercipitation shows that for a functional SOCE, STIM1 interacts with TRPC1 (Alicia *et al*., 2008), C2, C4, C5 channel (Liao *et al*., 2008; Worley *et al.,* 2007), and thereby, heteromultimerizes these channels. In addition, using siRNA, dominant negative suppression and biochemical pull-down assay showed that TRPC interacts with Orai (Liao *et al.*, 2009).

1.3.2.4.5. Regulation of SOCE

It has been shown that some factors can affect SOCE which I briefly made a list of them:

1) Ca^{2+} at the mouth of SOC channels is the main factor in SOC inhibition through negative feedback effect. Applying strong chelators and other ions like Ba^{2+} remove this inhibitory effect of Ca^{2+} on SOC channel function (Zweifach and Lewis, 1995).
2) Refilling of the intracellular store is able to terminate SOCE, but molecular mechanism of this function is not clear so far. Whether there is some modulator in ER membrane to sense refilling and triggers deoligomerization of STIM1 or there are some compounds which release from ER, is still needed to be clear (Parekh and Putney, 2005).
3) Calmodulin is another candidate for regulating SOCE. Very recent date from Lewis laboratory showed that calmodulin binds to Orai1 and deactivate CRAC channels (Mullins, 2009).
4) Cytosolic Ca^{2+} has a declustring affect on STIM1, and thus it terminates SOCE. Rising global Ca^{2+} in the cytosol declusters STIM1 and redistributes it in the endoplasmic reticulum (Malli *et al.*, 2008). In parallel with this idea, CRACR2A protein has been find very recently which looks to inhibit SOCE. Upon increasing of the concentration of cytosolic Ca^{2+} this protein interacts with this ion, get separated from SOCE units and leads to deactivation of this process (Carrasco and Meyer, 2010).
5) In some cell type like smooth muscle cells, tyrosin kinase looks to activate while protein kinase C inhibit CRAC channels (McElroy *et al*., 2009; Smani *et al*., 2008). In

line with this information it has shown that in mitotic cells phosphorilation of STIM1 plays a suppressing role on SOC channels activity (Smyth *et al*., 2009).

6) In some cells (like prostate cancer cell line), proteins which contributes in apoptosis have down-regulating effect on SOCE (Li *et al.,* 2008).
7) There is strong evidence in endothelial cells, that cytochrome p450 modulates formation of 5´, 6´-epoxyeicosatrienoic acid from anandamide and arachidonic acid and this derivative induces Ca^{2+} entry by activating of TRPV channel (Watanabe *et al*., 2003).
8) In addition to the molecules, mitochondria - with high buffer capacity - are also able to have a regulatory role on SOCE (see the following part).

1.2.3.4.6. Function of SOCE in the live system

The first explanation for the necessity of SOCE is refilling of intracellular organelles, and therefore it is speculated that any dysfunction in SOCE can influence the processes in the cell which regulated by Ca^{2+} signaling (Targos *et al*., 2005). Under physiological condition, studies on some immunodeficiency disease showed that SOCE is necessary for the correct function of T-cells (Dadsetan *et al.*, 2008; Oh-hora 2009). In addition, gene transcription (Dolmetsch *et al.*,1998; Ishikawa *et al*., 2003), apoptosis (Lampe *et al.,* 1995), and exocytosis (Fomina and Nowycky, 1999) are other processes which attributed to SOCE phenomenon. In addition, it has been shown that SOCE is responsible for suitable Ca^{2+} oscillation (Bird and Putney, 2005; Putney 2009), and transmitter secretion in excitable cells (Targos *et al*., 2005).

Most of the physiological functions of endothelial cells (like local control of vascular tone) are affected by Ca^{2+} signaling (Graier *et al*., 1994; Girardin *et al*., 2010). SOCE as a main component in shaping the pattern of Ca^{2+} signaling in this cell type, has been known to play a crucial role in appropriate function of endothelial cell (Abdullaev et al., 2008; Freichel *et al*. 2001; Girardin *et al*., 2010).

1.4. Mitochondria

Mitochondria are polymorphic and dynamic essential organelles that act as a source for producing energy (adenosine triphosphate (ATP)) and therefore involve in many metabolic pathways.

In addition, different anti or pro-apoptotic proteins (mostly from Bcl_2 family) bind (directly or indirectly) to inner or outer membrane of mitochondria and change the permeability of mitochondrial membranes. Changing the permeability of the membrane inhibits or promotes release of cytochrome c, which is an apoptotic factor (Er *et al*., 2006; Schwarz *et al*., 2007). This indicates that these organelles interfere in many pathways which are relevant to apoptosis and necrosis (Demaurex and Distelhorst 2003).

Indeed, mitochondria and cellular Ca^{2+} (as an important second messenger in eukaryotic cells) homeostasis have a mutual effect on each other. While, mitochondria involved in Ca^{2+} signaling and shaping of the spatial and temporal pattern of cellular Ca^{2+}, endoplasmic reticulum refilling, and SOCE activity (Graier *et al*, 2007), this ion control oxoglutarat dehydrogenas, isocitrate dehydrogenase, and pyruvate dehydrogenase enzymes activity and thereby has a regulatory effect on Krebs cycle and as a result ATP and ROS production. Ca^{2+} is also able to modulate transporters and exchangers for metabolites (e.g. aspartate-glutamate carriers) in the membrane of mitochondria (Demaurex *et al,* 2009). Also, there are some evidence showing that high increase of Ca^{2+} in the mitochondria induces cytochrome c release and thereby cell death (Ganitkevich, 2003).

1.4.1. Mitochondria Ca^{2+} uptake

Application of mitochondrial targeted protein sensors for Ca^{2+} in intact cells showed that mitochondria are able to uptake $Ca^{2+,}$ upon agonist stimulation in physiological condition (Rizutto *et al*. 1995; Graier *et al*., 2007).

The main driving force for mitochondrial Ca^{2+} uptake is negative membrane potential in inner membrane of this organelle and is around -150 to -180 mV. This negative charge is the result of respiratory chain activity that extrudes H^+ upon electron transfer to the space between outer and inner mitochondrial membranes (Mitchell 1969; Graier *et al*., 2007). In outer mitochondrial membrane, voltage dependent anion selective channel (VDAC) is the main way for Ca^{2+} transfer. This channel looks to be quite permeable to Ca^{2+} and increasing the number of this channel promotes Ca^{2+} entrance (Rapizzi *et al*., 2002).

Inner mitochondrial membrane is not permeable toward ions and is responsible for maintaining mitochondrial membrane potential. There are two pathways for Ca^{2+} transfer through this membrane: an uptake named mitochondrial Ca^{2+} uniporter (MCU), and a rapid uptake mode (RaM).

1.4.1.1. Mitochondrial Ca^{2+} uniporter

Ca^{2+} transfer to mitochondria occurs using a highly selective ruthenium red-sensitive pathway named mitochondrial Ca^{2+} uniporter (MCU). This uniporter exclusively transfers Ca^{2+} with a high rate and with the expense of membrane potential. Study on this uniporter performed using direct measurement of mitochondrial Ca^{2+} in matrix in living cells or patch clamping of mitoplasts (mitochondria without outer membrane).

Molecular constituents of MCU were not identified and very recently, uncoupling proteins 2 and 3 (UCP2 and UCP3) are known to be part of this uniporter (Trenker *et al*., 2007). These two proteins were initially recorded as uncouplers and carriers for H^+ under specific condition (isolated mitochondria), also involvement in other processes like apoptosis, fatty acids and glucose metabolism were speculated for these proteins (Brand and Steves 2005; Graier *et al.*, 2007).

Knockdown of these proteins decreases uptake of Ca^{2+} upon Ca^{2+} release from IP_3 receptor while overexpression of these proteins increases mitochondrial Ca^{2+} uptake upon Ca^{2+} release from intracellular organelle or Ca^{2+} influx. These genetic manipulations did not change H^+ concentration in the matrix of mitochondria and Ca^{2+} extrusion from mitochondria. Also, this study showed existence of MCU (ruthenium red sensitive pathway) is related to the expression of UCP2 and UCP3 (Trenker *et al*., 2007 & 2008).

Ca^{2+} (Kröner 1986), polyamine derivatives (spermine) (Nicchitta 1984), taurine (2-aminoethane sulfonic acid) (Palmi *et al*., 1999) activate MCU while ruthenium red, lanthanids (Reed and Bygrave, 1974), Mg^{2+} (Lenzen, *et al.*, 1986) and nucleotide (Litsky and Pfeiffer, 1997) inhibit this pathway. In addition, P38 MAPK inhibitor named SB202190 enhances MCU activity (Montero *et al.*, 2002). Nevertheless, most of these modulators are not highly specific for MCU and there are some problems with applying most specific ones, which is ruthenium red. This compound is impermeable for many cell

types and has some other side effect (effect on ryanodine receptor), so mostly to study MCU, researchers use compounds which disturb mitochondrial membrane potential (like FCCP and CCCP) and inhibit MCU indirectly (Demaurex *et al.*, 2009).

Comparing major Ca^{2+} extrusion pathways from cytosol, showed that in resting condition when the concentration of Ca^{2+} is about 10^{-7} M, PMCA and SERCA act against Ca^{2+} leaks. MCU starts Ca^{2+} uptake when the concentration is more than 10^{-5} M (figure 1.2) (Alonso *et al.,* 2006).

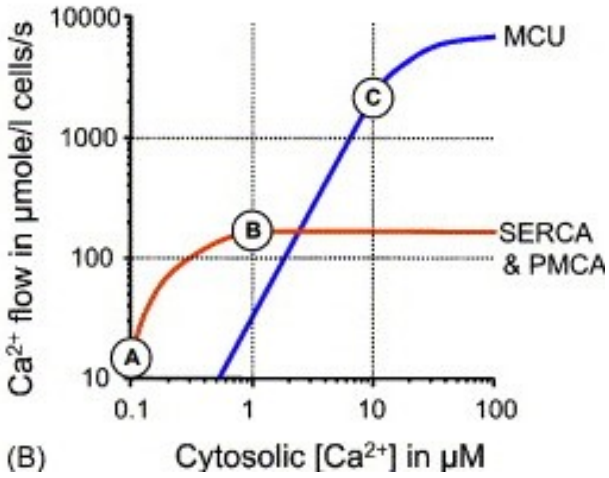

Figure 1.2. Comparison of Ca^{2+} extrusion pathways in adrenal chromaffin cells. Mitochondrial uptake is in blue and SERCA and PMCA activity in red. A, B and C showing the resting, moderate stimulation and maximal stimulation of the cell) (Villalobos *et al.*, 2002; Alonso *et al.,* 2006)

1.4.1.2. Rapid uptake mode (RaM)

In liver and heart, there is another route for Ca^{2+} uptake named rapid uptake mode (RaM). This uptake respond almost one hundred times faster than MCU to the transient increase concentration of Ca^{2+} pulses in physiological concentration (400 nM) and uptake Ca^{2+} very fast. RaM is deactivated when Ca^{2+} concentration reaches to almost 100 nM. Recovery from this deactivation took a very long time (about minutes). Therefore, it looks that this uptake is not for beat to beat mitochondrial Ca^{2+} (O'Rourke

2009; Ganitkevitch, 2007). The molecular characteristics of RaM are still not clear. This uptake is sensitive to ruthenium red in higher concentrations than MCU and is not affected by Mg^{2+}. Whether this mechanism is completely different from MCU or partially similar is still under debate (Rizutto, 2000).

1.4.1.3. Mitochondrial Na^+/Ca^{2+} exchanger in reverse mode

Depending on the Ca^{2+} and Na^+ concentration in cytosol (or under specific experimental condition) mitochondrial Na^+/Ca^{2+} exchanger (see the following part) works in reverse mode and is able to uptake Ca^{2+} (Graier *et al.*, 2007; Smets *et al.*, 2004).
There are various candidates for mitochondrial Ca^{2+} uptake. It looks that depends on the tissue and species there are other pathways that are not sensitive to ruthenium red.

1.4.2. Mitochondrial Ca^{2+} extrusion

1.4.2.1. Na^+/Ca^{2+} exchanger

Most of the authors believe that extrusion of Ca^{2+} from mitochondria is highly dependent on Na^+ flux and takes place through a Na^+/Ca^{2+} exchanger (NCX_{mito}). This exchanger is located in the mitochondrial inner membrane space. It assumes to transfer one Ca^{2+} in the exchange of 3 Na^+ from matrix to the space between two membranes (Pffeifer *et al.*, 2001). It has been investigated functionally using a pharmacological tool, Chloro-5- (2-chlorophenyl) -1, 5-dihydro-4, 1-benzothiazepin-2(3H) -one (CGP 37157), which is almost a specific inhibitor for this exchanger (Nicolau *et al.,* 2009). Molecular mechanism of NCX_{mito} and its contributors are not known. Very recently, Palty and his coworkers using Na^+ and Ca^{2+} sensors showed that NCX_{mito} is a NCLX which mediates Na^+ or Li^+ dependent Ca^{2+} extrusion. In this research, overexpression or knockdown of the protein had enormous effect on mitochondrial Ca^{2+} homeostasis. In addition, they showed that overexpression of NCLX in the cells that do not have this protein, rescues the Ca^{2+} extrusion (Palty *et al*., 2010).

1.4.2.2. Permeability transition pores

There is some evidence that increasing the Ca^{2+} level in mitochondrial matrix leads to transient formation of pores in the mitochondrial inner membrane and thereby Ca^{2+} effluxes through these pores (Evtodienko 2000; Graier *et al.*, 2007).

1.4.3. Mitochondria, Ca^{2+} signaling and SOCE regulation

Higher kinetics of MCU in comparison with NCX_{mito} and enough concentration of phosphate ions in the matrix of mitochondria, which make complex with Ca^{2+} entered the mitochondria, let this organelle to be a tool in Ca^{2+} buffering. It means the Ca^{2+} ions that enter the mitochondria in high rate and amount either captured by phosphates or they extrudes much slower by NCX_{mito} (Nicholls, 2008; Demaurex *et al.,* 2009).

Mitochondria are involved in the shaping of the spatial and temporal pattern of Ca^{2+} signals in the cell. Dependent on IP_3 receptor subtype, mitochondrial Ca^{2+} uptake is able to inhibit or promote cytosolic Ca^{2+} signals. Mitochondria inhibit the Ca^{2+} induced Ca^{2+} release, if IP_3 receptor has a linear Ca^{2+} activity and promote Ca^{2+} signal when the IP_3R has a bell-shaped Ca^{2+} activity (Graier *et al.,* 2007; Alonso *et al*., 2006).

While mitochondria buffer Ca^{2+} at the mouth of IP_3 receptor and thus modulating ER depletion and thus activating SOCE, it is also important for maintaining of SOCE. Mitochondria uptake the Ca^{2+} that enters the cell via SOC channel and therefore block the inhibitory effect of the ion on these channels (Graier *et al*., 2007; Parekh, 2008; Glitsch *et al.,* 2002). Disruption of mitochondrial membrane potential using ionophores (e.g. FCCP) and thus impeding Ca^{2+} uptake, dramatically decreases the Ca^{2+} concentration that has entered the cell upon SOCE activation (Malli *et al*., 2003a).

On the other hand, mitochondria are able to deactivate SOCE, and this can happen by the mitochondria that are in close contact with ER. A functional coupling between NCX_{mito} of this mitochondria and SERCA pump facilitates Ca^{2+} refilling of the endoplasmic reticulum through SERCA pump, and this leads to SOCE deactivation. Inconsistencies between the dual role of mitochondria in favoring and inhibiting the SOCE (through effect on Ca^{2+} cycling in ER), lead to a speculation that, in the commencement of SOCE mitochondria might play a role mostly in activating of the SOCE but later they might contribute mostly to the refilling of ER and thus, deactivating of SOCE (Parekh, 2008).

There are some reports showing that mitochondria might have a facilitating effect on SOCE not only by Ca^{2+} buffering but also by releasing some metabolites like pyruvic acid (Bakowski et al., 2007) and ATP (Montalvo *et al*., 2006; Glitsch *et al*, 2002). ATP is a Ca^{2+} buffer and it is likely that releasing ATP can have an effect on Ca^{2+} - dependent processes (Montalvo *et al*., 2006; Demaurex *et al.,* 2009).

Probably, pyruvic acid is able to prevent deactivaton of SOCE by either direct binding to the channel or by modulating of Ca^{2+} binding to the channel (Bakowski *et al*., 2007; Parekh, 2008).

In addition, there are some reports showing that the proximity of mitochondria to SOC channels is important for the efficient Ca^{2+} handling of this organelle and facilitation of Ca^{2+} entrance (Graier *et al*, 2007; Parekh, 2008; Demaurex *et al.,* 2009).

It has been shown in T-cell lymphocytes, upon depletion of the store and right before I_{CRAC} activity that mitochondria move toward entrance channel. Applying nocodazol (to disrupt movements of mitochondria toward the channels) decreases the amount of the Ca^{2+} entrance level (Quintana *et al.*, 2006). Supporting this data in Hela cells, overexpression of dynamitin which changes the spatial pattern of mitochondria and takes them away from Ca^{2+} entrance channel, decreases Ca^{2+} entered into the cell upon depletion of the store (Varadi *et al.*, 2004). Surprisingly, in the same cell type overexpression of hfis that changes the spatial pattern of mitochondria and aggregates them rather in prinuclear than in subplasmalemmal space, did not alter the level of Ca^{2+} entered the cell (Freiden *et al*., 2004). In addition to these discrepancies, structural coupling between STIM protein in ER and Orai protein in the plasma membrane upon SOCE activity result in a close contact between plasma membrane and endoplasmic reticulum. Therefore, one can speculate that the presence of mitochondria at the mouth of the channels is very unlikely and probably, mitochondria modulate the entrance channels activity by releasing metabolites. These metabolites diffuse towards the entrance channels and regulate SOCE activity without the presence of mitochondria (Demaurex *et al.,* 2009).

Mitochondrial uptake is dependent on the Ca^{2+} signaling shape in the cytosol. Depending on the stimulus for Ca^{2+} mobilization in the cytosol, and thereby having different Ca^{2+} signaling profile, mitochondrial uptake varies. When Ca^{2+} is released via IP_3 receptor, then the mitochondrial Ca^{2+} uptake is sharp, fast and shows the same

kinetics as Ca^{2+} elevation rate in cytosol. However, when Ca^{2+} provided with lower kinetic i.e. upon SOC channel activity, or leak from ER, the mitochondrial Ca^{2+} uptake is slower rate as compared to the cytosolic Ca^{2+} signal (Malli *et al*., 2003a).

1.4.4. Mitochondrial motility and its regulation by Ca^{2+}

Mitochondria are very dynamic organelles. They are in network or tubular form. Patterns of their movements are extremely complex and heterogeneous. Long distance movements, extension and contractions, fission and fusions are some examples of mitochondrial movement. These movements, which can be homogenous or move-pause-move, are necessary for the organelle to transmit ATP to the places where energy is required. Motility is also important for the efficient contribution of mitochondria in cellular processes and Ca^{2+} signaling (Yi and Hajnoczky, 2004).

Cytoskeleton machinery system is responsible for mitochondrial movement. In different cell types, microfilaments, microtubules or intermediate filaments contribute to mitochondrial movements (Yi *et al.,* 2004). For example, in yeast cells actin is the main player in mitochondrial movement (Frederick and Shaw, 2007). Other components, which are involved in the movements, include adaptor proteins and motor proteins. Adaptor proteins interact with a receptor on the mitochondrial outer membrane and connect mitochondria to motor proteins. Motor proteins (or “mechano enzymes’’ Hoyt *et al*., 1997) link this complex (mitochondria and adaptor) to the cytoskeleton network. The best-known receptor in the mitochondrial outer membrane, which is specific to motility, is Miro. Miro is a mitochondrial Rho GTPase in the mitochondrial outer membrane, and is highly conserved in different species. This protein is Ca^{2+} - affected by a pair of EF hand domain (Frederick *et al*., 2004; Liu and Hajnoczky, 2009). Three super families, myosins, dyneins and kinesins have been known to function as motor proteins in eukaryotic cells, which contribute in dynamicity of the cell, organelles or vesicles (Frederick and Shaw, 2007).

There is information from different cell lines showing cytosolic Ca^{2} modulates mitochondrial motility. In resting condition, mitochondria have maximum motility. However, by increasing cytosolic Ca^{2+} concentration this movement declines. Interestingly, mitochondrial movement recovered upon decay of Ca^{2+} signal in cytosol (Yi

A)

B)

C)

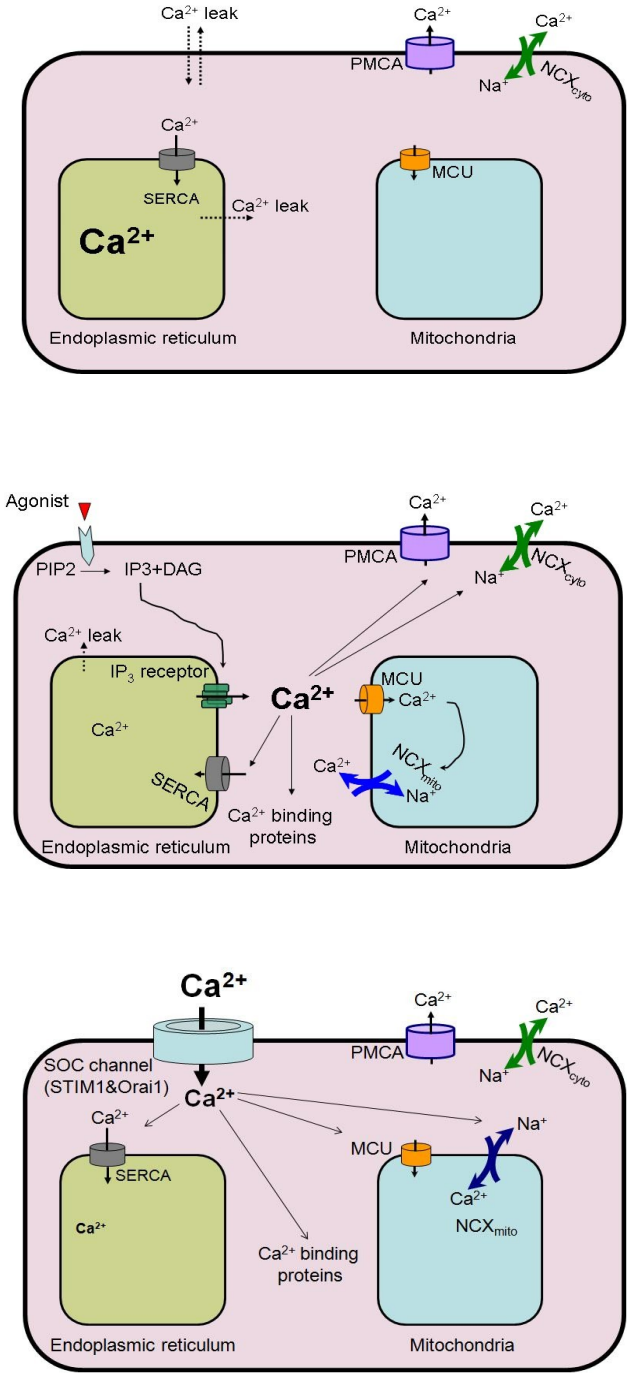

Figure 1.3. Schematic view of Ca^{2+} homeostasis in endothelial cells. Under resting condition, cytosolic Ca^{2+} level is low (100 nM) (A), However, upon cell stimulation with an IP_3 generating agonist Ca^{2+} ions release from ER and stores depleted (B). These ions extrude to extracellular space or intracellular organelles. Finally, readdition of the Ca^{2+} after ER depletion via IP_3 generating agonist or

SERCA inhibitor (C) will activate SOC channels, refill ER and uptake via mitochondria.

and Hajnoczky, 2004). Morphology of the mitochondria is modulated by proteins, which promote or inhibit fission (like DRP1) and fusion of the organelle. Studies show that Miro-Milton complex interacts with these proteins and thus, has a regulatory effect on the shape of mitochondria (Saotome *et al.,* 2008). Figure 1.3 shows a schematic view of Ca^{2+} homeostasis in endothelial cells.

1.5. Aim of the study

It has been a long time that SOCE phenomenon has been introduced by Putney (Putney, 1986), as an imperative mechanism which plays a role in different cellular signaling. On the other hand mitochondria is also known as not only as a power plant of cells but also as a major contributor in SOCE activation and/maintenance. However, very recently STIM1 and Orai1 has been known to be involved in SOCE mechanism and therefore, it was tempting to reconsider the effect of mitochondrial function specifically in the Ca^{2+} influx mediated by STIM1-Orai1 pathway. The aim of this study was first to indentify contributors of SOCE in EA.hy926 cells, second, to investigate the effect of mitochondrial Ca^{2+} sequestration on STIM1-Orai1 mediated SOCE and to test the effect of mitochondrial long distance motility on Ca^{2+} entering via SOC channels.

2. Material and methods

2.1. Materials.

Fura-2/AM, cell culture chemicals were provided from Invitrogen and fetal calf serum (FCS) is from PAA laboratories (Linz, Austria). CGP 37157 (7-chloro-5-(2-chlorophenyl)-1 was from Tocris Cookson Ltd. (Northpoint, Avonmouth, Bristol, UK). Other materials including, Dulbecco's modified eagle's medium (DMEM), EGTA, BHQ (2, 5–di–tert-butylhydroquinone), Ionomycin, FCCP (Carbonylcyanide p-trifluoromethoxyphenylhydrazone), Antimycine, Oligomycin, Histamine were provided from Sigma chemicals (St. Louis, MO, USA). JC1 (5, 5`, 6, 6´-tetrachloro-1,1´,3,3´-tetraethyl-benzimidazoylcarbocyanine iodide) and mitotracker green were from Molecular Probes Europe (Leiden, Netherlands).
NaCl, KCl, Na_2HPO_4, KH_2PO_4, $MgCl_2$, Hepes, D-glucose, $NaHCO_3$, KH_2PO_4, $CaCl_2$, β-Mercaptoethanol were, from Roth (Karlsruhe, Germany).

2.1.1. Solutions for cell physiology experiments:

For Ca^{2+} imaging the solutions mentioned below has been used:

1. Loading buffer was used for treatment cells with florescent dyes, washing cells or for equilibration of the cells after washing procedure. It contained: (mM) 2 $CaCl_2$, 138 NaCl, 1 $MgCl_2$, 5 KCl, 10 Hepes, 10 D-glucose, 2.6 $NaHCO_3$, 0.44 KH_2PO_4, 0.1 % vitamins, 0.2 % essential amino acids, 1 % penicillin/streptomycin, 1 % fungizone; pH adjusted to 7.4.
2. Ca^{2+}-buffer or so-called 2 $Ca^{2+}Na^{+}$ (mM): 2 $CaCl_2$, 138 NaCl, 1 $MgCl_2$, 5 KCl, 10 Hepes, 10 D-glucose pH adjusted to 7.4, depend on the protocols $CaCl_2$, were used to 0 (Ca^{2+}-free-buffer or so called 0 $Ca^{2+}Na^{+}$ buffer), 5, 10 or 20 mM.
3. EGTA buffer (mM): 1 EGTA, 138 NaCl, 1 $MgCl_2$, 5 KCl, 10 Hepes, 10 D-glucose, pH adjusted to 7.4.

For the experiments with low Na^{+} , NaCl were applied with 0 or 13 mM and for balancing of osmolarity, Cholin Chloride were used with 138 or 125 mM (respectively), in Ca^{2+}-buffer and EGTA buffer.

According to protocol, and experiments, pharmacological tool applied. A detail of these tools has been listed below:

1. Histamine, Mw : 184.07, stock concentration was 100 mM in water and final concentration was 100, 10 or1 µM
2. CGP 37157 (7-chloro-5-(2-chlorophenyl)-1, 5-dihydro-4, 1-benzothiazepin-2(3H), Mw: 324.22, stock concentration was 100 mM in DMSO and final concentration was 20 µM.
3. BHQ (2, 5-di-tert-butylhydroquinone), Mw : 222.33, stock concentration was 100 mM in DMSO and final concentration was 15 µM.
4. Rotenone, Mw : 394, stock concentration was 100 mM in DMSO and final concentration was 50 µM.
5. Oligomycine, Mw : 786.78, stock concentration was 10 mM in DMSO and final concentration was 2µM.
6. Antimycine, Mw : 534.645, stock concentration was 100 mM in EtOH abs and final concentration was 10 µM.
7. Ionomycine, Mw : 709.01, stock concentration was 3 mM in DMSO and final concentration was 5 µM.
8. Digitonin, Mw : 1229.34, stock concentration was 10 mM in water and final concentration was 5 µM.
9. FCCP (Carbonylcyanide p-trifluoromethoxyphenylhydrazone), Mw : 255.97, stock concentration was 10 mM in DMSO and final concentration was 4 µM.
10. JC1 (5, 5`,6,6´- tetrachloro- 1, 1´, 3, 3´-tetraethyl-benzimidazoylcarbocyanineiodide), Mw : 652.23, stock concentration was 2 mM in DMSO, and final concentration was 80 nM.
11. MitoTracker Green, Mw : 671.88, stock concentration was 1 mM in DMSO, and final concentration was 2 µM.

2.1.2. Plasmids.

Plasmids that have been used in this study listed in Table 2.1.

Construct	Characteristics	Original plasmid	Reference
pEYFP-C1	4.7kb, Km^r	pEYFPC1 (Invitogen)	Clontech
D1-ER	5.4kb, Km^r	pcDNA3 (Invitogen)	Palmer *et al*., 2003
mtDsRed	5.4kb, Amp^r	pcDNA3 (Invitrogen)	Malli *et al*., 2003a
STIM1-YFP	Km^r	pEYFP-N1 (Clontech)	Malli *et al*., 2008
Orai1-YFP	Km^r	p-EYFP-N1 (Clontech)	Malli *et al*., 2008
Orai1-CFP	Km^r	p-EYFP-N1 (Clontech)	Malli *et al*., 2008
NTRPC3-YFP	N terminal of TRPC3, Km^r	pEYFP-C1 (Clontech)	Eder *et al*., 2007
AKAP-RFP-CAAX	Km^r	?	Csordas *et al*., 2006; Liu et al., 2009

Table 1.2. Constructs have been used in this study.

2.2. Methods

2.2.1. Cell culture

In this study, EA.hy926 cell line, passage 50 to 85 (with or without permanently expressing RPmt) was used. EA.hy926 is an immortalized cell from hybridization of human umbeilical vein endothelial cells and human cell line A549 (derived from human lung carcinoma). The first aim of providing this cell line was to have an immortalized cell model, which permanently express factor VIII-related antigen. This factor is a trait of highly differentiated vascular endothelial cells (Edgell *et al.,* 1983).
Cells were cultured on 3 cm glass cover slips in Dulbecco's modified eagle's medium containing 10% fetal calf serum (FCS) and 1 % HAT (5 mM hypxanthin, 20 µM aminopterin and 0.8 mM thymidine), 50 units/ml penicillin, 50 µg/ml streptomycin at 37°C, 5 % CO_2.

2.2.2. Transfection

Transfection of the cells performed using Transfast^{TM} (Promega, Mannheim, Germany), and on the base of the company manual:

2.2.2.1. Transfection with DNA

Cells (80 % confluent) which has been grown on cover slips (with Ø 30mm) was treated with 1 ml (for each glass well) of FCS-free medium containing 1-2 µg DNA and 4 µl Transfast^{TM} tarnsfection reagent (for each well) added to plates. After one hour, transfection medium diluted with adding 1 ml of serum containing medium. 4 hours afterwards, transfection medium was exchange with new medium. Cells were employed for experiments 36 - 48 hours after transfection. It needs to be mentioned that if the gene of interest is not tagged with a fluorescent protein, to visualize transfected cells, an empty vector containing florescent tag co-expressed with the gene of interest (Malli *et al*., 2005).

2.2.2.2. Transfection with RNA

80 % confluent cells were transfected with 500 µl (for each glass well) of FCS-free medium containing 1 µg, empty vector (pEYFPC1 or mtDsRed), 2.5 µl siRNA nucleotides and 4 µl Transfast^{TM} transfection reagent (for each well). After one hour, 500 µl FCS-free medium was added to the transfection medium. After 16 hours, transfection medium exchanged with fresh serum containing medium, and after 24 hours cells were used for experiments.

2.2.2.2.1. siRNA sequences

STIM1 and Oria1 down regulate transiently using the siRNAs mentioned below:

Sense sequence for hOrai1-siRNA: CCCUUCGGCCUGAUCUUUAUCGUCU

Sense sequence for hStim1-siRNA: GGCUCUGGAUACAGUGCUCtt

Control: All-Star Neg. Control siRNA (Invitrogen)

2.2.3. Total RNA isolation

For isolation total RNA from EA.hy926, RNeasy Mini-Kit from Qiagen (Hilden, Germany) was used according to company instruction:

1. Cells washed 2 times with phosphate buffer saline (containing (for 1l): 8.00 g of NaCl, 0.20 g of KCl, 1.44 g of Na_2HPO_4, 0.24 g of KH_2PO_4, pH adjusted to 7.4).
2. In order to lysate the cells, RLT buffer containing 1 % β-Mercaptoethanol added to the cell culture dish (700 µl for 100 mm dish and 350 µl for 30 mm well respectively).
3. Cell lysate was collected with scarper and pipetted into a microcentrifuge tube and homogenized gently using an RNase free syringe by passing the sample at least 5 times through a 26-gouge needle.
4. One volume of 70 % ethanol was added to the lysate and mixed by pipetting.
5. The sample was applied to an RNeasy mini column placed in a 2 ml collection tube and centrifuged for 30 s at 8000 g
6. 700 µl RW1 buffer was added to the RNeasy column and the isolated RNA was washed by a 30 seconds centrifugation at 8000 g.

7. The RNeasy column was transferred into a new 2 ml collection tube and 500 µl of buffer RPE containing ethanol (RPE concentrate: EtOHabs = 1:4) was pipetted onto the RNeasy column and centrifuged for 30 seconds at 8000 g. Step 6 was repeated with 500 µl buffer RPE.
8. After discarding the flow-through, the RNeasy column containing the washed RNA was centrifuged another minute at full speed (13000 rpm) to dry the RNeasy silica-gel membrane.
9. The RNeasy column was transferred to a new 1.5 ml collection tube, and 30 – 50 µl of RNase free water was pipetted directly onto the RNeasy column and left for 5 minutes.
10. The column centrifuged for 1 min at max speed (13000 rpm). RNA concentration measured using Peqlab ND-1000 spectrophotometer. RNA was stored at -70 °C.

2.2.4. Reverse transcription from RNA to DNA (RT-PCR)

To remove all the possible contamination of DNA from RNA extracted, samples were treated with DNase from Promega:

- A mix prepared containing: 3 µg of RNA, 3 µl of 5x first strand buffer (Promega),1 µl DNase I (Promega) and x µl DEPC-water (RNase-free) With final volume of 15 µl, were prepared.
- Sample incubated at 37 °C for 15 minutes, and put on ice.
- 1.5 µl EDTA (20 mM) added
- Sample vortexed gently; centrifuged for a few seconds
- Sample incubated at -75 °C for 10 minutes
- Sample returned back immediately on ice
- Sample centrifuged and put on ice again.

For long time storage, RNA was kept at –70 °C.

For reverse transcription, the high capacity cDNA reverse transcription kit from Applied Biosystems (Woolsten, Warrington, UK) was used. To avoid RNA digestion the RNasin®RNase Inhibitor (Promega) was inserted into the reverse transcription mix. All the procedure was performed according to manufacturer manual. All the preparation

steps for RT master mix were performed on ice. 2X master mix reaction prepared as below (For each reaction:

- 10x RT buffer 2.0 µl
- 25x dNTP mix (100 mM) 0.8 µl
- 10x RT Random Primers 2.0 µl
- MultiScribe^{TM}Reverse Transcriptase 1.0 µl
- RNase Inhibitor 1.0 µl
- Nuclease-free H_2O 3.2 µl

2 ug of the RNA sample was added to the master mix composition (To prepare the appropriate amount of RNA, it has to be diluted with RNase-free water to provide a final volume of 20 µl), mixed and shortly centrifuged. Program for thermal cycler was:

25 °C for 10 min

37 °C for 120 min

85 °C for 5 sec

2.2.5. Specific Polymerase Chain Reaction (PCR)

For specific polymerase chain reaction (PCR), GoTaq® Green Master Mix (Promega, Mannheim, Germany) was used.

- 1-4 µl of cDNA or 5-50 ng of plasmid DNA
- 25-100 pmol of a gene specific forward primer
- 25-100 pmol of a gene specific reverse primer
- 25 µl of the master mix

ddH_2O added to a final reaction volume of 50 µl

Depend on the length of gene and the annealing temperature of the primers used the settings of the thermocycler is different, it was performed commonly as below:

1. 95 °C 15 min (Initial denaturizing step)
2. 94-95 °C 1 min (denaturizing)
3. 50-65 °C 1 min (primer annealing)
4. 72 °C 1 min (extension)
5. 72 °C 10 min (final extension step)

Step 2 to 4 repeated for 30 to 40 times.

The primers which used for RT-PCR in this study were:

hSTIM1 forward: 5'-ATGGATGTATGCGTCCGTCT-3'

hSTIM1 reverse: 5'-TCCAACTCCTCCTCAGCATA-3'

hOrai1 forward: 5'-TGTCCTGGCGCAAGCTCTAC-3'

hOrai1 reverse: 5'-ATGCCGCTGGTGCTGACGTT-3'

2.2.6. Preparation of competent *E.coli* strain TOP10

Preparing bacterial stocks for competent cells:

1. TOP10 cells were cultured on SOB plate contained (for 200 ml: 116.88 mg NaCl, 35.28 mg KCl, 20 ml of 0.1 M $MgSO_4$, 4 g Trypton,1 g Yeast extract pH adjusted to 7.4, 1.5 % Agar in solid mediums) and incubated at room temperature.
2. Single colonies were picked and inoculated in 2 ml of SOB medium, overnight, at room temperature and in shaker.
3. 15 % glycerol was added to tubes and the medium was aliquoted in 1 ml in -70 °C

Preparation of the competent cell for chemical transformation:

1. 1 ml of the TOP10 cells stock was inoculated in 250 ml and incubated for 16 h in shaking at room temperature (OD_{600} nm of 0.3).
2. Incubated medium was centrifuged at 3000 g at 4 °C for 10 min.
3. The pellet was resuspended in 80 ml of ice-cold CCMB80 buffer (Containing: 10 mM KOAC, 80 mM $CaCl_2.2H_2O$, 20 mM $MnCl_2$.4H2O,10 mM $MgCl_2.6H_2O$, 10 % glycerol, pH was adjusted to 6.4 with 0.1 HCl, sterile filtered and stored at 4 °C)
4. Sample was incubated on ice for 20 min and centrifuged at 4 °C
5. Pellet was resuspended in 10 ml of ice-cold CCMB80
6. OD of the sample was balanced to 1-1.5
7. After 20 min incubation on ice, sample was aliquoted in 50 µl portions in pre-cold tubes and stored at -70 °C.

2.2.7. Transformation of competent *E.coli* strains

1. 50 µl aliquots of competent cells were thawed on ice.
2. 2 µg DNA was added to the thawed TOP10 cells, mixed gently and incubated for 30 min on ice.
3. Cells were incubated for 60 second at 42 °C without shaking.
4. 250 µl SOB was added to the cells
5. Cells were incubated for 1 hour, in the shaker at 37 °C.
6. 50 µl of the medium containing cells was spreaded on the LB plate containing proper antibiotics and incubated overnight.

2.2.8. Real-time RT-PCR

The real-time RT-PCR technology was used to investigate the level of gene expression under different condition (e.g. Knockdown efficiency of functional siRNAs against gene of interest)

In this study, LightCycler 480 Instrument (Roche) was used which is equipped with the optical system of the fluorimeter. A light beam of 470 nm (excitation) is focused onto the individual wells of a 96 well plate and therefore onto the samples and the intensity of light records. The detection channel within the LightCycler fluorimeter has a filter that allow analyses at certain emission wavelengths, which does allow exact measurements of emission from a distinct fluorophore.

2.2.8.1. SYBR Green

SYBR Green I is a dye that binds specifically to double-stranded DNA. It's inherent fluorescence is enhanced when it binds to the minor groove of double-stranded DNA. During PCR, SYBR Green I binds to DNA products as soon as they are synthesized. Thus, the increase in SYBR Green I fluorescence, when measured at the end of each elongation cycle, indicates the amount of PCR product formed during that cycle. Dye staining can detect from nearly 1 to 10^9 copies of a target sequence. The maximum excitation of SYBR Green I dye occurs at 497 nm. Maximal emission wavelength of DNA stained with SYBR Green I is 521 nm.

2.2.8.2. Primers for Real-time

For amplifying the specific genes, QuantiTect® Primer Assays for (Qiagen Corporation, Hilden, Germany) were applied in the RT-PCR reaction. QuantiTect® Primer Assays are validated genome wide primer sets that provide highly specific and sensitive results in SYBR Green based real-time RT-PCR.

The Primer Assay for GAPDH (Hs_GAPDH_2_SG, Cat No.: QT01192646) was used for the amplification of human Glyceraldehyde-3-phosphate dehydrogenase in RT-PCR experiments acting as a housekeeping gene.

2.2.8.3. Preparation of samples

Cells were grown on 6 cm dishes (~10^6 cells) and each dish transfected with 10 µl (negative control siRNA or other siRNA (s), which had to be tested for its potency to a specific gene down regulation. 42 hours after transfection, Total RNA was isolated from dishes, Usually 2 µg of each RNA sample was subsequently reverse transcribed to cDNA. To quantify specific genes in cDNA samples with the LightCycler instrument, a pool of all samples containing an appropriate amount of cDNA from the various samples was prepared. Thereafter a serial dilution (1:10, 1:100 and 1:1000 from the pool) was prepared. This serial dilution was used to draw standard curve and to calculate the PCR efficiency. For each set of primers, a standard curve was prepared.

cDNA from different samples were diluted 1:50, and used for different conditions (e.g. siRNA treated samples of STIM1 and Orai1 versus control). Primers for housekeeping gene (GPDH) and the gene of interest were applied separately. All the experiments were performed in triplicate.

The data from the LightCycler instrument represented the crossing point value. This value is the cycle of PCR at which the fluorescence generated by sample, crosses the fluorescence threshold (that is the fluorescence level, which is significantly higher than background fluorescence). Thus, the efficiency of the active siRNAs was identified by reaching the threshold in higher cycles.

2.2.8.4. Reaction Setup

- 2 µl of cDNA sample was pipette in each well of the 96-well plate.
- 5 µl QuantiFast™SYBR Green PCR Master Mix, 1 µl QuantiTect®Primer Assay and 2 µl RNase free water were added to each well.
- 96-well was centrifuged at 1000 rpm for 10 sec and were placed on the LightCycler instrument

2.2.8.5. Real-Time PCR Conditions:

1. 95 °C for 15 min Denaturation
2. 95 °C for 10 s Denaturation
3. 60 °C for 30 s Combined annealing/extension

Step 2 and 3 were repeated for 40 cylces.

2.2.8.6. Analysis of Real Time PCR

The out coming crossing points of the particular PCR-reactions were analyzed by the REST software version 384® (Relative Expression Software Tool), which was downloaded from http://rest.gene-quantification.info/. The amount of downregulation of the gene of interest was calculated and plotted as percentage of the negative control.

2.2.9. Isolation of plasmids (Maxi prep)

For EA.hy926 transfection, plasmids isolated using PureYield™ Plasmid Maxiprep System (Promega, Madison, USA), and according to instruction manual:

1. Overnight culture of bacteria (200 ml) in LB medium (containing 10 gr NaCl, 10 gr Trypton and 5 gr yeast for 1000 ml, pH : 7.4, plus antibiotics, Ampicilin (100 µM) or Kanamycin (50 µM) centrifuged at 5000 g for 10 min.
2. Cells pellet resuspended in 12 ml of Cell Resuspension Solution
3. 12 ml of Cell Lysis Solution were added and the mixture was gently inverted for 3-5 times.
4. After 3 min, 12 ml of Neutralization Solution were added gently mixed for 10-15 min.
5. All the lysate, centrifuged at 14000 g for 20 min.

6. To purify the plasmid DNA the blue Clearing Column was assembled on top of the white Binding Column and the column stack was placed onto the vacuum manifold.
7. The lysate poured into the Clearing Column and vacuum maintained until the liquid pass through both columns.
8. The Binding Column washed once with 5 ml of Endotoxin Removal Wash and once with 20 ml of Column Wash until the solution was pulled through the column by the vacuum.
9. An additional 5 min exposition to vacuum applied to remove all the liquids.
10. The pure plasmid was collected by adding 1.5 ml of Nuclease-Free water to The Binding Column, which already was assembled on the collection tube using vacuum.

All the protocol for maxi prep was performed at room temperature but the pure plasmid stored at 4 °C.

2.2.10. DNA concentration measurement

DNA concentration was measured using Peqlab ND-1000 spectrophotometer; 2 µl of a nucleic acid sample was applied onto the measurement spot of the Nanodrop (ND) instrument. Absorption at 260 nm and 280 nm of sample(s), and concentration of them were calculated by system according to the formula mentioned below:

For RNA: OD_{600}*4 = Concentration of RNA (µg/µl)

For DNA: OD_{600}*5 = Concentration of DNA (µg/µl)

2.2.11. Molecular mechanism of Gene silencing using siRNA

One of the breakthroughs in molecular genetics is RNAi which is a post transcriptional gene regulation mechanism. Small interfering RNAs (siRNA), (~ 21bp), with an UU overhang at 3' end are the main items of this process. This small RNA can produce endogenously or it can be applied experimentally. In animal cells, these RNAs can down regulate the expression genes. Cells use this defensive reaction against any unknown nucleotides (like viruses). When a long chain double stranded RNA produce through reverse transcription or when it introduce exogenously into the cell the following reaction take place (figure 2.1):

1. dsRNAs is identified by Dicer (a member of RNAase III family) and cleaves to 21 bp double strands with 2 bp overhang at 3' end.
2. Other proteins like Argonaut2 (Ago2) and transactivating response RNA binding protein (TRBP) binds to the complex of dsRNAs - Dicer and form a new sophisticated complex named RISC loading complex (RLC).
3. ATP binds to this complex and activates it.
4. RLC unwinds the duplex of siRNA and Ago2 cleaves sense strand and the strand with less thermodynamically stability at 5' end stay with the complex.
5. The complex containing the single strand of RNA and Ago2 is called RISC (RNA-induced silencing complex). Ago2 modulate binding the complex to the mRNA which is highly specific complementary with the single strand of RNA and cleaves the mRNA.
6. The cleaved mRNA is recognized by nucleases as abnormal sequence and digests by them (Shukla *et al.,* 2009).

   In this study, ready to use double stranded siRNA were used to knockdown, the gene of interest.

2.2.12. Expression of dominant negative protein

One of the tactics in down regulation a gene function is applying dominant negative mutant. Dominant negative mutant is a mutant of the gene of interest, which is transfected to the cell. The product of the mutant is probably still able to interact with the partners of the protein that produced from normal genes. In the case of the proteins, which oligomerize, this mutant might bind to the normal protein and thus blocking the function of the protein. In this study, a mutant of TRPC channel was applied (Eder *et al.*, 2007).

2.2.13. Detection of DNA fragments

To detect DNA fragments, agarose gel, 1 % in 1x TAE buffer (40 mM Tris, 20 mM, Na^+-acetat, 1 mM EDTA, pH=7.2) in solid form were applied. 0.5 µg/ml Ethidium bromide

added to the gel, for staining the DNA. DNA samples in companion of an appropriate DNA ladder (GeneRuler™ DNA Ladder Mix, ready-to-use bought from Fermentas) were loaded. Gels were run in a horizontal gel-forming chamber using 1x TAE buffer at 100 V. Depend on the size of fragment and the length of the gels time for running was between 1 and 2 hour. To detect DNA fragment, gels were exposed to UV-light (360 nm).

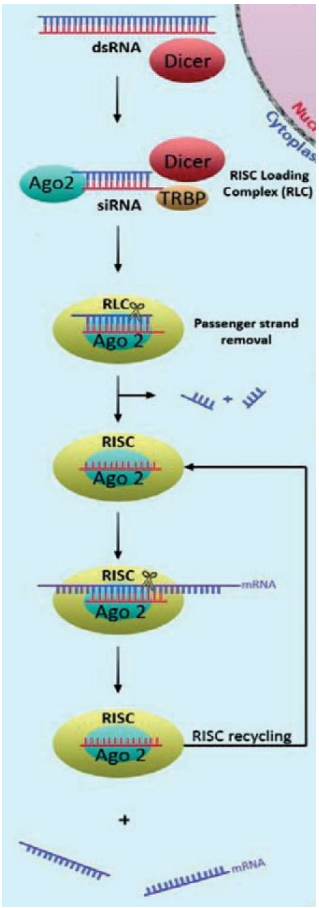

Figure 2.1. Scheme of molecular mechanism of knockdown using siRNA (Shukla *et al.,* 2009). Details are in the text.

2.2.14. Ca^{2+} ion measurement using fluorescent Ca^{2+} indicators

Fluorescent Ca^{2+} indicators are the chemical or biological compounds which specifically and reversibly bond to Ca^{2+} and change in physiochemical characteristics (e.g. spectral response).

Chemical indicators are mostly derivatives of Ca^{2+} chelators (like EGTA, and EDTA), with a very wide range of affinity of Ca^{2+} (Tsien, 1980). Sometimes there are some complications in the loading procedure of the chemical indicator. Conjugation of these indicators with lipophilic acetoxymethyl (AM) esters solved this problem (Rudolf *et al.,* 2003).

2.2.14.1. Ratiometric and non-ratiometric (intensity-based)

Fluorescent indicators with a spectral shift upon binding to Ca^{2+} are used for ratiometric measurement of Ca^{2+}. Indicators, which exhibit changes in the intensity of the fluorescent in the same wavelength, upon binding to Ca^{2+}, can be used for non-ratiometric measurement. Mostly ratiometric indicators are preferred because heterogonous dye loading, difference in cells thickness and bleaching will be accurate by using ratiometric indicators (Rudolf, *et al.* 2003).

2.2.14.2. Protein based indicators

Protein based indicators are from translation of nucleic acid sequence (proteins or peptides). These indicators involved at least a fluorescent part and a Ca^{2+} interacting part.

2.2.14.2.1. Pericam

These indicators are green fluorescent protein (GFP) based. Green fluorescent protein (GFP) has two peaks in the spectrum that are related to protonated and deprotonated condition of the protein. In other words, a proton network from polar amino acids that surrounds the chromophore, effects the conformation of this protein (Nagai, *et al.,* 2001)

Under intense study, researchers discover that insertion of a sequence (e.g. a Ca^{2+} reactive protein mostly calmodulin (CaM)) in the structure of green fluorescent protein (GFP) (tyrosine (Tyr) 145) does not change the chromophor properties of the protein. Binding of Ca^{2+} to inserted protein (CaM), decrease or increase the intensity of the emission light of GFP part. Another characteristic of GFP is the principle of circular permutated GFP indicators, named pericam. Connecting carboxyl and amino terminal by a spacer and cleaving the GFP between Tyr 145 and 146 does not make any difference in the fluorescence properties of the protein. The new ends can be linked to a variety of different proteins. In pericam indicators, engineered calmudolin (CaM) and its target peptide, M13 (skeletal muscle myosin light-chain kinase) applied for the new ends of one of GFP derivatives (yellow fluorescent protein (YFP)). Upon binding Ca^{2+}, calmodulin binds to M13 and apparently, this connection changes the pattern of protonation around GFP, which leads to changes in the spectral properties of this protein.

Ratiometric pericam construct was originally described to have a shift in the light intensity of the spectrum of GFP upon interaction with Ca^{2+} (Nagai *et al.,* 2001). However, later it was cleared that this sensor in 480 nm is more sensitive to proton than Ca^{2+} and in 430 nm it is sensitive to Ca^{2+} (Malli *et al*., 2003a). Therefore, in this study 480 nm was used exclusively for Ca^{2+} sensing.

2.2.14.2.2. Cameleon

Another group of fluorescent Ca^{2+} indicators is called cameleon. In these indicators, CaM and M13 have been fused together and inserted between CFP (cyan fluorescent protein) and YFP (yellow fluorescent protein). These indicators take advantage of FRET (Förster resonance energy transfer) mechanism. Upon binding Ca^{2+}, calmodulin interacts with M13 and the conformation of the construct changes in a way that the distance between chromophores decreases and thus, FRET signal increases (Ishii *et al.,* 2006; McCombs *et al.,* 2008).

2.2.14.3. FRET (Förster resonance energy transfer)

Theodor Förster proposed the idea of FRET (Förster resonance energy transfer) for the first time in 1949, as a non-radioactive distance dependent transfer of energy between a donor and acceptor chromophor. This process occurs when under a suitable distance (1-10 nm), the emission wavelength of the first chromophor overlaps with the excitation of the second one. This unique property of FRET put it in the center of researchers' interest as a very powerful technique in protein - protein or protein - DNA interaction studies in living cells (Miyawaki, 2003).

2.2.14.4. Comparison of characteristics' of protein based indicators and chemical indicators:

1. Protein - based indicators might localize in special intracellular compartments using a target sequence. These indicators remain in the cell longer than chemical indicators. However, targeting the chemical indicators to special organelle is almost impossible and the extrusion of chemicals is very fast.
2. Application of inducible promoters makes it possible to control the expression level of protein indicators.
3. The bleaching of chemical indicators is less than that of protein based indicators
4. Chemical indicators have higher ratio of signal to noise.
5. Kinetics of the response of chemical indicators is faster than protein based indicators.
6. Protein based indicators (especially GFP) are more pH sensitive than chemical indicators, which leads to decreased efficiency even under slight pH changes near neutral pH.
7. Chemical indicators are more preferable when the cells are resistant to transfection.
8. Some chemical indicators show tendency to bind to other ions like Mg^{2+} while protein based indicators are more specific to Ca^{2+}.

In addition, Ca^{2+} concentrations in different compartments are not similar. Therefore, it is important to apply an indicator with proper affinity (K_d). Compartments with low Ca^{2+} concentration need an indicator with higher Ca^{2+} affinity and vice versa (McCombs and Palmer, 2008).

2.2.14.5. Ca^{2+} imaging in different organelles

2.2.14.5.1. Cytosolic Ca^{2+} ($[Ca^{2+}]_{cyto}$) concentration measurement

As it has been already published (Graier *et al*., 1998, Paltauf-Doburzynska *et al*., 1998, Malli *et al*., 2005, Trenker *et al*., 2007), free cytosolic Ca^{2+} concentration was measured using a ratiometric dye, Fura-2/AM. This dye is UV-light excitable and a derivative of EGTA (a specific chelator for Ca^{2+}). Unbound form of Fura excites at 340 nm and when it interacts with Ca^{2+}, excitation wavelength shifts to 380 nm. The great advantages of ratiometric measurement (for Fura-2, F_{340}/F_{380}) is omitting of technical problems like different level of dye loading, difference of thickness of cells and bleaching (which commonly occurs during experiment). Another advantages, is application of esteric form of the Fura-2 (AM) which is permeable for the cells. Esteric format of Fura-2 cleaves upon esterase enzyme activity of the cell and captures in the cell. The Kd of Fura2/AM is about 148 nM, which is suitable for different changes of cytosolic Ca^{2+} in physiological states.

Cells which has been plated on cover slips (with Ø 30 mm), were washed with loading buffer and treated with 3.3 µM Fura-2/AM in loading buffer in room temperature, and in darkness. After one hour, cells were washed for 3 times with loading buffer and equilibrate for further 10 min in this buffer. Cover slip mounted on the special chamber and perfused with Ca^{2+} buffer (with the rate of 1 ml/min). Changes in F_{340}/F_{380} were interpreted as change of the level of cytosolic Ca^{2+}.

Cells were illuminated alternatively at 340 nm and 380 nm (340HTI15 and 380HTI15; Omega Optical Brattleboro, VT, USA), using a motorized filter-wheel (Ludl, Electronic Products, Hawthrone, NY, USA). Emission signals collected at 510 nm using 510WB40 emission filter from Omega Optical (Brattleboro, VT, USA).

2.2.14.5.2. Mitochondrial Ca^{2+} ($[Ca^{2+}]_{mito}$) concentration measurement

Mitochondrial Ca^{2+} measurements were performed using EA.hy926 cells expressing ratiometric pericam (RP-mt) permanently (Malli *et al*., 2003b, Malli *et al*., 2005; Trenker *et al*., 2007). Mt-RP was excited at 433 nm (433DF15, Omega Optical) and emitted light was collected at 535 nm (535AF26, Omega Optical, Brattleboro, USA). Because of the

sensitivity of mt-RP to pH at 480, $1-F_{430}/F_0$ was considered as representative for mitochondrial Ca^{2+} concentration. For fitting the curve and correcting the bleaching of the sensor (mt-PR), bleaching function (F_0) were calculated using one phase exponential decay equation and part of the data of F_{430} which were collected at the time points when the cells were in basal level of Ca^{2+}. Cells washed with loading buffer, at room temperature, before applying for experiments.

2.2.14.5.3. Endoplasmic reticulum ($[Ca^{2+}]_{ER}$) concentration measurement

Free Ca^{2+} concentration in the lumen of ER measured by Forster resonance energy transfer (FRET) technique. To this aim an ER targeted cameleon named D1-ER (Palmer *et al.*, 2004; Malli *et al.*, 2005; Trenker *et al.*, 2007) was used. Transfected cells were excited at 440 nm (440AF21, Omega Optical) and emission collected at 535 and 480nm simultaneously, using a beam splitter (530 and 480, Dual-view MicroImager^{TM}, Optical Insights, Visitron Systems, Puchheim, Germany).

For fitting the curve and correcting the bleaching of the sensor (D1-ER), bleaching function (F_0) were calculated. For calculating this function, one phase exponential decay equation and part of the data of F_{535}/F_{480} (which usually were collected from the time points when the cells were in basal level of Ca^{2+}) were applied. $(F_{535}/F_{480})/F_0$ was used for interpretation of Ca^{2+} signals in endoplasmic reticulum.

2.2.14.6. Protein-protein interaction

One of the applicability of FRET is in protein interactions studies. To this aim, the proteins, which are under research, tagged with fluorescence proteins (like CFP and YFP, which are capable to trigger FRET signal in proper distance). Binding of the proteins bring fluorescent tags in close distance and induce FRET. In this study, STIM1-YFP and STIM1-CFP were co-expressed in EA.hy926 and protein interaction was visualized using FRET between fluorescence tags (CFP and YFP). $(F_{535}/F_{480})/F_0$ was evaluated as interaction between proteins cloned with these tags.

For STIM1-STIM1 interaction study, STIM1-CFP and STIM1-YFP were expressed simultaneously. Cells were excited at 440±21 nm (440AF21, Omega Optical,

Brattleboro, VT) and emission was collected simultaneously at 535 (FRET channel, Omega Optical) and 480 nm (CFP channel, Omega Optical) using an optical beam splitter (535 and 480 nm, Dual-View MicroImager, Optical Insights, Visitron Systems) as described previously (Frieden *et al.,* 2002). To correct the decay in the F_{535}/F_{480}, the STIM1 dimerization was expressed as the ratio of $(F_{535}/F_{480})/R_0$.

2.2.15. Single mitochondria motility measurement

To quantify the single mitochondrial motility in EA.hy926, a journal designed by Malli, R. The following step performed in this journal:

1. A time – lapse series of image recorded by ASLCM with 1 second interval.
2. All the image planes were subtracted from background.
3. To omit effect of bleaching, and noises, a threshold was defined.
4. All the image planes were binerized.
5. A region of interest (ROI) was selected in a way that covered the space of one single mitochondria movement through all the planes. There should not be any interference of other mitochondria in this space.
6. The software recorded the X and Y value of middle point of the single mitochondria in each plan and transfer them to the excel sheet.
7. Using the X and Y values, the distance, the mitochondrion moves in each plan, calculated in Excel software.

2.2.16. Mitochondrial membrane potential ($\Delta\psi_m$)

Mitochondrial membrane potential ($\Delta\psi_m$) measured as it has performed by Trenker (Trenker *et al.*, 2007).

Cells expressing mAKAP-RFP-CAAX or mitochondria-targeted DsRed (mtDsRed) were treated with 40 nm JC-1 on the ACLSM using perfusion system. JC-1 was continuously present throughout all the experiments to hinder possible leakage of the potentiometric dye. JC-1 was excited with the 488 nm Ar-laser line and emission was recorded every 800 ms at 535 nm. The average intensity of the JC-1 fluorescence in mitochondrial

regions (F_{mito}), was divided by the average intensity of the JC-1 fluorescence in a region that was at least 3 μm away from these organelles (F_{cyto}). The F_{mito}/F_{cyto} ratio was used to asset changes in ψ_{mito}. In order to control the accuracy of experiment, after 7 min a combination of FCCP/oligomycin was used.

2.2.17. Imaging devices

For Ca^{2+} measurements in cytosol, mitochondria, and endoplasmic reticulum and also, for protein-protein interaction measurement (FRET) a deconvolution microscope consists of a Nikon inverted microscope (Eclipse 300TE,Nikon, Vienna) equipped with CFI Plan Flu or 40x oil immersion objective (NA 1.3;0.171 μm pixel-1, Nikon, Austria) was used. This system includes an epifluorescence system (150W XBO; Optiquip, Highland Mills, NY, USA), a computer controlled z-stage (Ludl Electronic Products, Haawthrone, NY, USA) and a liquid-cooled CCD camera (-30 °C; Quatix KAF 1400G2,Roper Scientific, Acton, MA, USA). Excitation wavelengths were selected using a computer controlled filter wheel (Ludl Electronic Products, Haawthrone, NY, USA). All devices were controlled: by Metafluor 7.6 (Visitron Systems, Puchheim, Germany)
For colocalization, motility, membrane potential and focal contacts Imaging, cells transfected with YFP-tagged proteins and/or mtDsRed or mAKAP-RFP-CAAX were monitored in performing z-scans or time-lapse experiments using a Nipkow-disk-based array confocal laser scanning microscope (ACLSM; Malli *et al*., 2003). The ACLSM was built on a Zeiss Axiovert 200M (Zeiss Microsystem, Jena, Germany) equipped with VoxCell Scan® (VisiTech, Sunderland, UK), a 150 mW Ar- laser (laser Physic; West Jordan, UT, USA) and controlled by Metamorph 6.2r6 (Universal imaging, Visitron System, Puchheim, Germany). Fluorescent proteins were imaged with a 100 x or 63 x objective (α Plan-Fluar 100 x (or 63 x)/ 1.45 oil objective, Zeiss Microsystem, Jena, Germany). The YFP probe targeted to the protein of interest was excited using the 488 nm Ar-laser line. The emitted light was filtered at 535 nm using an emission filter 535/30 (Chroma Technology Corp, Rockingham, VT, USA), which was mounted in a computer-controlled fast filter wheel (Ludl, Electronic Products, Hawthrone, NY, USA). The mtDsRed or mAKAP-RFP-CAAX probe was imaged with the 100 x or 63 x objectives as previously described and excited using the 514 nm Ar-laser line. The emitted light was

filtered at 570 nm with the emission filter E570LPv2 (Chroma Technology Corp., Rockingham, VT, USA), that was mounted as aforementioned. Zscans were performed in z-intervals of 0.1 µm between the planes. Mitochondrial motility was recorded in time-lapse experiments between 600 and 780 seconds by taking an image each second after 1000 ms exposure time. All the data were collected using a fluorescence microscope (Zeiss Axiovert 100/AxioObserver, Zeiss, Vienna, Austria) under controlling of Metaflour 7.6 (Malli *et al*., 2005; Trenker *et al*., 2007).

2.2.18. 3-Dimensional analyses

A Z-scan image series (form bottom to top) were recorded from the cells which were co-transfected with $D1_{ER}$ and mAKAP-RFP-CAAX (or mitochondria-targeted DsRed as controls) using a Nipkow-disk-based array confocal laser scanning microscope (ACLSM). The ACLSM details have been mentioned in imaging devices. The green fluorescent probe targeted to the ER (i.e. $D1_{ER}$) and the red fluorescence of RFP were alternatively imaged with a 100 x objective (α Plan-Fluar 100 x / 1.45 oil objective, Zeiss Microsystems, Jena, Germany) using the 488 nm and 514 nm Ar-laser lines for illumination. Z-interval between the planes was 0.1 µm. The emitted light was filtered at 535 nm and 570 nm using two different emission filters (535/30 and E570LPv2, Chroma Technology Corp., Rockingham, VT, USA), which were mounted in a computer-controlled fast filter wheel (Ludl, Electronic Products, Hawthrone, NY, USA). In the next step $D1_{ER}$ flourophore was bleached by exposing the cell to laser beam. After a few minutes mitochondria in mAKAP-RFP-CAAX expressing cells, were stained with MitoTracker® Green, and a new time series was recorded (with the same Z-interval between planes). The ER and mitochondria z-stacks were deconvoluted using the quick maximum likelihood estimation algorithm (QMLE) of Huygens 2.4.1p3 (SVI, Hilversum, Netherlands). Subsequently co-localisation analysis, were performed with Imaris 3.3 software (Bitplane AG, Zürich, Switzerland). Focal contacts between ER and mitochondria were defined as the percentage values of voxels (volume pixels) that contained both fluorescent proteins, which were obtained from the co-localisation analysis module in Imaris 3.3. Co-localization images were taken from the same Z-scan records (Trenker *et al*., 2007).

2.2.19. Statistics ananlysis

Analysis of variance (ANOVA) and Dunnett's Multiple Comparison Test were used for the analysis. $p < 0.05$ was determined to be significant.

3. Result

It is known that mitochondria have a controlling role on Ca^{2+} entered upon store depletion. However, until recently there was no information about molecular mechanism of the entering pathways upon SOCE dependent Ca^{2+} entry. Discovering of STIM1-Orai1 as the main components of SOCE was a motivation for this study to test the effect of mitochondria on STIM1-Orai1 specific store-operated Ca^{2+} entry. In addition, we tried to understand whether some typical characteristics of mitochondria including motility and proximity of mitochondria to the channels play a role in this Ca^{2+} entry.

3.1. SOCE is a collaborative effect of channels and exchanger

In the first step of this study the elements, which play a role in Ca^{2+} influx after readdion of Ca^{2+} upon depletion of ER were investigated. To this aim, the key elements that so far have been proposed by literature that are involved in Ca^{2+} entrance upon store depletion were checked.

3.1.1. Role of Na^+ /Ca^{2+} exchanger in Ca^{2+} entry upon SOCE activation

As it is generally accepted, NCX_{pm} is one of the main candidates in the extrusion of Ca^{2+} to extracellular space upon cell stimulation. Therefore this exchanger was manipulated using different concentration of Na^+.

Application of different concentration of extracellular Na^+ (138 and 19 mM) showed that Na^+/Ca^{2+} exchanger in plasma membrane play a role in Ca^{2+} entry (figure 3.1). EA.hy926 cells were stimulated with histamine and BHQ and then 2 mM Ca^{2+} readded. All the experiments were performed under two different concentration of Na^+. Upon release of Ca^{2+} from ER, there was a fast but transient increase in the Ca^{2+} of cytosol under both low and high concentration of Na^+ (data was not included in the figure 3.1). However, upon readdition of Ca^{2+} and under high concentration of Na^+ (138 mM), presumably, Na^+ loaded in the cell via TRP channels that in turn favored NCX_{pm} in reverse mode. Therefore, NCX_{pm} took up Ca^{2+} and extruded Na^+ out of the cell. In low concentration of Na^+, NCX_{pm} worked in forward mode and therefore involved in Ca^{2+}

extrusion. Upon less concentration of extracellular Na^+, the level of Ca^{2+} that entered to the cell reduced for almost 30 %. Thus, reduction of extracellular Na^+ reduces i) subplasmalemmal Na^+ loading (Paltauf-Doburzynska, 2000) and ii) counteracts with reversal mode of NCX_{pm}.

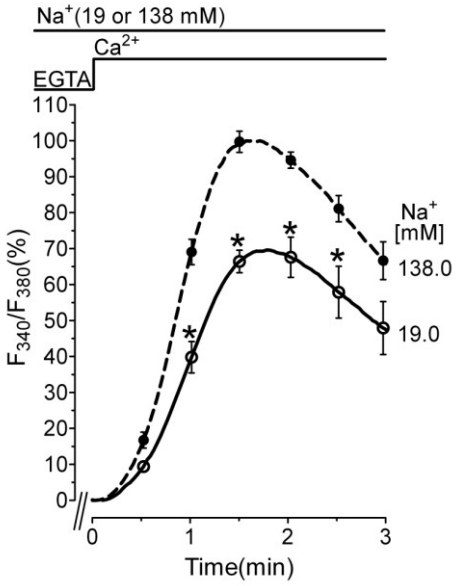

Figure 3.1: Contribution of plasma membrane Na^+/Ca^{2+} exchanger in Ca^{2+} entrance upon $[Ca^{2+}]_{cyto}$ increase after Ca^{2+} readdition to ER Ca^{2+} depleted cells. Cytosolic signals were measured using cells loaded with fura2/AM and presented as F_{340}/F_{380}. Cells were stimulated using 100 µM histamine and 15 µM BHQ in the absence of extracellular Ca^{2+} (1 mM EGTA) and later 2 mM Ca^{2+} added. Curves are averages of florescence signals from control cells (normalized to 100 percents) in the presence of 138 mM Na^+ (dotted line filled symbols n = 13) or from cells treated with low Na^+ (19 mM) buffer (continuous black line open symbols n = 13) which presented as the percent of control curve. *P<0.05 vs. the respective compared data set.

3.1.2. Role of TRPC family member in Ca^{2+} entry upon SOCE activation

To test the effect of TRP channels in Ca^{2+} influx into the cells, EA.hy926 cells were transfected with N-TRPC (N-dominant negative mutant of TRPC3 family) (figure 3.2). ER was completely depleted using histamine and BHQ in the absence of Ca^{2+} and with low

Na^+ buffer, later Ca^{2+} readded. Expression of the N-dominant negative mutant of TRPC3 family did not affect cytosolic Ca^{2+} increase upon ER Ca^{2+} release. However, it reduced 50 % of the Ca^{2+} influx into the cell upon store depletion and thus was proposed as a contributor in Ca^{2+} entrance to the cell.

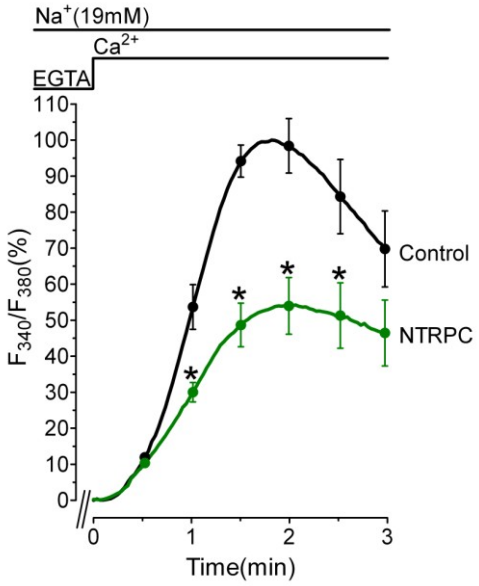

Figure 3.2: Contribution of TRPC channels in Ca^{2+} influx upon Ca^{2+} readdition after ER depletion. Cytosolic signals were measured using fura2/AM and presented as F_{340}/F_{380}.ER Ca^{2+} was depleted using 100 µM histamine and 15 µM BHQ and later 2 mM Ca^{2+} readded. To omit the effect of NCX_{pm} in reverse mode, all the experiments were in the present of low Na^+ (19 mM). Curves are averages of florescence signals from control cells (normalized to 100 %) in the presence of 138 mM Na^+ (dotted line filled symbols n = 13) or from cells treated with low Na^+ (19 mM) buffer (continuous black line open symbols n = 14) which presented as the percent of control curve.*P<0.05 vs. the respective compared data set.

3.1.3. Role of STIM1 and Orai1 as the main players of SOCE

Many reproducible studies in different laboratories introduce STIM1 and Orai1 proteins as the main elements of SOCE. These proteins were detected in our cell model,

EA.hy926 cells, at the level of mRNA by RT-PCR (figure 3.3) (Experiment performed by Markus Waldeck-Weiermair).

In addition, functionality of these proteins was tested using real-time-quantitative-PCR (RTq-PCR) versus a non-functioning siRNA Control (figure 3.4) (Experiment performed by Ismene Fertschai).

To test the contribution of STIM1 and Orai1 on Ca^{2+} influx after readdition of Ca^{2+} upon store depletion, cells transfected simultaneously with siRNAs against these two proteins. ER was completely depleted using histamine and BHQ in free Ca^{2+} EGTA containing buffer and later Ca^{2+} readded. To omit the effect of NCX_{pm} in reverse mode, low concentration Na^{+} buffer was applied in the experiment. While knockdown of these two proteins did not have any effect in cytosolic Ca^{2+} increase upon Ca^{2+} release from ER, the SOCE induced Ca^{2+} influx signal decrease to 50 % of that in control (figure 3.5).

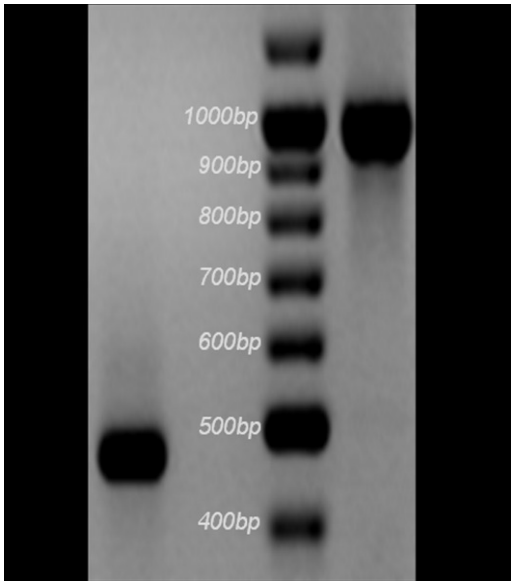

Figure 3.3: Detection of mRNA for hSTIM1 and hOrai1 in EA.hy926 cells.

The mRNA of hSTIM1 and hOrai1 was detected using RT-PCR (see methods).

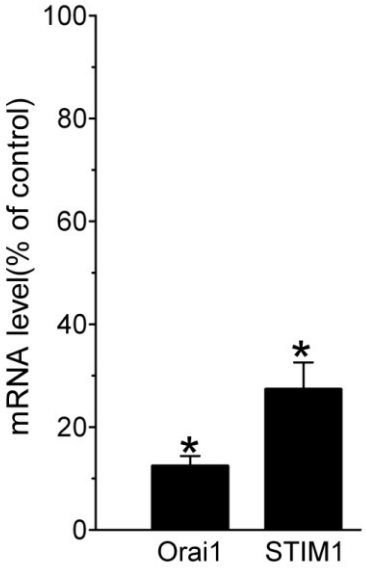

Figure 3.4: Knock-down efficiency of functional siRNAs against human Orai1 and human Stim1. n for all conditions including hOrai1, hStim1 and AllStar Neg. Control siRNA were three (see methods). *P<0.05 vs. the respective compared data set.

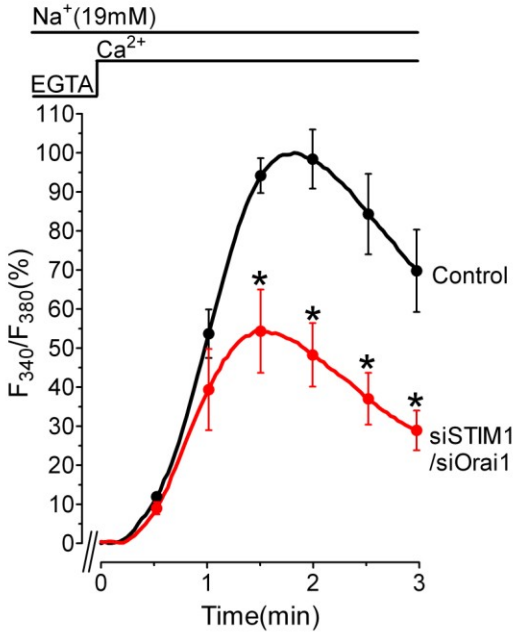

Figure 3.5: Effect of STIM1 and Orai1 knockdown in Ca^{2+} entry upon Ca^{2+} readdition after ER depletion. Cytosolic signals were measured using fura2/AM and presented as F_{340}/F_{380}. ER Ca^{2+} was depleted using 100 µM histamine and 15

μM BHQ and later 2 mM Ca^{2+} readded. All the experiments were in the present of low Na^{+} (19 mM). Curves are average of florescence intensity recorded from control cells (black line n = 13) which is normalized as 100 % and siRNA treated cells, (red line n = 11) which presented as the percent of control. *P<0.05 vs. the respective compared data set.

To test the cumulative effect of elements tested above, N-TRP expression and treatment for siRNA against STIM1 and Orai1 were performed concurrently and under low concentration of Na^{+} (figure 3.6). Cells were stimulated using histamine and BHQ in EGTA containing low concentration of Na^{+}, free concentration of Ca^{2+} and subsequently Ca^{2+} readded. As figure 3.6 shows, inhibition of Ca^{2+} entrance pathways including NCX_{PM} (in reverse mode), TRPC3 families and SOC channels (STIM1-Orai1 dependent pathway), reduced Ca^{2+} entry to almost 20 % of control.

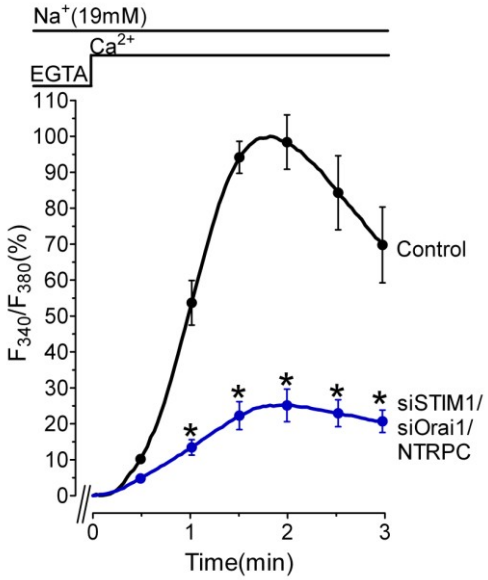

Figure 3.6: Effect of N-TRPC expression in the STIM1 & Orai1 knockdown cells in Ca^{2+} entry upon Ca^{2+} readdition after ER depletion. Cytosolic signals were measured using fura2/AM and presented as F_{340}/F_{380}. ER Ca^{2+} was depleted using 100 μM histamine and 15 μM BHQ and later 2 mM Ca^{2+} readded. All the experiments were in the present of low Na^{+} (19 mM). Curves are average of florescence intensity recorded from control cells (black line n = 13) which is normalized as 100 % and

siRNA treated cells which express N-TRPC, (blue line n = 8) which presented as the percent of control. *P < 0.05 vs. the respective compared data set.

Application of siRNA against STIM1 and Orai1 in our cell model showed that these proteins are involved in SOC entry. Prior to more investigation about STIM1-Orai1 dependent SOCE, we studied the mechanism of function of STIM1 as a sensor for ER Ca^{2+}.

components involved in Ca^{2+} entry upon Ca^{2+} readdition to prestimulated cells	Involvement level of the components (%)
NCX_{pm} in reverse mode	≈ 20
TRPC family	≈ 20
STIM1 and Orai1 dependent pathway	≈ 50

Table 3.1. Different components involved in Ca^{2+} entry upon Ca^{2+} readdition to prestimulated cells and the quantity of their involvement in this phenomenon.

3.2. STIM1 oligomerization in EA.hy926 cells

To investigate the pattern of STIM1 function, EA.hy926 cells were transiently transfected with STIM1-YFP. Localization of STIM1 was investigated prior and after histamine application (figure 3.7). As the figure shows, prior stimulation, STIM1 proteins had a homogenous distribution (a), but upon maximal ER depletion using 100 μM histamine and 15 μM BHQ in the absence of Ca^{2+} (1 mM EGTA), they oligomerized and aggregated to form clusters.

To quantify STIM1 dimerization and test the function of this protein as endoplasmic reticulum sensor, STIM1-YFP and STIM1-CFP were co-transfected in EA.hy926 cells. The fluorescent intensity from FRET signal between YFP and CFP was normalized (Δ max as 100 %) and considered as the amount of STIM1s interaction. The level of STIM1 dimerization compared with ER depletion level, which measured using cells co-expressing $D1_{ER}$ and STIM1-YFP (figure 3.8). There was a close correlation between ER depletion and STIM1 clustering. Depletion of ER and STIM1 clustering were

recorded almost at the same time course. However, STIM1 clustering was much faster than ER full depletion. 50 % of ER depletion was enough to exert maximal clustering of STIM1, thus indicating that the sensitivity of STIM1 to dimerize is very high in regard of ER depletion.

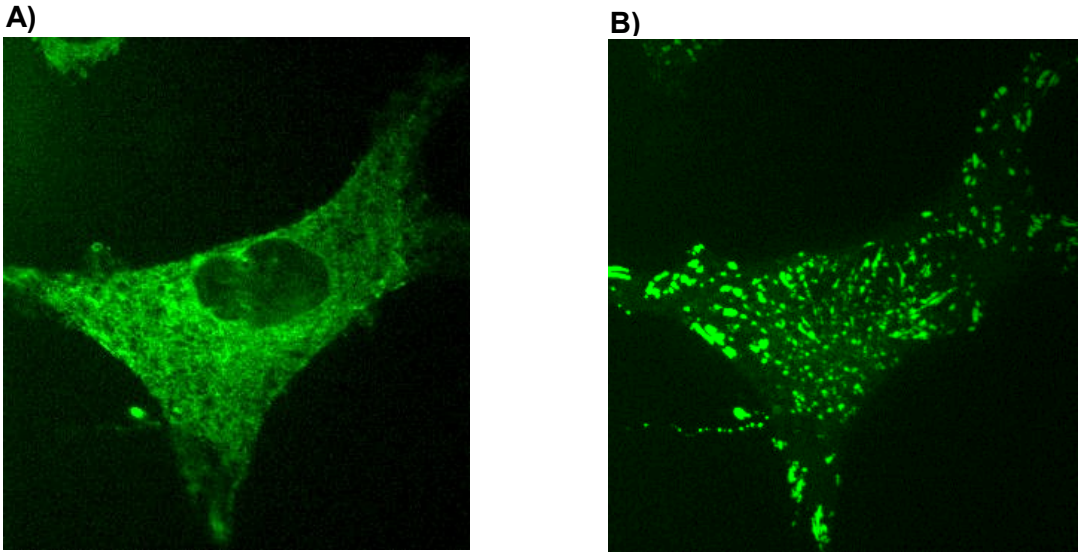

Figure 3.7: Visualization of STIM1-YFP before (A) and after (B) stimulation.
Cells transiently transfected with STIM1-YFP, stimulated with 100 µM histamine and 15µM BHQ in EGTA containing free Ca^{2+} buffer.

In addition, to test STIM1 clustering and its correlation with the amount of ER depletion, cells were transfected with STIM1-YFP and STIM1-CFP (simultaneously) or $D1_{ER}$ and STIM1-YFP. STIM1 clusters were investigated using different concentrations of histamine (10, 30 and 100 µM) followed by a combination of 100 µM histamine and 15 µM BHQ in the absence of extracellular Ca^{2+} (1 mM EGTA). Under these conditions, as figure 3.9.A shows, 10 µM histamine, only partially depleted ER, however, 30 µM and 100 µM histamine depleted ER faster and more remarkable. At the end of each experiment, maximal ER depletion was achieved by addition of 100 µM histamine and 15 µM BHQ. In all the cases, STIM1 clustering correlated to the level of ER depletion (fig 3.9.B). Applying 10 µM histamine triggered a diminutive STIM1 clustering. 30 µM

histamine application lead to a moderate clustering which in some cases was closed to the maximal level of clustering which achieved upon 100 µM histamine application. This set of data showed that in our cell model, STIM1 dimerized upon depletion of the store and the amount of this dimerization had a direct relation with the amount of store depletion. Moreover, maximum depletion of ER by using a combination of 100 µM histamine and BHQ triggered the highest level of clustering in all conditions.

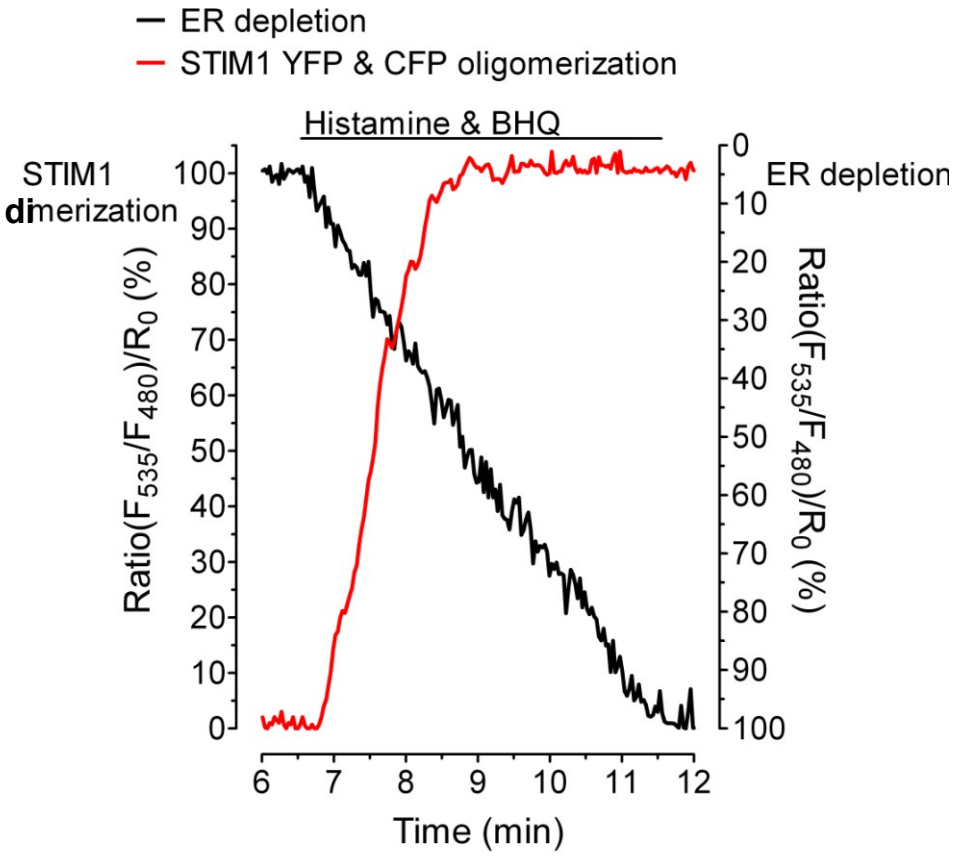

Figure 3.8: Comparison of the time course of STIM1 dimeraization with that of ER depletion. Cells were transiently trasnfected with STIM1-YFP and -CFP and their interaction measured using FRET and presented as the Ratio $(F_{535}/F_{480})/R_0$. ER release was measured in the cells overexpressing STIM-YFP and ER targeted cameleon ($D1_{ER}$) and presented as the Ratio $(F_{535}/F_{480})/R_0$. Maximum dimerization of STIM1 and maximum depletion of ER, were achieved using 100 µM histamine and 15 µM BHQ in EGTA containing free Ca^{2+} buffer and were presented as 100 %. Red

trace is a representative of florescence intensity recorded from STIM1- STIM1 interaction (n = 9) and black trace is a representative florescence intensity recorded from ER release (n = 10).

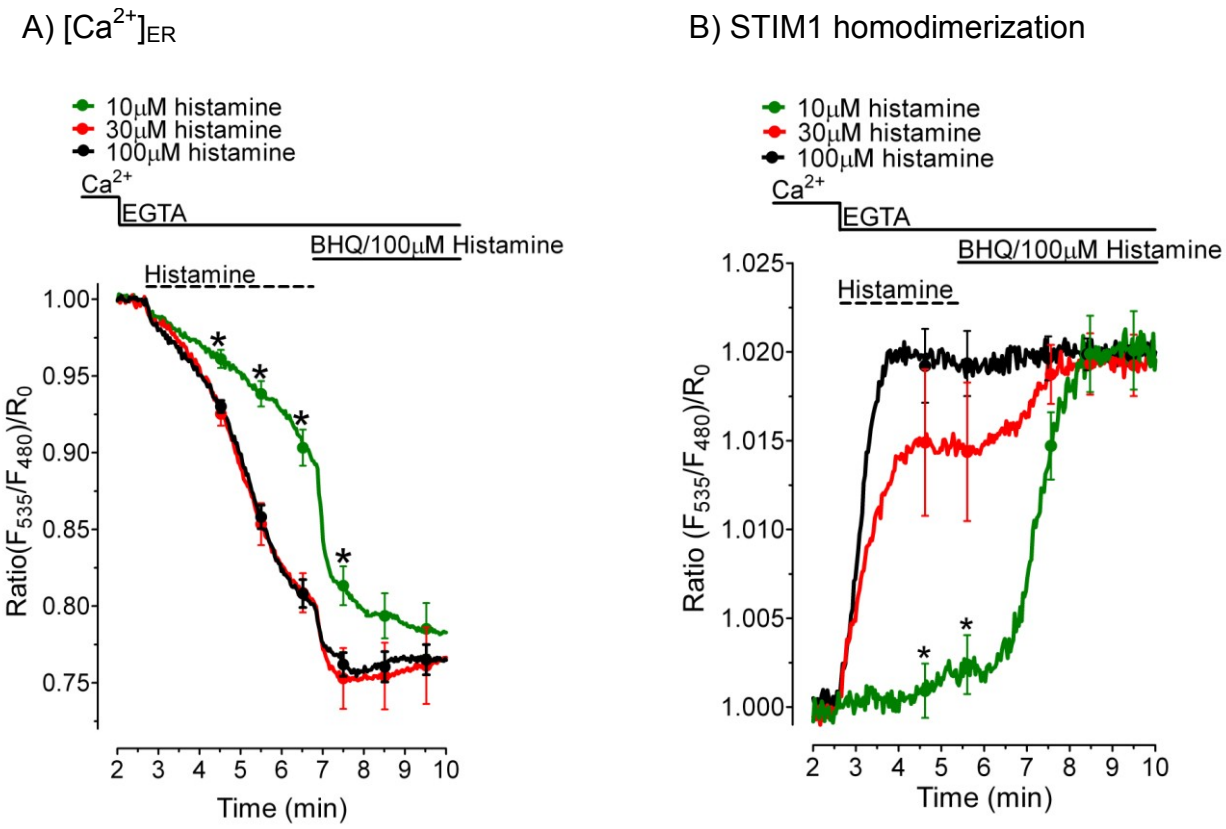

Figure 3.9: Effect of different concentrations of histamine on ER Ca^{2+} depletion and STIM1 dimerization. (A) Cells transiently transfected with STIM1-YFP and cameleon targeted to ER ($D1_{ER}$). ER Ca^{2+} depleted using 10, 30 or 100 μM histamine which followed by exhaustive depletion of ER with 100μM histamine and 15 μM BHQ in free Ca^{2+} EGTA containing buffer. Traces are average curves from FRET signal presented as the Ratio $(F_{535}/F_{480})/R_0$ and recorded from cells stimulated with 100 μM (black, n = 8), 30 μM (red, n = 7) and 10 μM (green, n = 6) histamine. *P<0.05 vs. cells stimulated with 100 μM histamine (Black trace)

(B) Cells transiently transfected with STIM1-YFP and -CFP and stimulated using 10, 30 or 100 μM histamine and followed by exhaustive depletion of ER with 100 μM histamine and 15 μM BHQ in free Ca^{2+} EGTA containing buffer. Traces are average curves from FRET signal presented as the Ratio $(F_{535}/F_{480})/R_0$ and recorded from

cells stimulated with 100 μM (black, n = 8), 30 μM (red, n = 6) and 10 μM (green, n = 6) histamine. *P<0.05 vs. cells were stimulated with 100 μM histamine (Black trace).

As it already indicated, application of siRNA against STIM1 and Orai1 showed that these proteins are involved in SOCE phenomenon in our cell model. To check mitochondrial effect on this phenomenon, mitochondrial function efficiency was manipulated and the effect of this manipulation on STIM1 and Orai1 dependent SOCE was studied. To reach this aim, first the effect of overexpression of these components in SOCE in our cell model was tested.

3.3. Effect of STIM1 and Orai1 overexpression on cytosolic and ER Ca^{2+} in endothelial cells

Cells were transiently transfected with STIM1, Orai1 or STIM1 and Orai1. To investigate SOCE, ER was depleted and then Ca^{2+} readded.

As figure 3.10 A shows, application of histamine and BHQ released Ca^{2+} from ER, which leads to a transient Ca^{2+} elevation in the cytosol. There was no difference in the amplitude and kinetic of this Ca^{2+} signal in the cells overexpressing STIM1 or Orai1 or STIM1 and Orai1 comparing with controls. In addition, there was no difference in the extrusion (decay) of the Ca^{2+} signal upon release. In readdition of Ca^{2+}, presence of BHQ kept endoplasmic reticulum empty and inhibited SOCE deactivation. Cells overexpressing STIM1 or Orai1 showed no difference for cytosolic Ca^{2+} increase versus controls. However, cells overexpressing STIM1 and Orai1 showed higher amplitude of Ca^{2+} signal in the cytosol comparing with that in control. Analyzing of the kinetic of the Ca^{2+} elevation signal showed that increase of Ca^{2+} in the cells overexpressing Orai1 is almost similar to that in control but in the cells, expressing STIM1 the velocity of uptake is slightly higher than controls.

In the cells overexpressing STIM1 and Orai1 the kinetics of elevation (R_{max}) is almost 4 times faster than control cells (figure 3.10 B). In parallel, we kept a track of Ca^{2+} homeostasis in ER upon overexpression of STIM1 as the main sensor of Ca^{2+} in ER.

Cells expressing STIM1 and cameleon targeted to ER ($D1_{ER}$) were prestimulated with histamine and BHQ in free Ca^{2+} EGTA containing buffer and compared with cells

expressing $D1_{ER}$ and mtDsRed as control. As figure 3.11 shows, to inhibit fast refilling of ER and better monitoring of this phenomenon, 0.3 mM and later 2 mM Ca^{2+} readded to the cells overexpressing STIM1 and the vector. Upon readdition of low concentration of Ca^{2+} (0.3 mM) to the cells overexpressing STIM1, ER refilled faster than control cells. However, increasing the concentration of extracellular Ca^{2+} achieved similar refilling amount in STIM1 overexpressing cells comparing control cells.

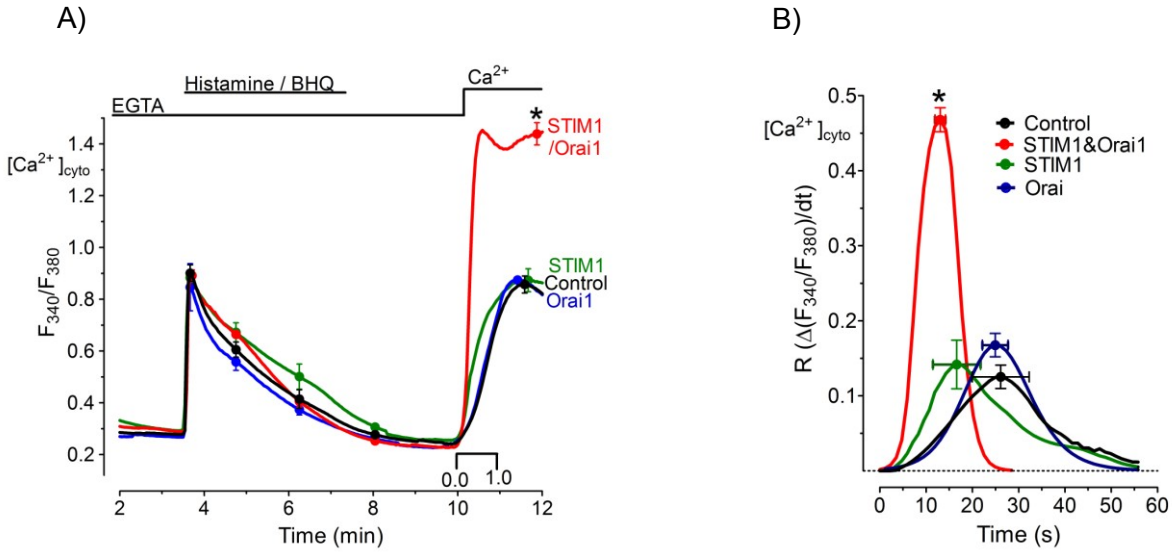

Figure 3.10: Effects of overexpression of STIM1 and Orai1 on $[Ca^{2+}]_{cyto}$ signals in endothelial cells. $[Ca^{2+}]_{cyto}$ signals were measured in fura-2/AM loaded cells.
(A) ER Ca^{2+} was depleted using 100 µM histamine and 15 µM BHQ in the presence of 1 mM EGTA. Later 2 mM Ca^{2+} was added which yielded SOCE-induced $[Ca^{2+}]_{cyto}$ increase in control cells (black trace n = 12), cells overxpressing STIM1 alone (green trace n = 12), Orai1 alone (blue trace n = 9), and both STIM1 and Orai1 proteins (red trace n = 22). *P<0.05 vs. control.
(B) Changes in the rate of Ca^{2+} influx upon readdition of Ca^{2+} after SOCE activation in one minute which expressed as $R(\Delta(1-F_{340}/F_{380})/dt)$. *P<0.05 vs. control

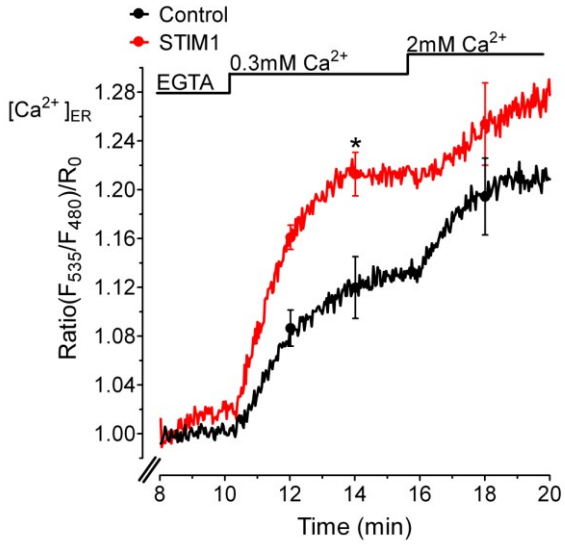

Figure 3.11: Effect of STIM1 overexpression on ER Ca^{2+} refilling. ER Ca^{2+} signals were obtained using a cameleon targeted to ER ($D1_{ER}$) and presented as the ratio $(F_{535}/F_{480})/R_0$. Cells were transefected with $D1_{ER}$ and STIM1-YFP or mtDsRed. ER Ca^{2+} was depleted using 100 µM histamine and 15 µM BHQ, and partially refilled with 0.3 mM Ca^{2+} and later 2 mM Ca^{2+} readded. Black curve is the average of florescence intensity recorded from control cells (n = 4). Red curve is average from florescence intensity recorded from cells overexpressing STIM1 (n = 12).

In addition, the effect of knockdown of the STIM1 and / or Orai1 in ER Ca^{2+} homeostasis was investigated (figure 3.12). Upon readdition of Ca^{2+} in the presence of BHQ, in all the conditions, ER refilled for around 40 %. Washing of BHQ triggered complete refilling which was almost similar in cells transfected with siRNA against STIM1 and Orai1, or cells transfected with siRNA against STIM1 comparing with cells transfected with All star Negative as control.

3.4. Effect of lanthanum on STIM1 and Orai1 mediated SOCE in the cells overexpressing STIM1 and Orai1

As it has been mentioned in literature, one of the specific inhibitors of SOCE is lanthanum (Bird *et al*., 2008). In an experiment, sensitivity of cytosolic Ca^{2+} signal upon SOCE activation and after readdition of Ca^{2+} was tested in the cells overexpressing

STIM1 and Orai1, in the absence and presence of Lanthanum. As the figure 3.13 shows, La^{3+} completely blocked the Ca^{2+} influx upon readdition of Ca^{2+} to prestimulated cells in both STIM1/Orai1 overexpressing and control cells. Washing of La^{3+} using EGTA buffer and readdittion of Ca^{2+} triggers Ca^{2+} influx into the cells, which in cells expressing STIM1 and Orai1 was significantly higher extent than control cells.

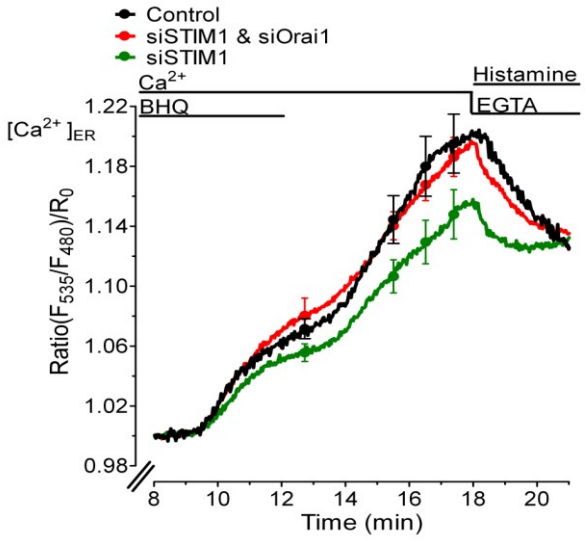

Figure 3.12: Effect of STIM1 and Orai1 knockdown on ER Ca^{2+} refilling. ER Ca^{2+} signals were obtained using a cameleon targeted ER ($D1_{ER}$) and presented as the ratio $(F_{535}/F_{480})/F_0$. Cells were transefected with $D1_{ER}$ and siRNA against STIM1 and Orai1 or All star Negative as control. ER Ca^{2+} was depleted using 100 µM histamine and 15 µM BHQ, and Ca^{2+} readded in the presence of BHQ and later BHQ washed out. Black curve is average of florescence intensity recorded from control cells (n = 7). Red curve is average of florescence intensity recorded from cells transefected with siRNA against STIM1 and Orai1 (n = 10). Green curve is average of florescence intensity recorded from cells transefected with siRNA against STIM1 (n = 10).

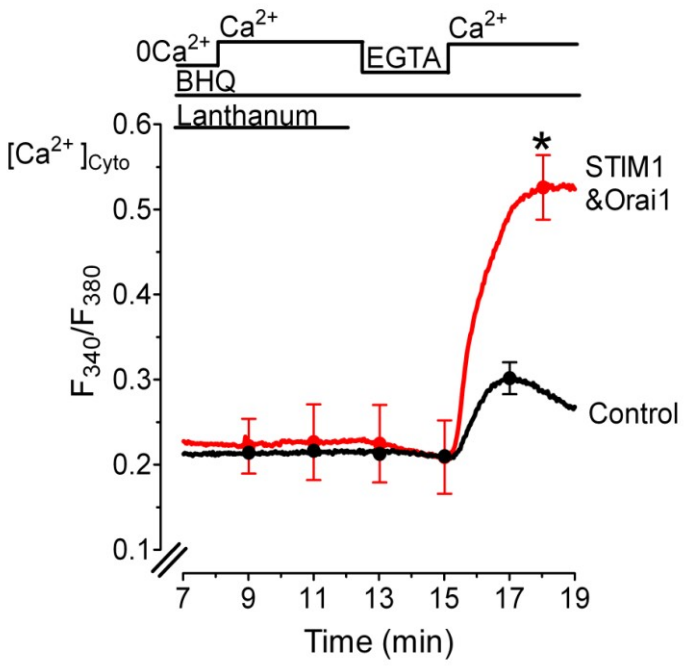

Figure 3.13: Effect of lanthanum (La^{3+}) on STIM1 and Orai1 dependent SOCE. Cytosolic Ca^{2+} signals were obtained using cells loaded with fura2/AM and presented as the F_{340}/F_{380}. Cells were transefected with STIM1 and Orai1 or mtDsRed as control. ER Ca^{2+} was depleted using 100 µM histamine and 15 µM BHQ, in free Ca^{2+} EGTA containing buffer. To block the inhibitory effect of EGTA on lanthanum, cells treated for two minutes with La^{3+} in free Ca^{2+} buffer and then Ca^{2+} readded in the presence of La^{3+}. After 4 minutes, La^{3+} washed out. Black curve is average of florescence intensity recorded from control cells (n = 10). Red curve is average of florescence intensity recorded from cells overexpressing STIM1 and Orai1 (n = 8).

3.5. Effect of mitochondria on SOCE phenomenon

It is believed that Ca^{2+} ions that entered to the cell upon SOCE activity have an inhibitory effect on the related channels (Hoth *et al.*, 1997).

Disrupting of mitochondrial Ca^{2+} sequestration by depolarization of mitochondrial membrane potential using FCCP and oligomycin decreased cytosolic Ca^{2+} influx upon depletion of the stores (figure 3.14) (Malli *et al*., 2003b). In addition, applying CGP 37157 as an inhibitor for NCX_{mito} decreased cytosolic Ca^{2+} influx upon readdition of the Ca^{2+} after depletion of the stores (figure 3.14). Consequently, it is speculated that

mitochondria uptake some part of Ca^{2+} ions which entered to the cell therefore, blocked the inhibitory role of Ca^{2+} on the channels.

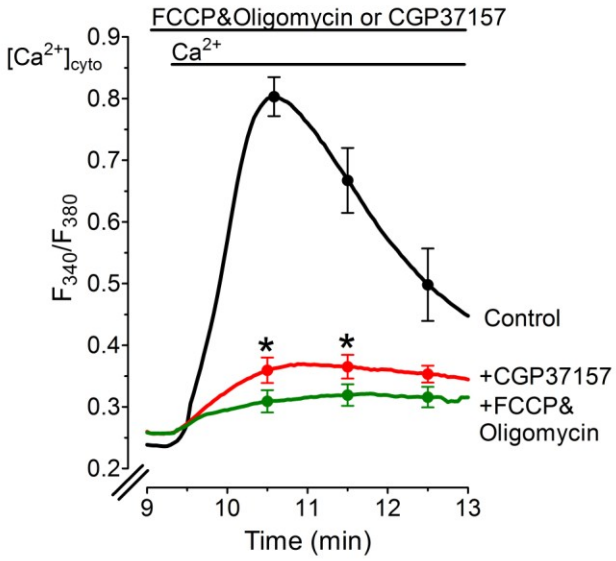

Figure 3.14: Effect of FCCP/oligomycin or CGP 37157 on SOCE – dependent Ca^{2+} entry. $[Ca^{2+}]_{cyto}$ signals were measured in fura-2/AM loaded cells. ER Ca^{2+} was depleted using 100 µM histamine and 15 µM BHQ in the absence of extracellular Ca^{2+} (1 mM EGTA) and later 2 mM Ca^{2+} added. 2 min before Ca^{2+} readdition, cells were treated using 2 µM FCCP and 2 µM oligomycin or 20 µM CGP 37157 and $[Ca^{2+}]_{cyto}$ signals were measured using fura2/AM. Black curve is average of florescence intensity of fura2/AM in control cells (n = 16), red curve is average of florescence intensity of fura2/AM of the cells treated with CGP 37157 (n = 11) and green curve is average of florescence intensity of fura2/AM for cells treated with FCCP and oligomycin (n = 7).*P<0.05 vs. control.

Figure 3.15 A and B shows the mechanism of the function of FCCP and oligomycin or CGP 37157 on mitochondrial Ca^{2+} uptake upon release of Ca^{2+} from ER and subsequent readdition of 2 mM Ca^{2+}, respectively. NCX_{mito} mostly involved in Ca^{2+} efflux of mitochondria in uptake upon ER release (A) and it works in reverse mode in Ca^{2+} uptake upon readdition of Ca^{2+} upon SOCE activation (B). As the result shows in control cells release of Ca^{2+} from ER (by histamine) make a transient signal in mitochondria, however treatment of the cell before stimulation with CGP 37157 leads to a Ca^{2+} signal

with less amplitude which sustained. In SOCE-induced Ca^{2+} influx, treatment of the cell with CGP 37157 decreased the mitochondrial Ca^{2+} uptake. Application of FCCP in both release from ER and influx from extracellular environment dramatically decreased the signal.

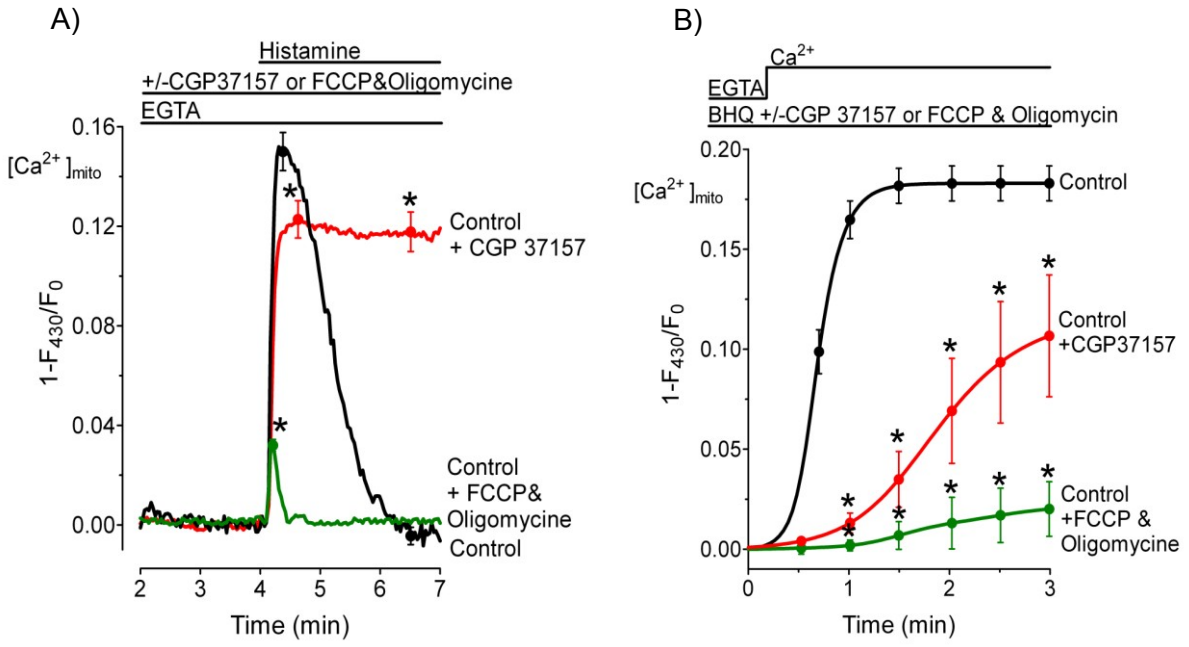

Figure 3.15: Effect of FCCP/oligomycin or CGP 37157 on mitochondrial Ca^{2+} signaling. Mitochondrial Ca^{2+} signals were measured using cells, which permanently express mt-RP. Florescence intensity of 430 nm was measured and data was normalized and presented as $1\text{-}F_{430}/F_0$. (A) Cells were stimulated using 100 µM histamine in the absence of extracellular Ca^{2+} (1 mM EGTA). Cells were treated with 2 µM FCCP and 2 µM oligomycin or 20 µM CGP 37157, 2 minutes before histamine application. Black trace is average for the florescent signal achieved from control cells (n = 20). Red trace is the average for the florescent signal of the cells treated with CGP 37157 (n = 16), and green traces is the average for the florescent signals achieved from the cells treated with FCCP/oligomycin (n = 16).*P<0.05 vs. control.
(B) ER Ca^{2+} was depleted with 100 µM histamine and 15 µM BHQ in the absence of extracellular Ca^{2+} (1 mM EGTA) and then 2 mM Ca^{2+} readded in the presence of 15 µM BHQ. Cells were treated with 2 µM FCCP and 2 µM oligomycin or 20 µM CGP 37157, 2 minutes before Ca^{2+} readdition. Black trace is the average for the florescent signal achieved from control cells (n = 20). Red trace is the average for the florescent

signal of cells treated with CGP 37157 (n = 12), and green traces is the average for the florescent signals achieved from cells treated with FCCP/oligomycin (n = 17).*P<0.05 vs. control.

To test the contribution of mitochondrial Ca^{2+} buffering function to special SOCE pathway including STIM1 and Orai1, we overexpressed these proteins and tested the mitochondria effect on the Ca^{2+} entry upon depletion of the store. Cells transiently were transfected with STIM1-YFP and Orai1-CFP or mtDsRed as control. ER fully depleted using 100 µM histamine and 15 µM BHQ in the absence of extracellular Ca^{2+} (1 mM EGTA) and subsequently 2 mM Ca^{2+} readded. In this, experiment cells treated with FCCP and oligomycin for 2 min before Ca^{2+} readdition. As figure 3.16 A and B show, depolarization of mitochondria decreased the Ca^{2+} influx to the cell upon depletion to 10 % of control. However, in STIM1 and Orai1 overexpressing cells, mitochondrial depolarization, partially (30 %) decreased the signal.

The result was similar when we applied CGP 37157 to block NCX_{mito}. As figure 3.16 C and D show blocking of NCX_{mito} using CGP 37157, decreased Ca^{2+} influx upon ER depletion in control cells (approximately 90 %) while in cells overexpressing STIM1 and Orai1, effect of CGP 37157 was trivial comparing to control (around 20 % decrease in CGP 37157 treated STIM1 and Orai1 overexpressing cells versus that cells without treatment).

As the results indicate, STIM1 and Orai1 pathway is less sensitive to FCCP and oligomycin or CGP 37157 comparing to control condition. Seemingly, the proportion of the number of functional channels to subplasmalemmal mitochondria decreases upon overexpression of the STIM1 and Orai1 proteins and therefore local mitochondrial buffering function does not play a major role. To test this idea, cells were transiently overexpressed with STIM1-YFP and mtDsRed and the proximity of STIM1 clusters and subplasmalemmal mitochondria were investigated upon ER depletion. As the result shows, upon depletion of ER using histamine and STIM1 clustering (3.17.A), only 13 % of STIM1 clusters colocalized with mitochondria.

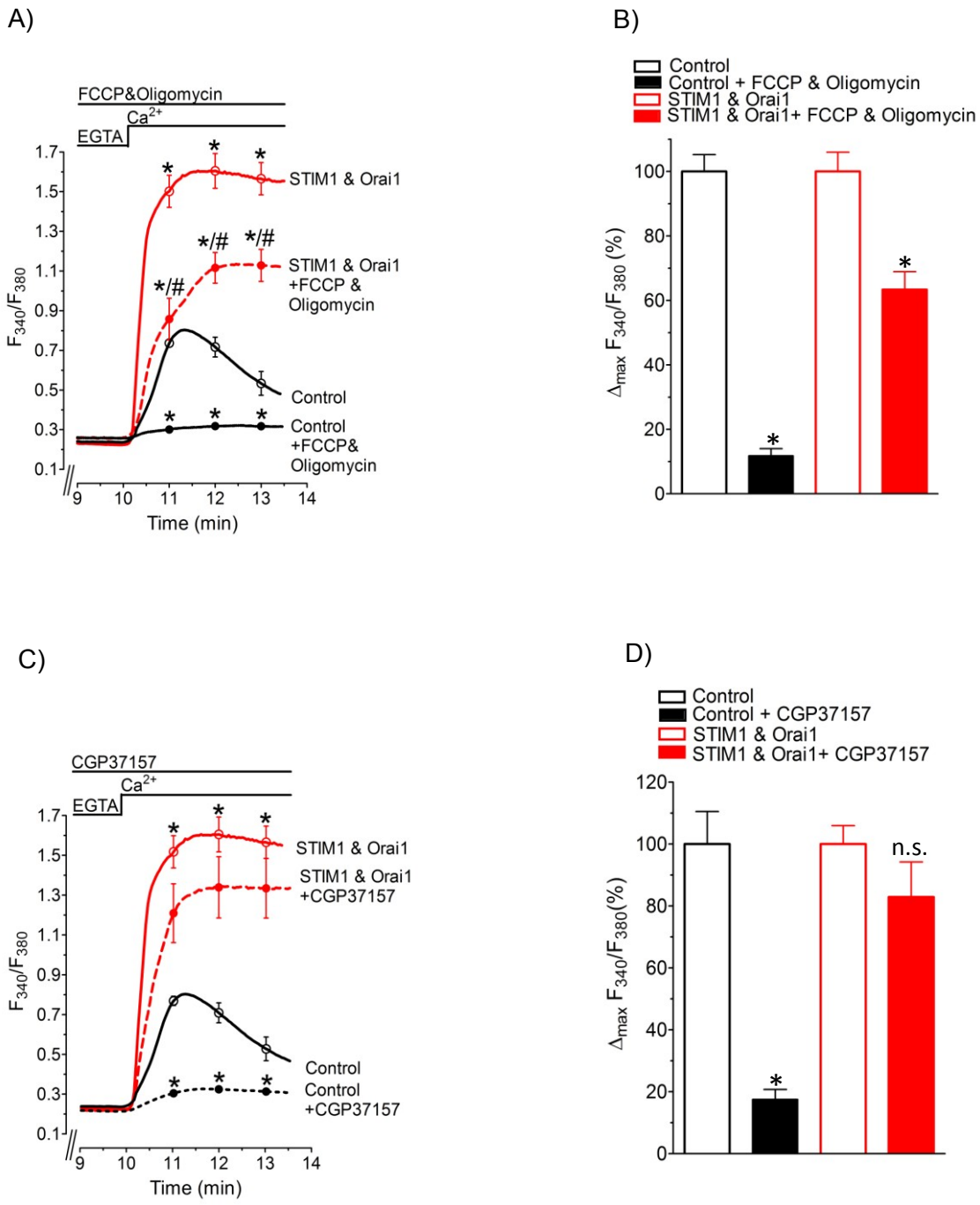

Figure 3.16: Effects of Ψ_{mito} depolarization and NCX_{mito} inhibition on SOCE-dependent Ca^{2+} entry in cells overxpressing STIM1 and Orai1. ER Ca^{2+} depleted using 100 µM histamine and 15 µM BHQ and then 2 mM Ca^{2+} readded. (A) SOCE induced $[Ca^{2+}]_{cyto}$ signals in control cells under control conditions (without FCCP and oligomycin, black continuous line n = 16) and upon Ψ_{mito} depolarization with 2 µM

FCCP and 2 µM oligomycin (black dotted line n = 11). Similar experiments were performed with cells overexpressing STIM1 together with Orai1 (red continuous line n = 19) and in the presence or absence of FCCP and oligomycin (red dotted line n = 12). *P<0.05 vs. control. #P<0.05 vs. STIM1 and Orai1 overexpressing cells without FCCP and oligomycin.

(B) Statistical analysis of maximal $[Ca^{2+}]_{cyto}$ signals presented in panel A. Control or overexpressing cells without treatment were presented as 100 % and treated groups was presented as percent of non treated groups.*P<0.05 vs. control.

(C) SOCE induced $[Ca^{2+}]_{cyto}$ signals in control cells under control conditions (without CGP 37157, black continuous line n = 16) and upon NCX_{mito} inhibition with 20 µM CGP 37157 (black dotted line n = 7). Analog experiments were performed with cells overexpressing STIM1 together with Orai1 under control conditions (red continuous line n = 19) and in the presence of CGP 37157 (red dotted line n = 9). *P<0.05 vs. the respective compared data set.

(D) Column graph presenting the delta max of the extent of Ca^{2+} influx upon Ca^{2+} readdition in the (C) panel, which is normalized in percent for control condition or STIM1 & Orai1 overexpressing cells.

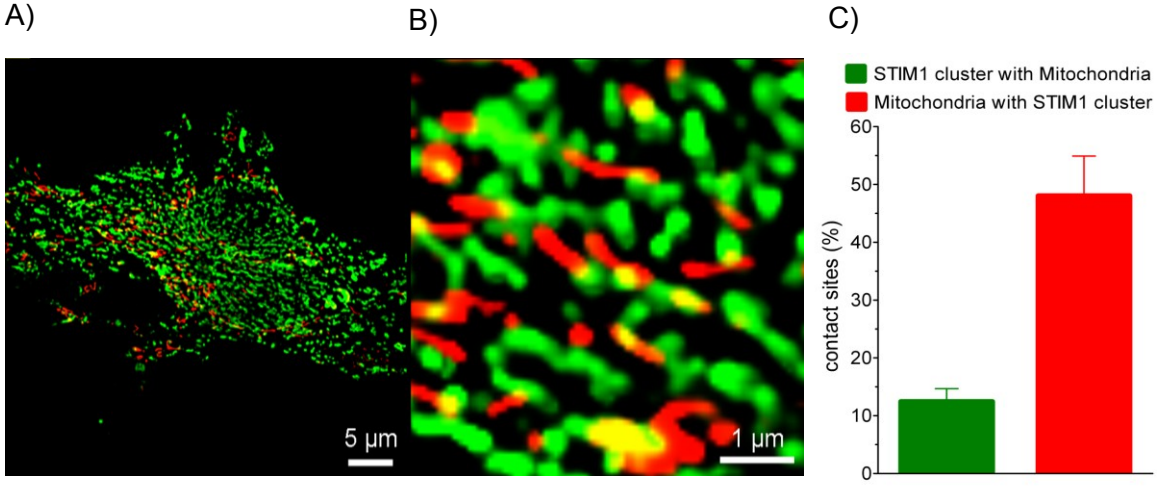

Figure 3.17: Analysis of contact sites between subplasmalemmal STIM1 clusters and mitochondria. High-resolution fluorescence microscopy of cells expressing YFP-STIM1 and mitochondrial targeted DsRed were used to assess the vicinity of mitochondria to subplasmalemmal STIM1 clusters. Prior to image

acquisitions, ER Ca^{2+} depletion was achieved by cell stimulation with 100 µM histamine and 15 µM BHQ in EGTA containing Ca^{2+} free solution.
(A) Representative endothelial cell with subplasmalemmal STIM1 cluster (green) and mitochondria (red). Image was taken with an ACLSM (see methods) at a z-position where the apical plasma membrane was in the focus.
(B) Zoomed section of subplasmalemmal STIM1 clusters (green), mitochondria (red) and merged areas (yellow) pointing to contact sites between mitochondria and STIM1 clusters.
(C) Statistic analysis of contact sites between STIM1 clusters and mitochondria (n = 7)

This result further supports the idea of less dependency of SOCE units upon STIM1-Orai1 overexpression to mitochondrial local buffering function.

Another interpretation of the result regarding insensitivity of the STIM1 and Orai1 overexpressing cells to the mitochondrial toxin would be the cooperation of two different mitochondrial entrance pathways; including mitochondrial membrane potential - dependent pathways and NCX_{mito} in reverse mode. In cell overexpressing STIM1-Orai1 and upon inhibition of one of these pathways, local increase of Ca^{2+} upon Ca^{2+} readdition boosts the alternative pathway and rescues the signal.

To test the possibility of different mitochondrial Ca^{2+} uptake contribution upon SOCE activation, we manipulated SOCE strength using different concentration of Ca^{2+} upon depletion of ER and we investigated mitochondrial Ca^{2+} uptake upon blocking one or both of these pathways by CGP 37157 (figure 3.18 B) or/and by FCCP and oligomycin (figure 3.18 C and D). In both mentioned conditions, there was a direct relation between concentration of Ca^{2+}, which was applied, and the rate and amplitude of mitochondrial Ca^{2+} uptake upon SOCE induction. By increasing the concentration of extracellular Ca^{2+} in Ca^{2+} readdition upon store depletion, kinetic and amount of the Ca^{2+} entered to the cells increased.

In the lowest concentration (0.5 mM), application of either FCCP and olgimycin or CGP 37157 abolished mitochondrial Ca^{2+} uptake.

In 2 mM concentration, of extracellular Ca^{2+}, which readded upon ER depletion, treatment with FCCP and oligomycin significantly decreased the mitochondrial Ca^{2+} uptake. However, in the same concentration, treatment the cells with CGP 37157 only

partially decreased the signal. This indicates that under physiological concentration of extracellular Ca^{2+}, FCCP and oligomycin - dependent pathways play the main important role. In higher concentrations (10 and 20 mM), despite of the application of either FCCP and oligomycin or CGP 37157, mitochondria is able to uptake Ca^{2+}. In addition, upon treatment the cells with FCCP and oligomycin, sensitivity of mitochondrial uptake upon Ca^{2+} readdition, decreased considerably comparing to control cells (figure 3.18 E). EC_{50} for mitochondrial Ca^{2+} uptake upon readdition after ER depletion using histamine for control cells was 1.02 (0.65 – 1.61) mM while in cells treated with FCCP and oligomycin was 8.24 (7.14 – 9.52). However, in the cells treated with CGP 37157, EC_{50} (2.00 (0.82 – 4.85) mM) did not change significantly comparing to control cells.

This data shows that there are two distinguishable mitochondrial Ca^{2+} uptake pathways and upon blocking one of those pathways, the second route is able to overtake the Ca^{2+} up taking role.

To further investigate two different uptake pathways, cells were stimulated with histamine and BHQ and subsequently, different concentration of Ca^{2+} readded. FCCP, oligomycin and CGP 37157 were applied simultaneously 2 minutes before Ca^{2+} readdition. As figure 3.18 D shows, in all concentration of Ca^{2+}, no detectable mitochondrial Ca^{2+} uptake was recorded. This data support our speculation toward the presence of two different mechanisms, which provide mitochondrial Ca^{2+} uptake. Interestingly, under total blocking of mitochondrial uptake and therefore blocking of mitochondrial Ca^{2+} sequestration, upon depletion of ER and subsequent readdition of high concentration (10 mM) of Ca^{2+} (figure 3.18 F), a large amount of Ca^{2+} entered to the cell and was detected in the cytosol.

This information clearly shows that there might be some Ca^{2+} influx pathways upon ER depletion, which are independent from mitochondrial buffering role.

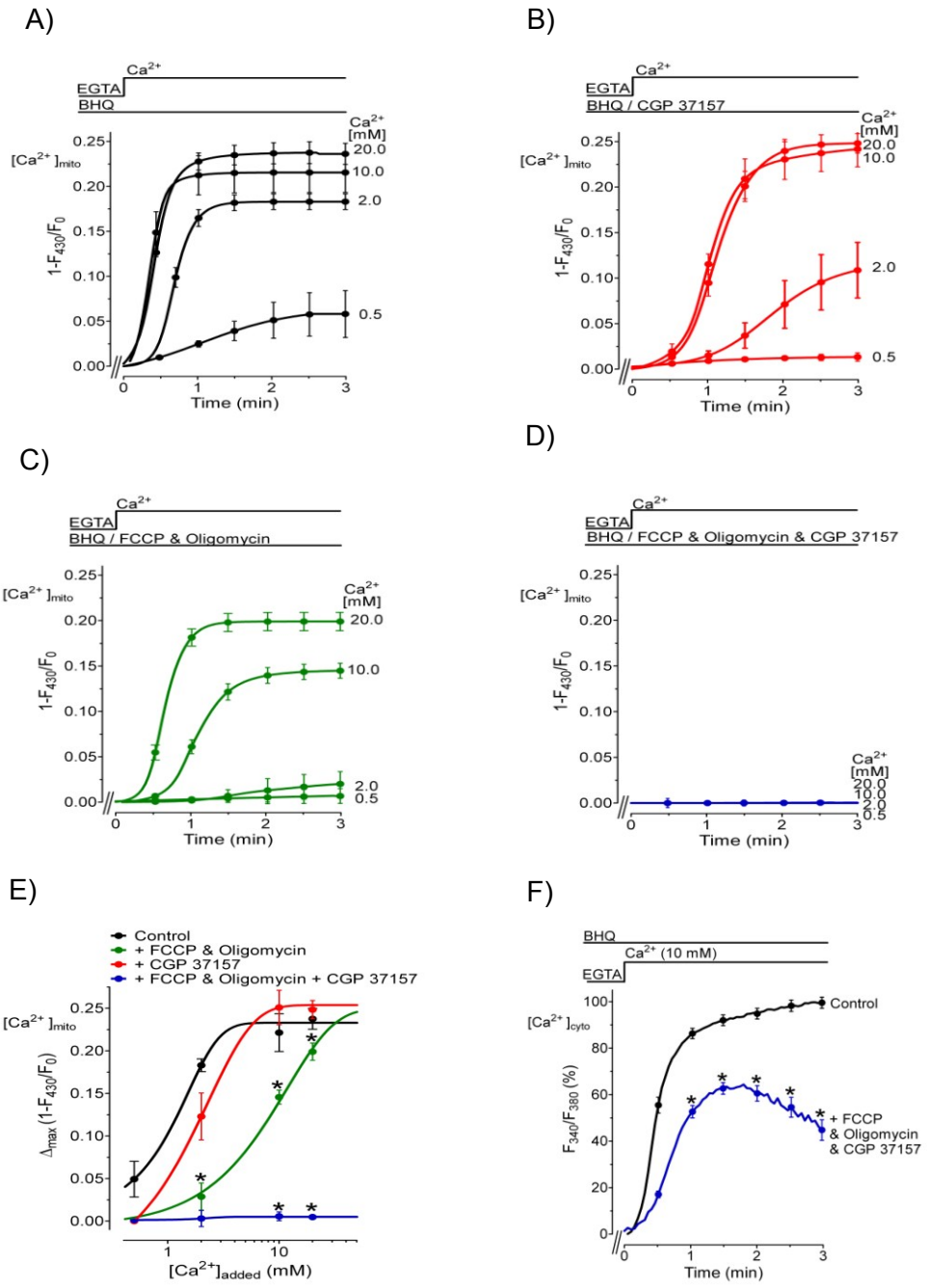

Figure 3.18: Analysis of mitochondrial Ca^{2+} uptake upon SOCE induced Ca^{2+} influx, which were achieved by the readdition of different Ca^{2+} concentrations to ER Ca^{2+} depleted cells and effects of Ψ_{mito} depolarization and NCX_{mito} inhibition on SOCE- induced $[Ca^{2+}]_{mito}$ and $[Ca^{2+}]_{cyto}$ signals. ER Ca^{2+} depletion was achieved by cell stimulation with 100 µM histamine and 15 µM BHQ in EGTA containing Ca^{2+} free solution. Subsequently different Ca^{2+} concentrations were added

in the presence of BHQ. $[Ca^{2+}]_{mito}$ signals upon Ca^{2+} readdition were measured in cells expressing RP-mt and $[Ca^{2+}]_{cyto}$ signals upon Ca^{2+} readdition were measured using fura2/AM.

(A) Mitochondrial Ca^{2+} uptake, $[Ca^{2+}]_{mito}$ increased upon the readdition of 20 mM (n = 8), 10 mM (n = 15), 2.0 mM (n = 20) and 0.5 mM (n = 6) Ca^{2+} to ER Ca^{2+} depleted cells.

(B) Mitochondrial Ca^{2+} uptake $[Ca^{2+}]_{mito}$ increased under conditions of Ψ_{mito} depolarization with 2 µM FCCP and 2 µM oligomycin upon the readdition of 20 mM (n = 17), 10 mM (n = 21), 2.0 mM (n = 17) and 0.5 mM (n = 8) Ca^{2+} to ER Ca^{2+} depleted cells.

(C) Mitochondrial Ca^{2+} uptake $[Ca^{2+}]_{mito}$ increased in the presence of 20 µM CGP 37157 upon the readdition of 20 mM (n = 6), 10 mM (n = 19), 2.0 mM (n = 12) and 0.5 mM (n = 9) Ca^{2+} to ER Ca^{2+} depleted cells. (D) SOCE-fueled $[Ca^{2+}]_{mito}$ increased under conditions of Ψ_{mito} depolarization with 2 µM FCCP and 2 µM oligomycin and NCX_{mito} inhibition with 20 µM CGP 37157 upon the readdition of 20 mM (n = 14), 10 mM (n = 13), 2.0 mM (n = 15) and 0.5 mM (n = 7) Ca^{2+} to ER Ca^{2+} depleted cells. (E) Concentration response curves of $[Ca^{2+}]_{mito}$ signal that were induced by the readdition of different Ca^{2+} concentrations to ER Ca^{2+} depleted cells as described in panels (A) to (D). (F) Ca^{2+} influx upon readdition of 10 mM Ca^{2+} to ER Ca^{2+} depleted cells, $[Ca^{2+}]_{cyto}$ in percentage of the control, under control conditions (black line n = 32) and in the presence of 2 µM FCCP, 2 µM oligomycin and 20 µM CGP 37157 (blue line n = 40). *P<0.05 vs. control.

3.6. STIM1 and Orai1 dependent Ca^{2+} uptake needs mitochondria for its function

We tested the functionality of the mentioned different pathways of mitochondrial uptake, and mitochondrial contribution in Ca^{2+} handling upon overexpression of STIM1 and Orai1. To this aim, cells were overexpressed with STIM1 and Orai1 proteins. They were stimulated by histamine and BHQ and subsequently 2 mM Ca^{2+} readded. To inhibit SOCE termination Ca^{2+} readded in the present of BHQ. Ca^{2+} influx upon ER depletion was recorded after depolarization of mitochondria using FCCP and oligomycin or blocking of NCX_{mito} using CGP 37157.

As figure 3.19 B shows, blocking of NCX_{mito}-dependent uptake pathway using CGP 37157, partially (25 %) decreased the signal. Inhibition of mitochondrial membrane

potential - dependent pathway using FCCP and oligomycin decreased the mitochondrial Ca^{2+} uptake more pronounced (60 %). Blocking both mitochondrial Ca^{2+} uptake completely abolished Ca^{2+} signal (to less than 5 %).

Finally, Ca^{2+} entry upon SOCE activity in the cell overexpressing STIM1-Orai1 was investigated (figure 3. 20).

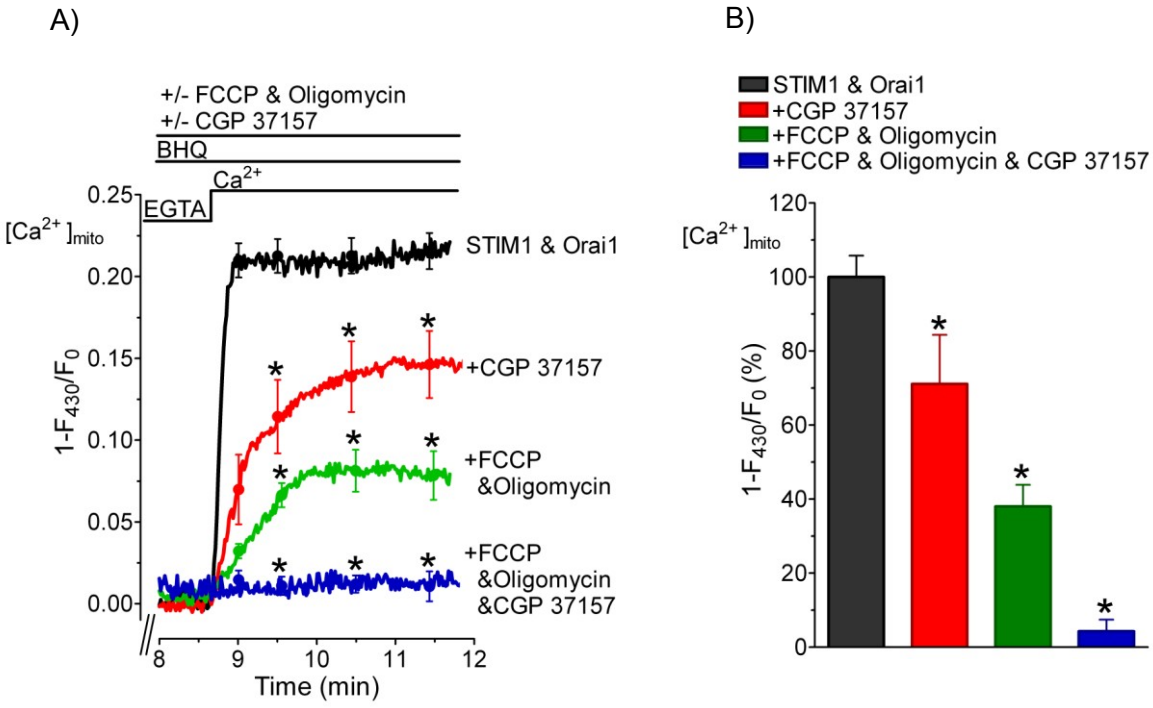

Figure 3.19: Effects of Ψ_{mito} depolarization and NCX_{mito} inhibition on mitochondrial Ca^{2+} uptake, $[Ca^{2+}]_{mito}$, upon SOCE activation in cells overexpressing STIM1 and Orai1. $[Ca^{2+}]_{mito}$ signals presented as $1\text{-}F_{430}/F_0$, were measured in cells overexpressing STIM1-Orai1 by imaging the fluorescence of mt-RP. SOCE mediated Ca^{2+} influx were induced by a readdition of 2 mM Ca^{2+} to ER Ca^{2+} depleted cells. (A) Mitochondrial signals recorded from STIM1-Orai1 overexpressing cells (black line n = 41), in the presence of 20 µM CGP 37157 (red line n = 18) or 2 µM FCCP and 2 µM oligomycin (green line n = 34) or under combination of FCCP, oligomycin and CGP 37157 (blue line n = 23). *P<0.05 vs. cells overexpressing STIM1-Orai1. (B) Statistical analysis of maximal $[Ca^{2+}]_{mito}$ signals presented in panel A. The maximal delta of $1\text{-}F_{430}/F_0$ value of the average signals in cells overexpressing STIM1-Orai1 was defined as 100 % and other

condition presented as the percent of the maximal delta in cells overexpressing STIM1-Orai1.*P<0.05 vs. cells overexpressing STIM1-Orai1.

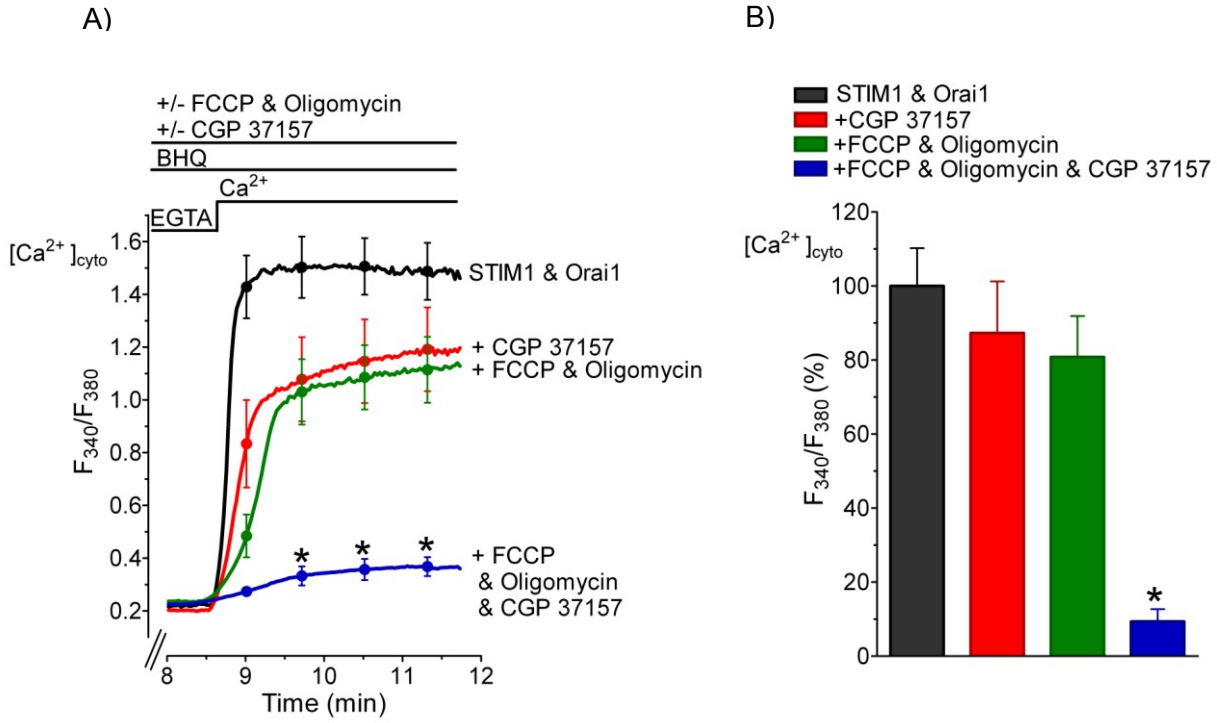

Figure 3.20: Effects of Ψ_{mito} depolarization and NCX_{mito} inhibition on SOCE induced $[Ca^{2+}]_{cyto}$ signals in cells overexpressing STIM1-Orai1. $[Ca^{2+}]_{cyto}$ signals were measured in cells overexpressing STIM1-Orai1 by imaging the fluorescence of fura 2/AM. Ca^{2+} influx were induced by a readdition of 2 mM Ca^{2+} to prestimulated, ER Ca^{2+} depleted cells. (A) $[Ca^{2+}]_{cyto}$ signals recorded upon the readdition of 2 mM Ca^{2+} in prestimulated STIM1-Orai1 overexpressing cells (black line n = 8), in the presence of 20 µM CGP 37157 (red line n = 12), in the presence of 2 µM FCCP and 2 µM oligomycin (green line n = 17) and under conditions of Ψ_{mito} depolarization and NCX_{mito} inhibition (FCCP and oligomycin and CGP 37157, blue line n = 14). *P<0.05 vs. cell overexpressing STIM1-Orai1.

(B) Statistical analysis of maximal $[Ca^{2+}]_{cyto}$ signals of the experiments presented in panel (A) in percentage. The maximal delta F_{340}/F_{380} value of the average signals in cells overexpressing STIM1-Orai1 was defined as 100 % and other conditions were

presented as the percent of maximal delta in STIM1-Orai1 overexpressing cell. *P<0.05 vs. cell overexpressing STIM1- Orai1.

Cells overexpressing STIM1-Orai1 stimulated using histamine and BHQ and thereafter 2 mM Ca^{2+} was readded. Cells were treated with CGP 37157 or FCCP and oligomycin or treated simultaneously with CGP 37157, FCCP and oligomycin. As the result shows, while CGP 37157, FCCP and oligomycin alone only partially decreased the signal, application of all three compounds reduced the signal for approximately 95 %.

This set of data shows that blocking of one of mitochondrial Ca^{2+} uptake pathways barely prevents mitochondria from Ca^{2+} uptake upon STIM1-Orai1 overexpressoin. Blocking one of the pathways does not prohibit mitochondrial contribution, upon SOCE activation. On the other hand, complete blocking of mitochondrial Ca^{2+} uptake and thus excluding mitochondrial buffering/uptake function, inhibited SOCE activation and Ca^{2+} signal.

Result shows that in the cells overexpressing STIM1-Orai1, STIM1-Orai1 - dependent Ca^{2+} entry is dependent on mitochondrial Ca^{2+} buffering/uptaking function.

3.7. Effect of mitochondrial motility on cytosolic Ca^{2+} homeostasis

As it has been supported so far by our data, mitochondria are important for Ca^{2+} entry upon SOCE activation. Whether it is Ca^{2+} uptaking/buffering which is important for Ca^{2+} entrance to the cell or releasing a factor from mitochondria (which may works as a chelator (Montalvo *et al*., 2006), or simply as a modulator (Bakowski and Parekh, 2007)) is not known yet.

In our study about mitochondrial regulatory function and Ca^{2+} signaling, we consider some of unique characteristics of this organelle. One of the most prominent ones was mitochondrial dynamic entity, which let this organelle to be probably like a rapid carrier for (maybe) ATP to different locations of the cell. Mitochondrial motility lets this organelle to be in demanded locations on time. We were interested to know whether motility and the following effects of it are important in mitochondrial function in cellular Ca^{2+} signaling (with focus on SOCE).

3.7.1. Effect of mAKAP-RFP-CAAX expression on motility and structure of mitochondria in EA.hy926 cells

To test the effect of mitochondrial motility on Ca^{2+} signaling, we applied a new construct, called mAKAP-RFP–CAAX (figure 3.21) (Csordas *et al*., 2006; Liu *et al*., 2009). This construct includes a part of N-terminal of mouse mitochondrial AKAP protein, which targets the protein to outer membrane of mitochondria. C-terminal of the protein is CAAX box, which is specific for targeting proteins to plasma membrane. These two parts link together with a red fluorescent protein (RFP). We assume that expression of this construct links mitochondrial to plasma membrane that in turn inhibits mitochondrial motility.

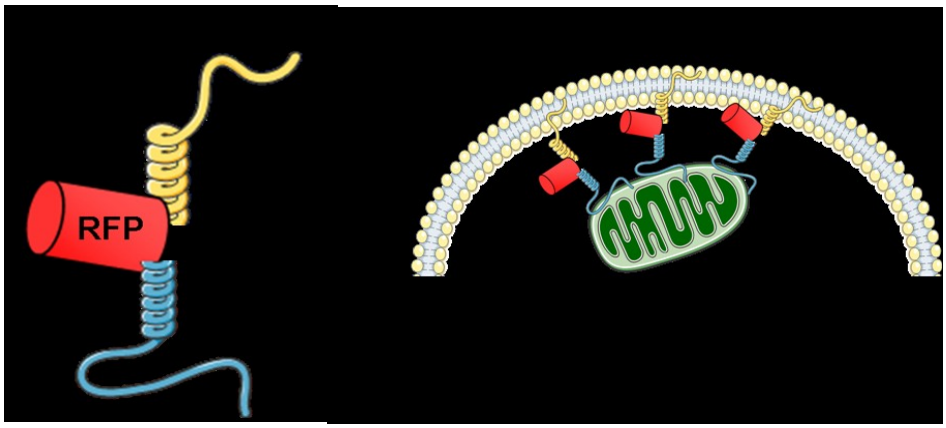

Figure 3.21: Schematic view of mAKAP-RFP–CAAX and its function upon expression in the cells.

Overexpression of this construct in our cell model was visualized and three dimensional images from ER and mitochondria were reconstructed using z- scanning planes of the cells expressing mAKAP-RFP-CAAX and $D1_{ER}$ and stained with mitoTracker green^{TM}. Line florescence scanning (from the middle part of the cells imaged in the figure 3.22) indicated that in control cells, mitochondria and subdomains of ER, randomly distributed (3.22 & 3.23 A). However, upon expression of mAKAP-RFP-CAAX in the cells, mitochondria mostly colocalized with mAKAP-RFP-CAAX in plasma membrane and ER

structure did not change upon expression of mAKAP-RFP-CAAX (3.22 & 3.23 A) (3-dimensional analysis performed by Roland Malli).

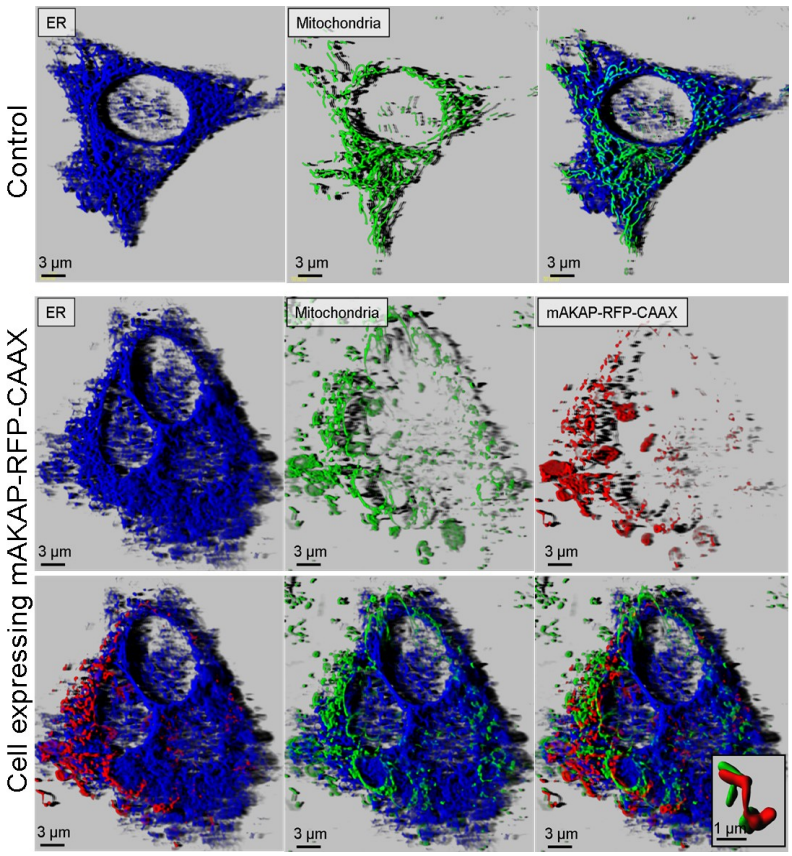

Figure 3.22: Effect of expression of mAKAP-RFP–CAAX on distribution of mitochondria. (A) Representative 3D-rendering of ER (blue) and mitochondria (green) and respective overlays in control cells (upper panel) and in cells expressing mAKAP-RFP-CAAX (lower panels). The inserted image in the lower right panel indicates the colocalization of individual mitochondria (green) with mAKAP-RFP-CAAX (red). 3-dimensional analysis was performed by Roland Malli.

Distribution of ER (figure 3.24 A) and mitochondria (figure 3.24 B), further investigated by detecting the total florescence intensity recorded from these organelles in all the planes along with z-axis of the cells. As the figure 3.24 confirmed last data, florescence intensity recorded from ER did not change upon expression of mAKAP-RFP-CAAX

comparing with control. However, regarding mitochondria, upon expression of mAKAP-RFP-CAAX, maximum florescence intensity from almost middle planes of z-scan (in controls) shifted to the lower planes of z-scan. The spindle-shape of endothelial cells let us to speculate that this shift indicates the link between mitochondria and maximal plasma membrane that is at the bottom of the cell.

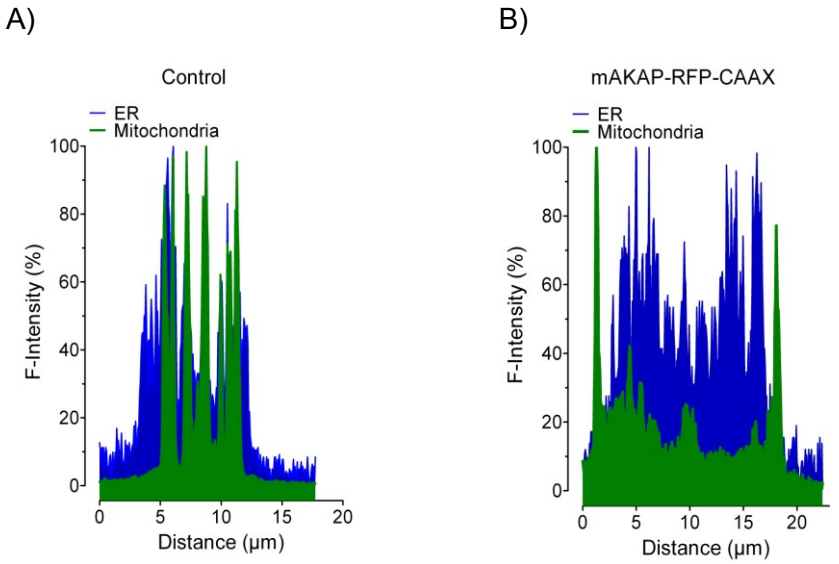

Figure 3.23: Linescans analysis from a section of control cells and cells expressing mAKAP-RFP-CAAX. Linescans showing the fluorescence intensity of an ER targeted cameleon ($D1_{ER}$) and MitoTrackerGreen® at lines showed in overlay images in figure 3.22 in a control cell (A) and a cell expressing mAKAP-RFP-CAAX (B). This data was presented by Roland Malli.

Mitochondrial motility was investigated upon expressing the mAKAP-RFP-CAAX. Single mitochondria movement was analyzed for three minutes, using a time dependent series of images recorded by confocal laser scanning microscope. While in control cells, there were different patterns of movements including long distance that accompanied by fission-fusion, wiggling, contraction and extension, in cells expressing mAKAP-RFP-CAAX construct there were no distance movements. Figure 3.25 A compares a representative movement pattern of a single mitochondrion in a control cell versus that of a mAKAP-RFP-CAAX expressing cell.

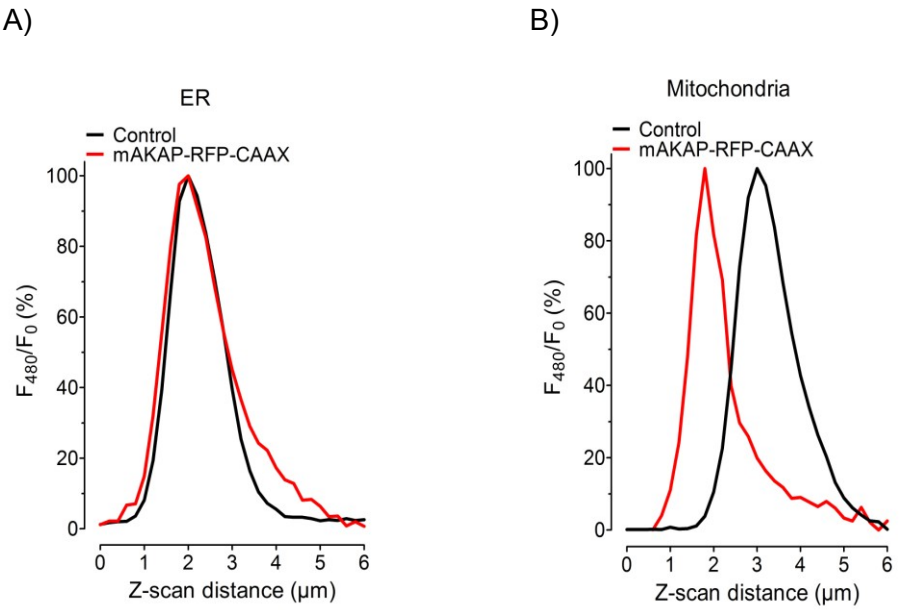

Figure 3.24: Effect of expression of mAKAP-RFP–CAAX on distribution of mitochondria and ER in z-scanning series analysis. (A) The average fluorescence intensity of MitoTrackerGreen® within distinct planes along the z-axis of control cells (black curve n = 6) and cells expressing mAKAP-RFP-CAAX (red curve n = 4). (B) Distribution of fluorescence coming from ER targeted cameleon ($D1_{ER}$) along the z-axis of control cells (black trace n = 6) and cells expressing mAKAP-RFP-CAAX (red trace n = 4).

In addition, the maximal distance that a mitochondrion moved in three minutes - called maximal radius - were calculated. Figure 3.25 B shows that maximal average of the distance covered by mitochondria (maximal radius) in control cells was approximately 26 µm while in mAKAP-RFP-CAAX expressing cells was less than 2 µm. Tracking of the single mitochondria and Maixmal redius was described by Roland Malli.

Moreover, knowing X and Y position for each individual mitochondrion in every time-series image made it possible to calculate speed of the mitochondria. Figure 3.26 shows that speed in cells expressing mAKAP-RFP-CAAX dramatically decreased comparing with control cells.

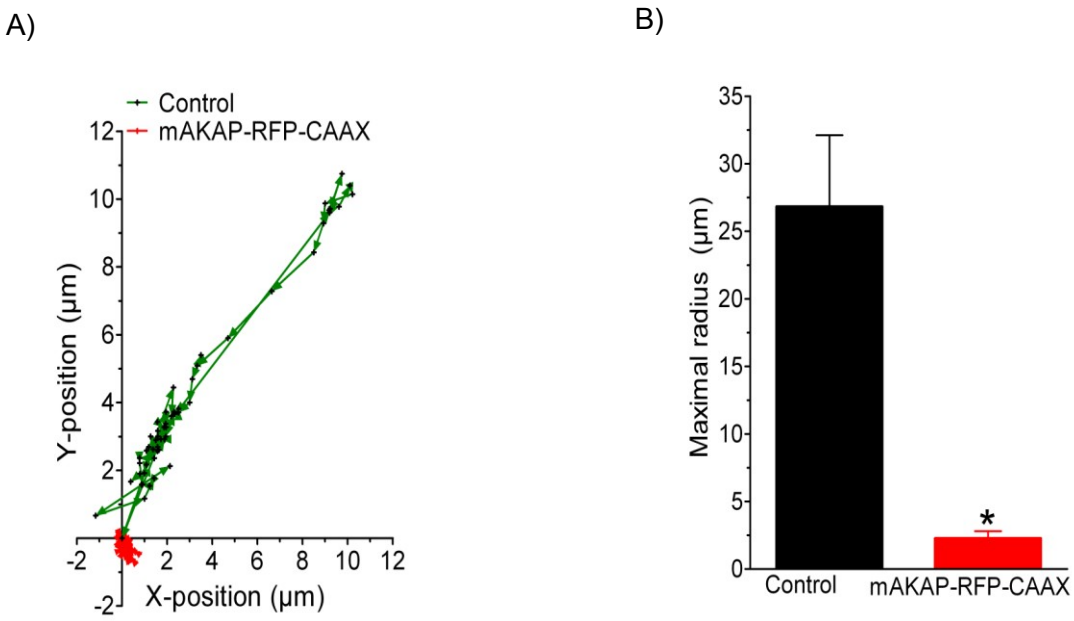

Figure 3.25: Impact of mAKAP-RFP-CAAX expression on the movement pattern of mitochondria. (A) Tracking of a representative single mitochondrion under control condition (green trace) and upon the expression of mAKAP-RFP-CAAX (red trace). (B) Statistical analysis of the maximal distance covered by single mitochondrion within 3 minutes (defined as maximal radius in µm) in control cells (n = 27) and cells expressing mAKAP-RFP-CAAX (n = 16). *P < 0.05 vs. Control. Tracking of single mitochondria was described by Roland Malli and Phillip Peinhoff.

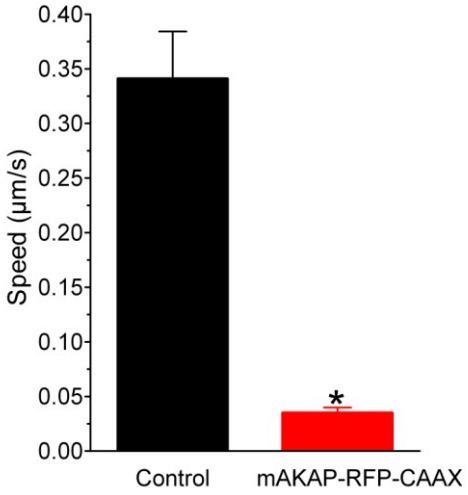

Figure 3.26: Effect of mAKAP-RFP–CAAX on mitochondrial mobility. Columns represent the average speed in µm/s of single mitochondria in control cells (n = 27) and cells expressing mAKAP-RFP-CAAX (n = 16). *P < 0.05 vs. control.

3.7.2. Effect of mAKAP-RFP-CAAX expression on cytosolic and mitochondrial Ca^{2+} signal upon Ca^{2+} release from ER.

Analyzing of the motility clearly showed that upon expressing of the mAKAP-RFP-CAAX, mitochondria hooked to plasma membrane and fixed to this compartment. This knowledge about characteristics of the linker gave us the chance to apply the construct as a tool to manipulate mitochondrial movements and check this parameter in Ca^{2+} signaling specially on Ca^{2+} entrance upon SOCE activation. To this aim, cells transfected with mAKAP-RFP-CAAX or mtDsRed as control and Ca^{2+} measured in different compartments. As figure 3.27 A shows, upon release from ER, the rate and the extent of Ca^{2+} increased in the cytosole was similar in mAKAP-RFP-CAAX expressing cells comparing with control. However, mitochondrial Ca^{2+} uptake (figure 3.27 B) significantly decreased comparing with mtDsRed expressing cell as control. In mitochondrial Ca^{2+} signal, extrusion of Ca^{2+} did not change upon expression of the mAKAP-RFP-CAAX construct (figure 3.27 C).

This data indicates that expression of the linker that fixes mitochondria to plasma membrane, did not change the amount of ER Ca^{2+} release in the cell while it had effect on mitochondrial uptake.

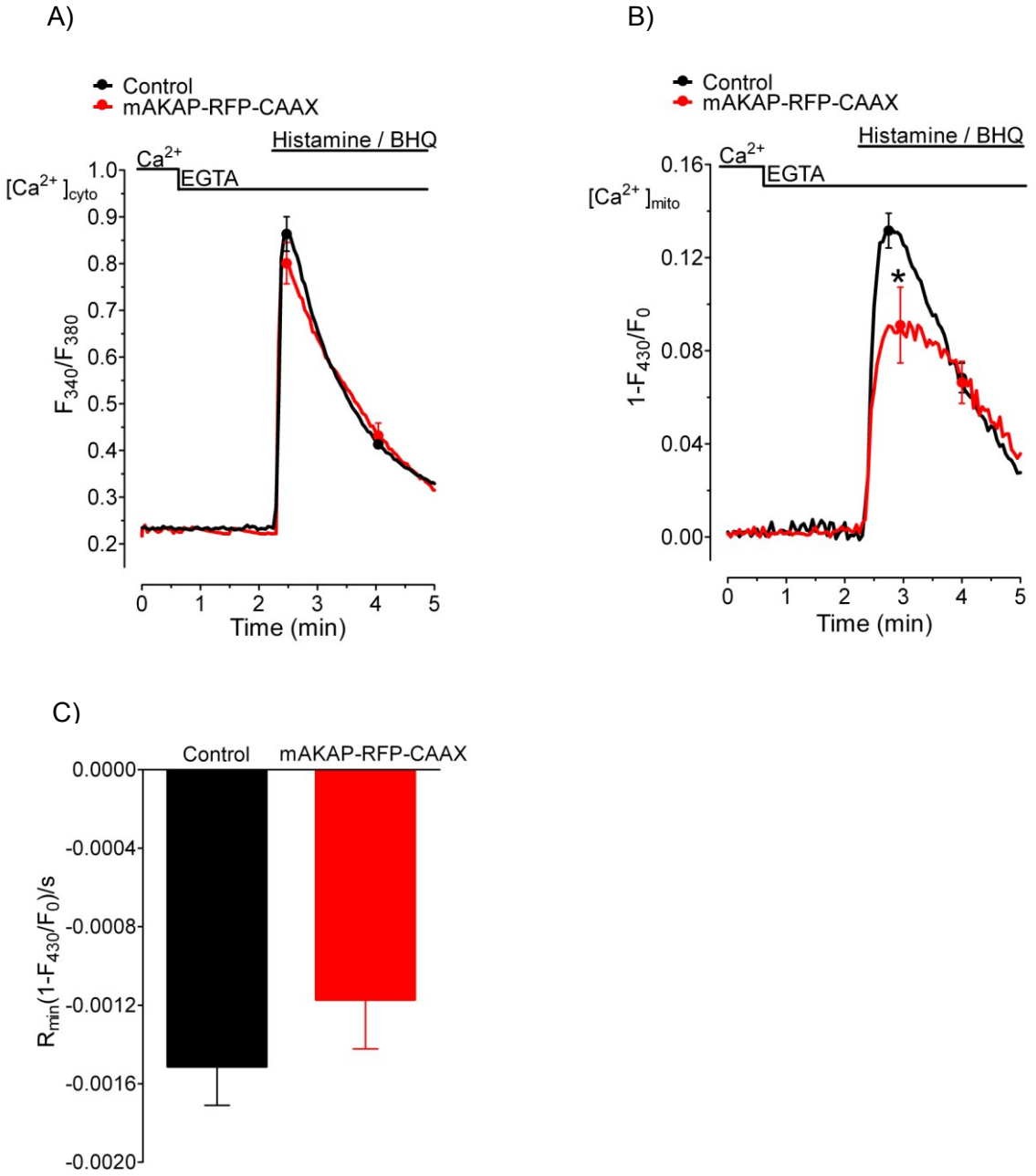

Figure 3.27: Effect of mAKAP–RFP–CAAX on cytosolic and mitochondrial Ca^{2+} signal, $[Ca^{2+}]_{cyto}$ and $[Ca^{2+}]_{mito}$ upon Ca^{2+} release from ER. (A) Mitochondrial Ca^{2+} signals were measured in cells expressing mt-RP. ER Ca^{2+} depletion was achieved with 100 µM histamine and 15 µM BHQ in an EGTA (1 mM) containing Ca^{2+} free solution under control conditions (n = 30) and in cells expressing mAKAP-RFP-CAAX (n = 18). *P < 0.05 vs. control. (B) Average curves indicating cytosolic Ca^{2+}

signals in response to 100 µM histamine and 15 µM BHQ in the presence of 1 mM EGTA under control conditions (n = 19) and in cells expressing mAKAP-RFP-CAAX (n = 13). (C) Column graph showing the averages of the rate of the decay of mitochondrial Ca^{2+} signal upon Ca^{2+} release from ER in control (black column n = 28) and in mAKAP-RFP-CAAX expressing cells (red column n = 18). All signals were recorded with an exposure time of 800 ms yielding an acquisition rate of 2.586 s.

3.7.3. Effect of mAKAP-RFP-CAAX expression on mitochondrial membrane potential (Ψ_{mito})

To know whether reduction of mitochondrial Ca^{2+} uptake can be the effect of less mitochondrial membrane potential in mAKAP-RFP-CAAX expressing cells, mitochondrial membrane potential was measured in mAKAP-RFP-CAAX expressing cells and compared with control cells using JC-1 (figure 3.28 A). JC-1 is a cationic dye and specifically targeted to mitochondria. Upon loading the dye, it mostly aggregated in mitochondria (min 9th). Treating the JC1-stained cells with FCCP, collapsed mitochondrial membrane potential and decreased the florescence intensity of dye which was aggregated in mitochondria (min 12th).

Figure 3.28 B shows the average of the ratio of the florescence intensity of JC-1 in mitochondria to the florescence intensity of the dye in cytosole. Comparing of this ratio between different conditions - cells expressing mAKAP-RFP-CAAX versus controls - showed that expression of mAKAP-RFP-CAAX does not make any change in mitochondrial membrane potential of the cells.

3.7.4. Effect of mAKAP-RFP-CAAX expression on mitochondrial Ca^{2+} uptake upon applying different concentration of histamine

Linking mitochondria to plasma membrane might change the coupling efficiency between ER and mitochondria. To test this probability, we study mitochondrial Ca^{2+} uptake upon applying different concentration of histamine (1, 3, 10, 30 and 100 µM) in the absence of extracellular Ca^{2+} (1 mM EGTA) (figure 3.29). In control cells by

increasing the concentration of histamine, mitochondrial Ca^{2+} uptake increased. It was the same in the cells expressing mAKAP-RFP-CAAX. However, on the same concentration of histamine, cells expressing mAKAP-RFP-CAAX had less mitochondrial Ca^{2+} uptake comparing with that of control cells. This reduction in Ca^{2+} uptake was more significant upon higher concentration of histamine.

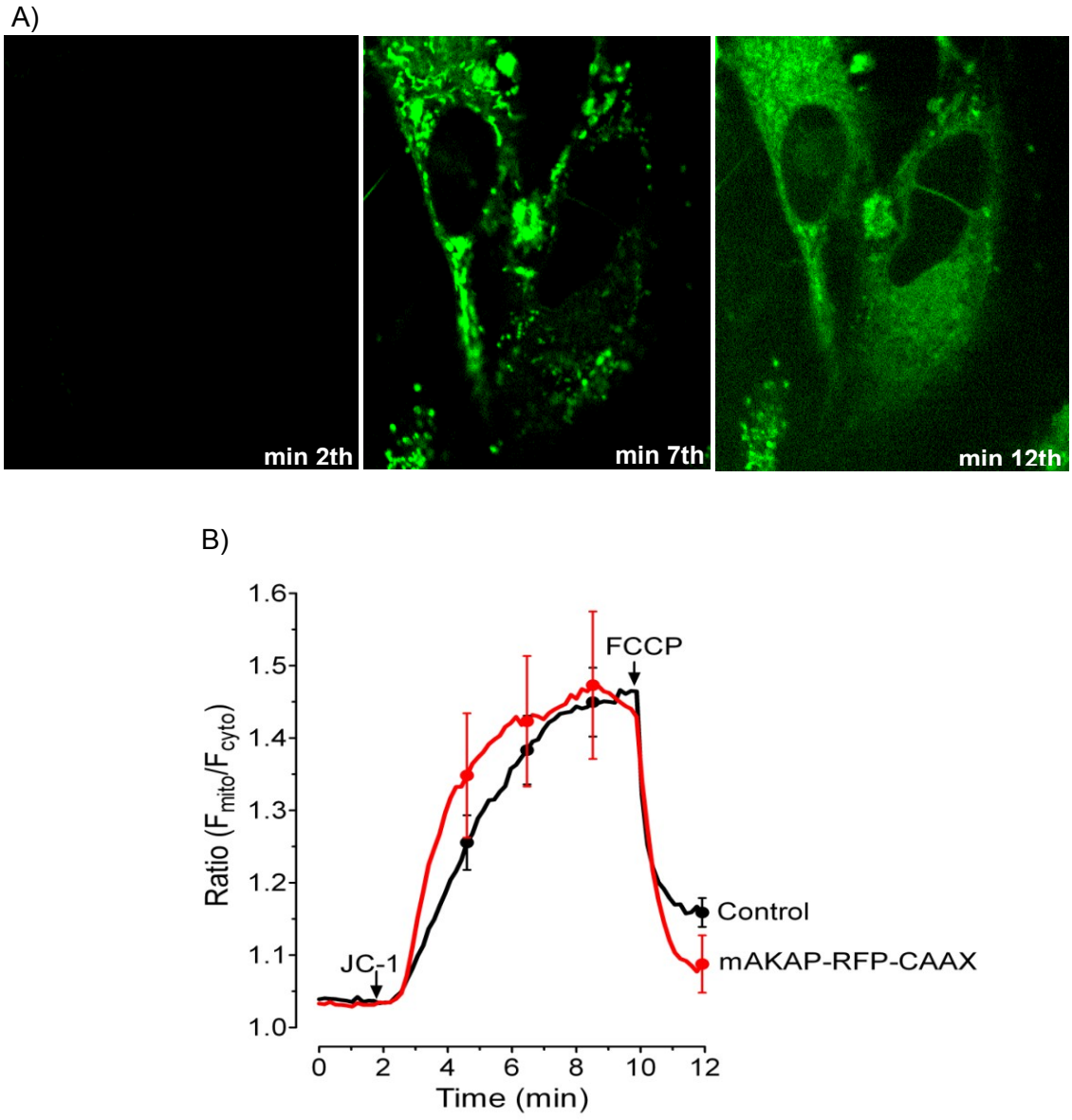

Figure 3.28: Effect of mAKAP-RFP-CAAX on mitochondrial membrane potential (Ψ_{mito}). Ψ_{mito} was assessed using a cationic dye, called JC-1 (Trenker et al., 2007). (A) Steps of treatment of cells with JC1. Middle panel shows the accumulation of the dye in mitochondria and right panel shows the collapse of

mitochondrial membrane potential upon FCCP application in a representative field of microscope. Times mentioned in the figures are according to the one in panel (B). (B) Traces represent ratio of JC-1 florescence in mitochondrial to this dye intensity in cytosole in control cells (black trace, n = 21) and in cells expressing mAKAP-RFP-CAAX (red trace, n = 14). Once the fluorescence intensity in mitochondria (F_{mito}) and the cytosol (F_{cyto}) reached the equilibrium, 2 µM FCCP was added in order to achieve complete mitochondrial depolarization.

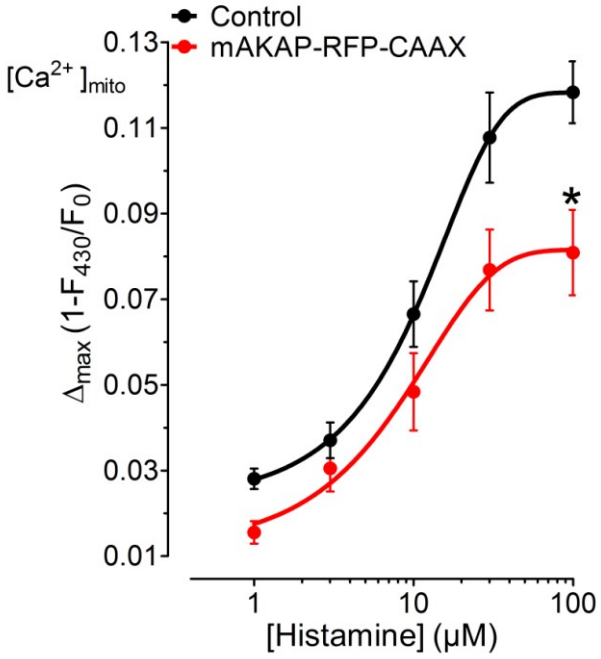

Figure 3.29: Effect of mAKAP-RFP-CAAX expression on concentration response curve presenting the relation between different concentrations of histamine used to release Ca^{2+} from the ER (in the presence of 1 mM EGTA) and the respective maximal mitochondrial Ca^{2+} uptake.

Mitochondrial maximal uptake presented as Δ_{max} $(1\text{-}F_{430}/F_0)$ in control cells (black curve n = 21 for 1 µM histamine, n = 26 for 3 µM histamine, n = 31 for 10 µM histamine, n = 21 for 30 µM histamine, n = 28 for 100 µM histamine) and in cells expressing mAKAP-RFP-CAAX (red curve n = 12 for 1 µM histamine, n = 17 for 3 µM histamine, n = 16 for 10 µM histamine, n = 11 for 30 µM histamine, n = 18 for 100 µM histamine). *P < 0.05 vs. control.

Rate of mitochondrial Ca^{2+} uptake (figure 3.30 A) and time needed to reach to maximal rate (T_{Rmax}) (figure 3.30 B) was calculated. As figure 3.30 A shows in both control cells and cells expressing mAKAP-RFP-CAAX, by increasing the concentration of histamine, the speed of mitochondrial Ca^{2+} uptake increased. In each concentration that applied for histamine, the maximum kinetics of control was higher than cells expressing mAKAP-RFP-CAAX. Interestingly, upon applying higher concentrations of histamine (30 and 100 µm), maximum kinetic of mitochondrial Ca^{2+} uptake in cell expressing mAKAP-RFP-CAAX was significantly less than controls.

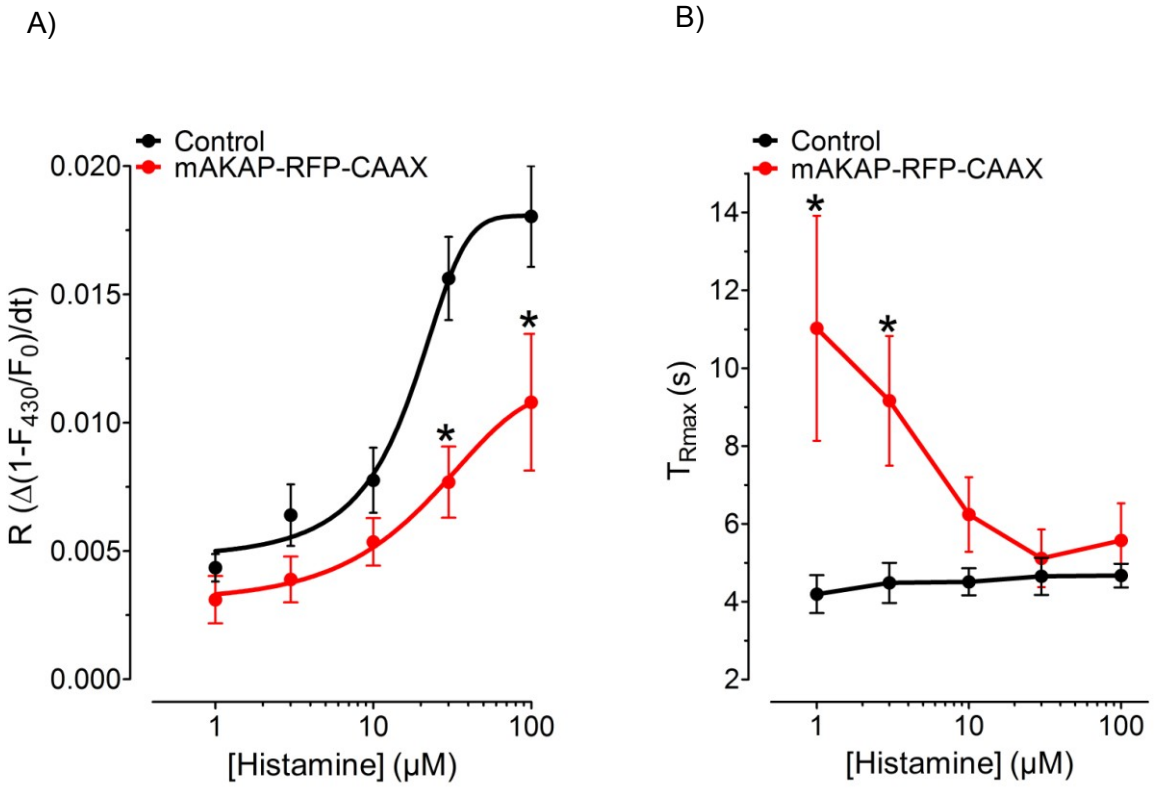

Figure 3.30: Effect of mAKAP-RFP-CAAX expression on the velocity of mitochondrial Ca^{2+} uptake and time to reach to this maximal velocity. (A) Analysis of the maximal rate of mitochondrial Ca^{2+} accumulation expressed as $\Delta(1-F_{430}/F_0)/dt$ upon cell stimulation with different histamine concentrations in the absence of extracellular Ca^{2+} (1 mM EGTA). Black sigmoid curve represents the data obtained under control conditions (n = 21 for 1 µM histamine, n = 26 for 3 µM histamine, n = 31 for 10 µM histamine, n = 21 for 30 µM histamine, n = 28 for 100

μM histamine). Red sigmoid curve represents the data obtained with cells expressing mAKAP-RFP-CAAX (n = 12 for 1 μM histamine, n = 17 for 3 μM histamine, n = 16 for 10 μM histamine, n = 11 for 30 μM histamine, n = 18 for 100 μM histamine). All signals were recorded with an exposure time of 800 ms yielding an acquisition rate of 2.586 s. *P < 0.05 vs. control. (B) Correlation of the time from the initiation of mitochondrial Ca^{2+} elevations until the maximal rate of mitochondrial Ca^{2+} accumulation (expressed as T_{Rmax} in s) with the strength of Ca^{2+} mobilized by cell stimulation upon using different histamine concentrations in free Ca^{2+}, EGTA containing (1 mM) buffer. As indicated, cells were stimulated with 1 μM histamine (n = 21 in controls, n = 12 in mAKAP-RFP-CAAX expressing cells), 3 μM histamine (n = 26 in controls, n = 17 in mAKAP-RFP-CAAX expressing cells), 10 μM histamine (n = 31 in controls, n = 16 in mAKAP-RFP-CAAX expressing cells), 30 μM histamine (n = 21 in controls, n = 11 in mAKAP-RFP-CAAX expressing cells) and 100 μM histamine (n = 28 in controls, n = 18 in mAKAP-RFP-CAAX expressing cells). *P < 0.05 vs. control.

Analysis of the time needed to reach to maximal rate for mitochondrial Ca^{2+} uptake indicated that in control cells, treatment the cells with different concentration of histamine did not change the time needed to reach to maximum rate. In all applied concentration of histamine, it took approximately 4 second to reach to maximal velocity of uptake. In cell expressing mAKAP-RFP-CAAX, the time to reach to maximum velocity was slightly longer than controls. Using lower concentration of histamine (1 and 3 μM), showed more delay in the time to reach to maximum velocity comparing with that of controls.

3.7.5. Effect of mAKAP-RFP-CAAX on mitochondrial ER focal contacts

This set of data confirmed that upon expressing the linker, various characteristics of mitochondrial uptake have changed which might be the effect of uncoupling between ER and mitochondria. Figure 3.31 shows analysis of focal contact between ER and mitochondria in the cells expressing mAKAP-RFP-CAAX, which decreased approximately by 75 %.

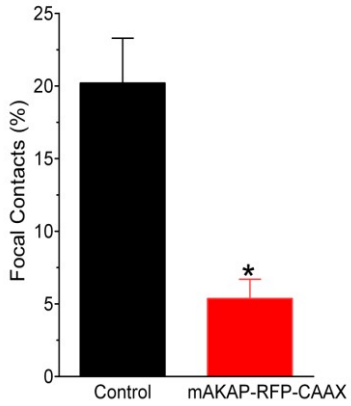

Figure 3.31: Analysis of focal contact between mitochondria and ER upon mAKAP-RFP-CAAX expression.

Columns represent the percentage of colocalized voxels (volume pixels) of fluorescence signals from the ER with that of mitochondria in control cells (black column, n = 3) and cells expressing mAKAP-RFP-CAAX (red column, n = 4). *P < 0.05 vs. control. The analysis of colocalization was performed with Imaris 3.3 software

3.7.6. Effect of mAKAP-RFP-CAAX on ER Ca^{2+} homeostasis

It is already published that mitochondrial-ER crosstalk is important for Ca^{2+} homeostasis in ER especially if the agonist (histamine) present in refilling of the organelle (Malli R. *et al.* 2007). In this condition in our cell model, mitochondrial Ca^{2+} handling interruption had an effect on ER refilling. To check the effect of uncoupling between ER and mitochondria upon expression of mAKAP-RFP-CAAX, Cells were transiently transfected with mAKAP-RFP-CAAX and $D1_{ER}$ or mtDsRed. Ca^{2+} signal was measured in ER (figure 3.32). Cells were pre-stimulated with histamine and BHQ in the absence of extracellular Ca^{2+} (1mM EGTA) and 2mM Ca^{2+} was readded in the presence of histamine. Subsequently, histamine was washed out and after full refilling of ER; cells were depleted using histamine and BHQ in the absence of extracellular Ca^{2+} (1mM EGTA).

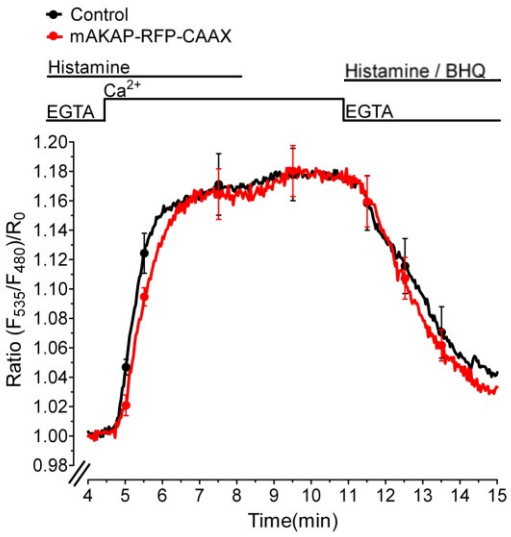

Figure 3.32: Effect of mAKAP-RFP-CAAX on ER Ca^{2+} refilling and ER Ca^{2+} release. Exhaustive ER Ca^{2+} depletion was achieved with 100 µM histamine and 15 µM BHQ in the absence of extracellular Ca^{2+} (1 mM EGTA). Subsequently, ER Ca^{2+} refilling was measured upon the addition of 2 mM Ca^{2+} in the presence of 100 µM histamine followed by a washout of the agonist. Later, ER depleted for the second time using 100 µM histamine and 15 µM BHQ in the absence of extracellular Ca^{2+} (1 mM EGTA). Changes of the ER Ca^{2+} concentrations are presented as the Ratio $(F_{535}/F_{480})/R_0$ in control cells (black curve, n = 13) and in cells expressing mAKAP-RFP-CAAX (red curve, n = 15).

As the figure 3.32 shows, fixing of mitochondria to plasma membrane by expressing mAKAP-RFP-CAAX does not have any significant effect on Ca^{2+} refilling of ER.

3.7.7. Effect of mAKAP-RFP-CAAX on mitochondrial Ca^{2+} signal in SOCE induced Ca^{2+} influx.

In line with our idea about mitochondrial importance in SOCE induced Ca^{2+} entry, it was interesting to know what the effect of mitochondrial linking to plasma membrane is on mitochondrial and cytosolic Ca^{2+} signal upon SOCE activation. First, we checked this

effect in mitochondrial uptake (upon SOCE mediated Ca^{2+} entry). Cells expressing mt-RP were transiently transfected with mAKAP-RFP-CAAX or mtDsRed and mitochondrial Ca^{2+} uptake recorded upon store depletion using histamine and BHQ. As figure 3.33 shows, in spite of close vicinity between mitochondria and plasma membrane in the cells expressing mAKAP-RFP-CAAX, the extent of Ca^{2+} taken by mitochondria upon SOCE activation in these cells decreased to almost half of the control cells.

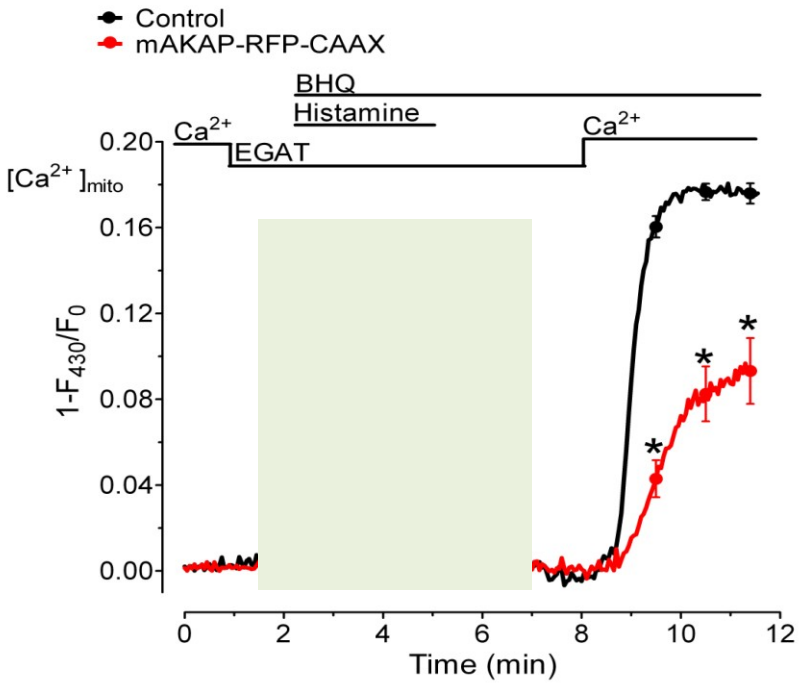

Figure 3.33: Effect of mAKAP–RFP–CAAX on mitochondrial Ca^{2+} uptake upon SOCE dependent Ca^{2+} influx. Mitochondrial Ca^{2+} signals, $[Ca^{2+}]_{mito}$ were measured in the cells expressing mt-RP and presented as $1\text{-}F_{430}/F_0$. Cells were stimulated using 100 µM histamine and 15 µM BHQ in EGTA containing free Ca^{2+} buffer and subsequently 2 mM Ca^{2+} readded. Black curve is average of the florescence signal recorded from control cells (n = 30) and red curve is the average florescence intensity achieved in cells expressing mAKAP-RFP-CAAX (n = 18). Gray square covers the part of signal that already explained in figure 3.31. *P < 0.05 vs. control.

3.7.8. Effect of mAKAP-RFP-CAAX on SOCE mediated Ca^{2+} influx.

In next step, we tried to find out the effect of immobilization of mitochondria on SOCE signal in our cell model. To this aim, cells expressing mAKAP-RFP-CAAX or mtDsRed as control were stimulated and then Ca^{2+} readded. As figure 3.34 shows, regardless of significant reduction in mitochondrial uptake upon SOCE activation (figure 3.32), there was no difference in the extent of Ca^{2+} entered the cell, in the cells expressing mAKAP-RFP-CAAX versus controls (figure 3.34).

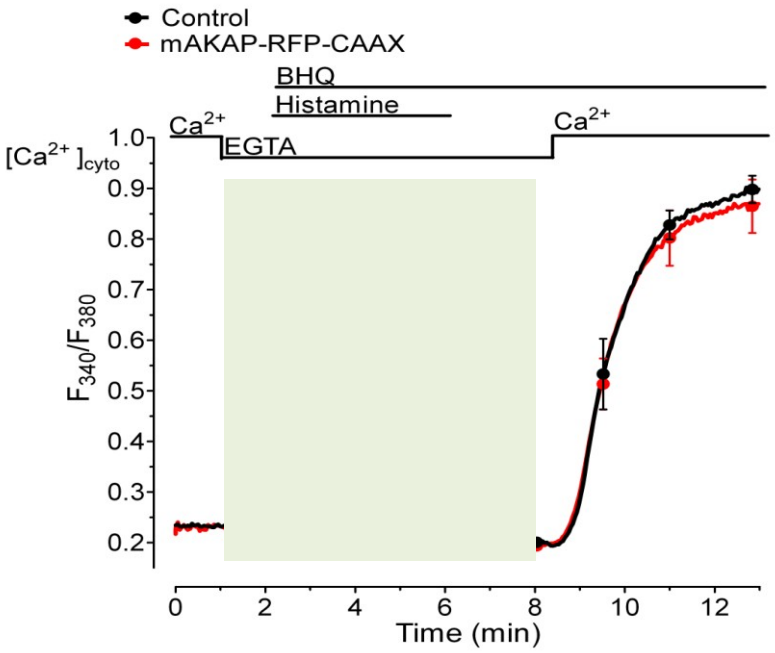

Figure 3.34: Effect of mAKAP–RFP–CAAX on cytosolic Ca^{2+} increase upon readdition of Ca^{2+} after store depletion. Cytosolic Ca^{2+} signals were measured in the cells loading with fura2/AM and presented as F_{340}/F_{380}. Cells were stimulated using 100 μM histamine and 15 μM BHQ in EGTA containing free Ca^{2+} buffer and subsequently 2 mM Ca^{2+} readded. Black curve is the average of the florescence signal recorded from control cells (n = 19) and red curve is the average of florescence intensity achieved in cells expressing mAKAP-RFP-CAAX (n = 13). Gray square covers the part of signal that already has been explained in figure 3.23. *P < 0.05 vs. control.

3.7.9. Effect of mAKAP-RFP-CAAX on mitochondrial and cytosolic Ca^{2+} signal in SOCE induced Ca^{2+} influx in cells overexpressing STIM1 and Orai1.

The data presented, suggest that mitochondrial motility and location does not have any effect on non-specific SOCE efficiency. Knowing about dependency of STIM1 and Orai1 - Ca^{2+} entry to mitochondrial Ca^{+} uptake/buffering function, persuaded us to test whether linking of mitochondria to plasma membrane and immobilizing of this organelle may have any effect on mitochondrial Ca^{2+} uptake and SOCE in STIM1 and Orai1 overexpressing cells. Cells were transiently transfected with STIM1–YFP or –CFP, Orai1 or mtDsRed and/or mAKAP-RFP-CAAX. ER was depleted using 100 μM histamine and 15 μM BHQ in the absence of extracellular Ca^{2+} (1 mM EGTA) and later Ca^{2+} readded. To avoid SOCE deactivation, BHQ was present until the end of experiment.

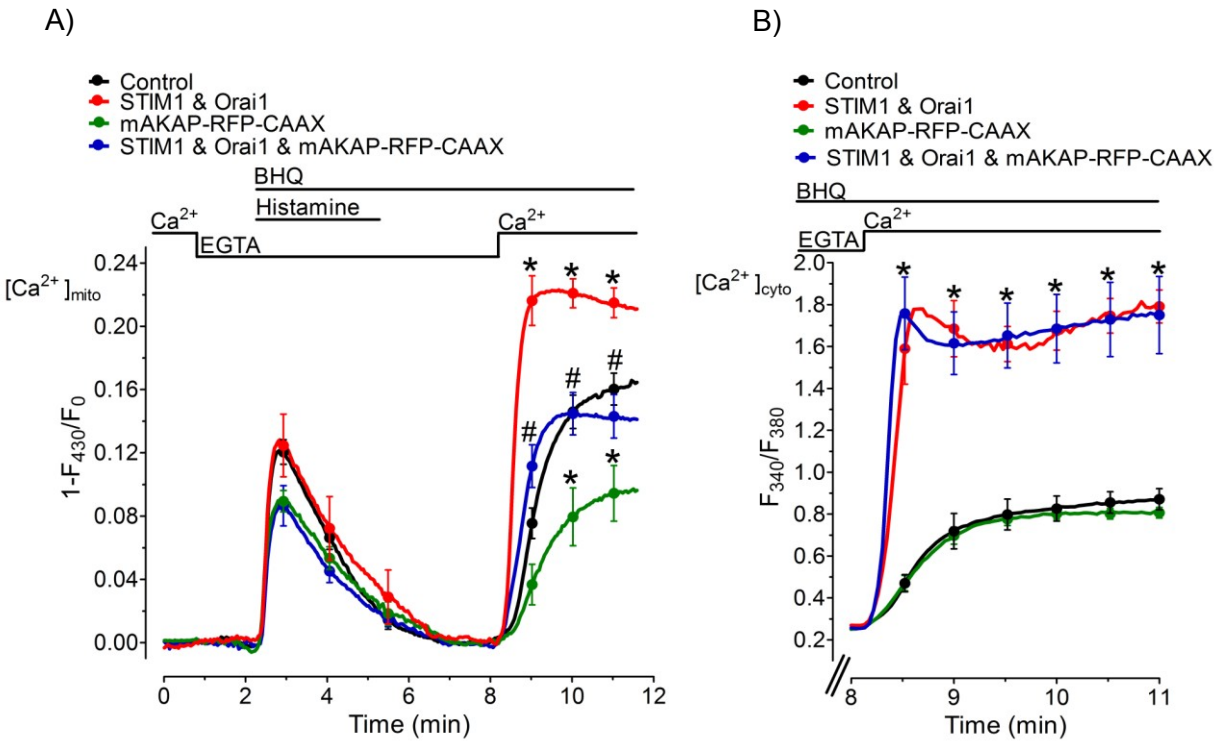

Figure 3.35: Effect of expression of mAKAP-RFP-CAAX on mitochondrial and cytosolic Ca^{2+} signal upon SOCE activation in the cells overexpressing STIM1 and Orai1. Mitochondrial and cytosolic Ca^{2+} signals were measured in the cells expressing mt-RP or cells loaded with fura2/AM. SOCE was activated by ER Ca^{2+}

depletion with100 μM histamine and 15 μM BHQ in EGTA (1mM). Subsequently, 2 mM Ca^{2+} was added in the presence of BHQ.
(A) Curves are average for the florescence intensity recorded from control cells (black line n = 27), cells overexpressing STIM1 and Orai1 (red line n = 10), cells expressing mAKAP-RFP-CAAX (green line, n = 14) and in STIM1 and Orai1 overexpressing cells expressing mAKAP-RFP-CAAX (blue line n = 15, $^{\#}P < 0.05$ vs. cells overexpressing STIM1 and Orai1 without mAKAP-RFP-CAAX). (B) Cytosolic Ca^{2+} increased by Ca^{2+} readdition to prestimulated cells. Experiments were performed with control cells (black line n = 8), cells overexpressing STIM1 and Orai1 (red line n = 7), cells expressing mAKAP-RFP-CAAX (green line, n = 16) and in STIM1 and Orai1 overexpressing cells expressing mAKAP-RFP-CAAX (blue line, n = 9). $^{*}P < 0.05$ vs. control.

As the figure 3.35 A shows similar to control cells, linking of mitochondria to plasma membrane in the cells overexpressing STIM1 and Orai1, decreased mitochondrial Ca^{2+} uptake upon Ca^{2+} release from ER. Moreover, in readdition phase in cells overexpressing STIM1 and Orai1, immobilizing of mitochondria reduced the mitochondrial Ca^{2+} uptake. The extent of reduction was the same with the one in control cells.

To see the effect of mitochondrial immobilization effect on Ca^{2+} signal upon SOCE activation in cells overexpressing STIM1 and Orai1, we did the same experiment and measured cytosolic Ca^{2+} increase upon readdition of Ca^{2+} after ER depletion (figure 3.35 B). Confirming the data presented before, mitochondrial immobilization did not affect Ca^{2+} influx upon SOCE activation in cells overexpressing STIM1 and Orai1.

3.7.10. Effect of mitochondrial membrane depolarization on SOCE fueled Ca^{2+} influx and SOCE induced mitochondrial Ca^{2+} uptake in cells overexpressing STIM1 and Orai1

To test the dependency of recorded cytosolic Ca^{2+} in cells expressing mAKAP-RFP-CAAX to mitochondrial Ca^{2+} handling, we applied FCCP and oligomycin to disrupt mitochondrial Ca^{2+} uptake and we recorded cytosolic Ca^{2+} signal upon SOCE activation.

As it already mentioned mitochondrial Ca^{2+} sequestration, plays a role in SOCE establishment and maintenance. Moreover, the result presented in last two figures indicated while there is less extent of mitochondrial Ca^{2+} uptake in cells with immobilized mitochondria, there is no effect on the cytosolic Ca^{2+} signal. To test the sensitivity (or in other word mitochondrial dependency) of the Ca^{2+} entry upon SOCE activation in the cells expressing mAKAP-RFP-CAAX, we applied FCCP and oligomycin. ER was depleted using 100 µM histamine and 15 µM BHQ in the absence of extracellular Ca^{2+} (1 mM EGTA) and then 2 mM Ca^{2+} in the presence of BHQ readded. As figure 3.36 shows, in control cells as well as STIM1 and Orai1 overexpressing cells, expression of mAKAP-RFP-CAAX did not change the extent of sensitivity level of SOCE fueled Ca^{2+} influx to mitochondrial depolarization (using FCCP and oligomycin).

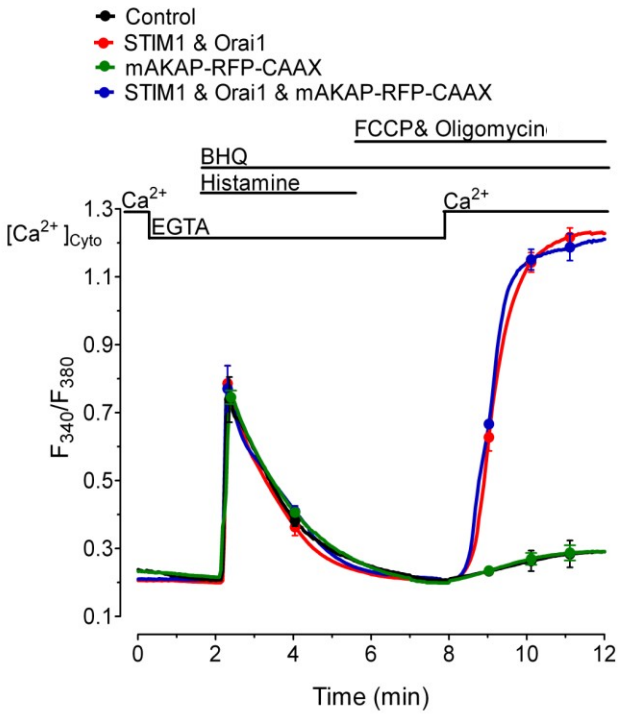

Figure 3.36: Effect of mitochondrial membrane depolarization on SOCE induced Ca^{2+} influx in the cells overexpressing STIM1 and Orai1 expressing mAKAP-RFP–CAAX. Cytosolic Ca^{2+} signals were measured in the cells loaded with fura2/AM and presented as F_{340}/F_{380}. Cells were transiently transfected by STIM1 and Orai1 and/or mAKAP-RFP–CAAX or mtDsRed as control. SOCE was activated by ER Ca^{2+} depletion with100 µM histamine and 15 µM BHQ in EGTA (1mM) and

subsequently, 2 mM Ca^{2+} was added in the presence of BHQ. 2 μM FCCP and 2 μM oligomycin added 2 minutes before Ca^{2+} readdition.

Traces are average of florescence intensity earned from control cells (black, n=12), cells expressing mAKAP-RFP-CAAX (green, n = 11), STIM1 and Orai1 (red, n = 10), STIM1 and Orai1 and mAKAP-RFP-CAAX, (blue, n = 8).

4. Discussion

In endothelial cells, stimulation of cells using an agonist triggers a two-step Ca^{2+} signal in cytosol. First, a fast elevation that is transient and provided from intracellular organelle and mostly via IP_3 receptor. The second phase of signal takes place upon readdition of extracellular Ca^{2+} and mostly is a combination of SOCE-dependent and independent entry pathways. Non-selective TRP channels that are highly expressed in this cell type are the candidates for SOCE-independent Ca^{2+} entry (Girardin *et al*. 2010, Graier *et al*., 1994; Nilius 2003; Nilius *et al.,* 1993).

In our endothelial cell line, EA.hy926, manipulation of extracellular Na^+ showed that under high concentration of the Na^+ loaded in the cell, NCX_{pm} functions in reverse mode. This finding is in agreement with the work of Girardin and co-workers that verified this entry pathway by path clamp method (Girardin *et al*. 2010). As we expected counteracting TRPC family channels activity by expression of N-dominant negative in EA.hy926 cells reduced the level of Ca^{2+} entered to the cell simulation with agonist.

In addition, we showed that STIM1 and Orai1 are components of SOCE in our cell model, however knocking down of these proteins showed that their contribution in agonist mediated Ca^{2+} entry is only 50 %.

It has been shown that the Ca^{2+} ions, which entered the cell upon stimulation with agonist, is highly sensitive to pharmacological tools, which effect mitochondrial Ca^{2+} sequestration (Malli *et al*., 2003; Malli *et al*., 2005). Therefore, it has been hypothesized that mitochondrial Ca^{2+} handling (uptake/buffering) is essential in the regulation of the Ca^{2+} entered to the cell upon agonist stimulation.

We next tried to answer whether mitochondria plays a role for STIM1-Orai1 mediated Ca^{2+} entry or not. But due to multiple Ca^{2+} entry pathways in our cell model, to find out the importance of mitochondrial regulatory function specifically in STIM1 and Orai1 - dependent pathway we designed the experiment with overexpression of these proteins. Overexpression of these proteins leads to increasing the number of influx channels and thereby, enhancing the Ca^{2+} influx upon SOCE activation. However, overexpression of one of these proteins did not change the level of Ca^{2+} entering the cell. It means that the ratio of the numbers of different components of these entrance units is important. These findings are in line with previous reports (Soboloff *et al*, 2006). Overexpression of both of

these proteins simultaneously or STIM1 alone changed the kinetics of Ca^{2+} entered the cell. Increasing the kinetics might indicate that increasing the number of STIM1 protein boost the possibility of the formation of SOCE units more quick than that in controls. Moreover, overexpression of STIM1 alone was enough to increase the rate of ER Ca^{2+} refilling while knockdown of this protein alone or together with Orai1 did not change the rate and extent of ER Ca^{2+} refilling. Considering the contribution of other Ca^{2+} influx pathways in our cell model, the fact that ER is refilled in the knockdown condition is not surprising.

This study showed that in cells overexpressing STIM1 and Orai1, the amplitude of Ca^{2+} that entered upon agonist mediated store depletion, is partially sensitive to the toxins that impair mitochondrial Ca^{2+} handling. Moreover, localization of subplasmalemal mitochondria in cells expressing STIM1 and Orai1 showed that many of SOCE units containing STIM1 and Orai1 (almost 50 %) are not in close vicinity to mitochondria. Therefore, we assumed that increasing the SOCE units out of mitochondrial accessibility might make these units independent form mitochondrial function.

Application of the FCCP as an ionophore showed that most of mitochondrial Ca^{2+} uptake under physiological condition is mostly dependent on mitochondrial membrane potential. Moreover, depend on the applied protocol NCX_{mito} in reverse mode performs a very small part of the uptake.

Applying higher concentration of Ca^{2+} showed that these two pathways, mitochondrial membrane potential dependent (Mitochondrial Ca^{2+} uniporter(s)) and NCX_{mito} in reverse mode) might cooperate with each other. Under high concentration of Ca^{2+}, inhibition of one of these pathways, leads to mitochondrial uptake rescued by another one. This cooperation in mitochondrial uptake results in insensitivity of Ca^{2+} that entered to the cell to the pharmacological tools, in higher concentration of extracellular Ca^{2+} comparing with that effect of these tool under physiological situation.

Similar to the higher concentration of Ca^{2+}, in cells overexpressing STIM1 and Orai1, applying of mitochondrial toxins does not dramatically decrease the cytosolic Ca^{2+} signal in SOCE mediated Ca^{2+} entry.

Blocking of both uptake pathways confirmed our speculation. Under physiological condition or under higher amount of extracellular Ca^{2+}, simultaneous blocking of both pathways fully inhibited mitochondrial uptake. Under such as condition, mitochondrial

dysfunction had a dramatic effect on Ca^{2+} entry upon SOCE activation. Similar to this condition in STIM1-Orai1 overexpressing cells, blocking of mitochondrial uptake had a strong effect on Ca^{2+} entry upon SOCE activation.

These data clearly shows that mitochondrial function strongly regulates SOCE phenomenon, however upon increasing the Ca^{2+} level via STIM1-Orai1 overexpression, mitochondrial Ca^{2+} uptake boosts, in a way that blocking of one of mitochondrial Ca^{2+} entrance pathway does not harm the function (uptake/buffering) of this organelle. Upon complete mitochondrial function disturbance, Ca^{2+} entry upon SOCE activation fully inhibited in cells expressing STIM1 and Orai1.

Our result regarding location of subplasmalemmal mitochondria showed that the ratio between number of these organelles and number of SOCE units does not play a major role in mitochondrial function (uptake/buffering) on regulation of the Ca^{2+} entered via SOC channels. Increasing the number of entrance units does not exclude mitochondria from regulatory effect on SOCE.

In order to better understanding the role of mitochondria on SOCE phenomenon, we manipulated different characteristics of mitochondria. We applied a construct (mAKAP-RFP-CAAX), that contained CAAX box, which takes this construct to membrane and AKAP which links this construct to mitochondria (Csordas *et al.*, 2006; Liu *et al.*, 2009). A-kinase anchoring proteins (or AKAPs) are a family of about 50 scaffold proteins. The common characteristic of this family is a conserved motif, which binds typically to phosphokinase A and other enzymes in signaling pathways (that can be other kinases or phosphatase) (Lohmann *et al*., 1984). In different cell type, a variety of anchoring proteins targeted to specific compartments like mitochondria, centrosome and vesicules (Alto *et al*., 2002). They act as a platform for proteins, make a joint between proteins and compartments and therefore, facilitate and coordinate the function of the localized signaling process (Lorene *et al.,* 2005). Expression of this construct links mitochondria to plasma membrane. The main affect of this construct was blocking of long distance movements of mitochondria. Moreover, data from focal contacts between ER and mitochondria showed that expression of this construct, uncouples mitochondria and ER, thus mitochondrial Ca^{2+} uptake decreased. In addition, the rate of uptake decreases comparing with control. However, it did not change the extrusion rate of Ca^{2+} from this organelle.

Not only mitochondrial Ca^{2+} uptake upon Ca^{2+} release from ER decreases but also, it decreases when is fueled by SOCE activation. Interestingly, it seems that close vicinity of mitochondria to plasma membrane does not facilitate SOCE – mediated mitochondrial Ca^{2+} uptake. Further investigation showed that immobilizing of mitochondria using mAKAP-RFP-CAAX did not affect on Ca^{2+} entered via SOC channels. In other words, immotile mitochondria are able to play the same role as the motile ones, showing that movement is not important for mitochondrial conribution to the SOCE phenomenon. Applying FCCP/oligomycine in the cells expressing mAKAP-RFP-CAAX decreased the extent of Ca^{2+} entered the cell through SOCE channels, suggesting that even under this condition which mitochondrial Ca^{2+} uptake is less than control condition, mitochondrial function is still pivotal for SOCE phenomenon.

We assumed that in mAKAP-RFP-CAAX expressing cells, the alignment of mitochondria toward channels has changed and this might be effective in less mitochondrial Ca^{2+} uptake.

Overall, this study showed that in the cells overexpressing STIM1 and Orai1, SOCE mediated Ca^{2+} entry is less sensitive to mitochondrial membrane potential depolarizing (using FCCP/oligomycin) or blocking of NCX_{mito} (using CGP 37157), however, entire blocking of mitochonrial Ca^{2+} sequestration blocks SOCE mediated Ca^{2+} entry signal, suggesting that mitochondrial Ca^{2+} sequestration plays a crucial role in Ca^{2+} enry in this condition. In addition, we showed that mitochondrial motility is not important in mitochondrial Ca^{2+} sequestration upon SOCE activity.

5. References:

1. Abdullaev, I.F., Bisaillon, J.M., Potier, M., Gonzalez, J.C., Motiani, R.K., Trebak, M. (2008). Stim1 and Orai1 mediate CRAC currents and store-operated calcium entry important for endothelial cell proliferation. Circ Res 103, 1289–1299.

2. Alicia, S., Angélica, Z., Carlos, S., Alfonso, S., Vaca, L. (2008). STIM1 converts TRPC1 from a receptor-operated to a store-operated channel: moving TRPC1 in and out of lipid rafts. Cell Calcium 44, 479-491.

3. Alonso, M.T., Villalobos, C., Chamero, P., Alvarez, J., García-Sancho, J. (2006). Calcium microdomains in mitochondria and nucleus. Cell Calcium 40, 513-525.

4. Alto, N. M., Soderling, J., Scott, J. D. (2002). Rab32 is an A-kinase anchoring protein and participates in mitochondrial dynamics. J. Cell Biol. 158, 659-668.

5. Ayoub, K., Hallet, M.B. (2004). The mitochondrial ADPR link between Ca^{2+} store release and Ca^{2+} influx channel opening in immune cells, FASEB J. 18,1335-1338.

6. Bakowski, D. and Parekh A. B. (2007). Regulation of store-operated calcium channels by the intermediary metabolite pyruvic acid, Curr. Biol. 17, 1076-1081.

7. Bautista D.M., Lewis, R.S. (2004). Modulation of plasma membrane calcium-ATPase activity by local calcium microdomains near CRAC channels in human T cells. J. Physiol. 556, 805-817.

8. Benitah, J.P., Alvarez, J. L., Gómez, A.M. (2010). L-type Ca^{2+} current in ventricular cardiomyocytes. J. Mol. Cell Cardiol. 48, 26-36.

9. Berridge, M.J. 2002. The endoplasmic reticulum: a multifunctional signaling organelle, Cell Calcium 32, 235–249.

10. Berridge MJ. (2006). Calcium microdomains: organization and function. Cell Calcium. 40, 405-412.

11. Berridge M.J., Bootman, M.D. and Roderick, H.L. (2003). Calcium signaling: Dynamics, Homeostasis and remodeling. Nat. Rev. Mol. Cell Biol. 4, 517-529.

12. Berridge, M.J., Bootman, M.D., Roderick, H.L. (2003). Calcium signalling: dynamics, homeostasis and remodelling. Nat. Rev. Mol. Cell Biol. 4, 517-29.

13. Biel, M., Michalakis, S. (2009). Cyclic nucleotide-gated channels. Handb. Exp Pharmacol. 191, 111-36.

14. Bird, G.S. (2008). Methods for studying store operated calcium entry. Methods 46, 204-212.

15. Bird, G.S., DeHaven, W.I., Smyth, J.T., Putney, J.W. Jr. (2008). Methods for studying store-operated calcium entry. Methods 46, 204-412.

16. Bird, G.S., Putney, J.W. Jr. (2005). Capacitative calcium entry supports calcium oscillations in human embryonic kidney cells. J. Physiol. 562, 697-706.

17. Boehning, D., Patterson, R.L., Sedaghat, L., Glebova, N.O., Kurosaki, T., Snyder, S.H. (2003). Cytochrome c binds to inositol (1, 4, 5) trisphosphate receptors, amplifying calcium-dependent apoptosis. Nat. Cell Biol. 5, 1051-1061.

18. Bolotina, V.M., Csutora, P. (2005). CIF and other mysteries of the store-operated Ca^{2+}-entry pathway. Trends Biochem. Sci. 30, 378-387.

19. Bolotina, V.M. (2008). Orai, STIM1 and iPLA2beta: a view from a different perspective. J. Physiol. 586, 3035-42.

20. Brand, M.D., Esteves, T.C. (2005). Physiological functions of the mitochondrial uncoupling proteins UCP2 and UCP3. Cell Metab. 2, 85-93.

21. Bryant, N., Govers, J.N., James D.E. (2002). Regulated transport of the glucose transporter GLUT4. Nature Rev. Mol. Cell Biol. 3, 267-277.

22. Cahalan, M.D. (2009). STIMulating store operated Ca^{2+} entry. Nat. Cell Biol. 11, 669-677.

23. Cancela, J.M., Coppenolle, F., Galione, A., Tepikin, A.V., Petersen O.H. (2001). Transformation of local Ca^{2+} spikes to global Ca^{2+} transients: the combinatorial roles of multiple Ca^{2+} releasing messengers. EMBO J. 21, 909-919.

24. Carafoli, E. (1991). Calcium pump of the plasma membrane. Physiol. Rev. 71, 129-153.

25. Carafoli, E. (1994). Biogenesis: plasma membrane calcium ATPase: 15 years of work on the purified enzyme. FASEB J. 8, 993-1002.

26. Caride, A. J., Filoteo, A.G., Penheiter, A.R., Paszty, K., Enyedi, A., Penniston, J. T. (2001). Delayed activation of the plasma membrane calcium pump by a sudden increase in Ca^{2+} : fast pumps reside in fast cells. Cell Calcium 30, 49-57.

27. Carrasco, S., Meyer, T. (2010). Cracking CRAC. Nat. Cell Biol.12, 416-418.

28. Cines, D.B., Pollak, E.S., Buck, C.A., Loscaloz, J., Zimmermn G.A. McEver R.P., Pober, J.S., Wick, T.M., Konkle, B.A., Schwartz B.S., Barnathan, E.S., McCrae, K.R., Hug, B.A.,Schmidt, A.M., Stern, D.M. (1998). Endothlial cells in physiology and in the pathophysiology of vascular disorders. Blood 91, 3527-3561.

29. Clapham, D.E. (2007). Calcium signaling. Cell 131, 1047-1058.

30. Collins, T.J., Lipp, P., Berridge, M.J., Bootman, M.D. (2001). Mitochondrial Ca^{2+} uptake depends on the spatial and temporal profile of cytosolic Ca^{2+} signals. J. Biol. Chem. 276, 26411-26420.

31. Collins, T.J., Berridge, M.J., Lipp, P., Bootman, M.D. (2002). Mitochondria are morphologically and functionally heterogeneous within cells. EMBO J. 21, 1616-1627.

32. Csordás, G., Renken, C., Várnai, P., Walter, L., Weaver, D., Buttle, K.F., Balla, T., Mannella, C.A., Hajnóczky, G. (2006). Structural and functional features and significance of the physical linkage between ER and mitochondria. J. Cell Biol. 174, 915-921.

33. Csutora, P., Peter, K., Zarayskiy, V., Kilic, H., Park, K.M., Bolotina, V.M. (2008). Novel role of STIM1 as a trigger for CIF production. J. Biol. Chem. 283, 14524-14531.

34. Dadsetan, S., Zakharova, L., Molinski, T.F., Fomina, A.F. (2008). Store-operated Ca^{2+} influx causes Ca^{2+} release from the intracellular Ca^{2+} channels that is required for T cell activation. J. Biol. Chem. 283, 12512-12519.

35. Dean, W.L., Chen, D., Brandt, P.C., Vanaman, T.C. (1997). Regulation of platelet plasma membrane Ca^{2+}-ATPase by cAMP-dependent and tyrosine phosphorylation. J. Biol. Chem. 272, 15113-15119.

36. DeHaven, W.I., Jones, B.F., Petranka, J.G., Smyth, J.T., Tomita, T., Bird, G.S., Putney, J.W. Jr. (2009). TRPC channels function independently of STIM1 and Orai1. J. Physiol. 587, 2275-98.

37. Demaurex, N., Distelhorst, C. (2003). Cell biology Apoptosis-the calcium connection. Science 300, 65-67.

38. Demaurex, N., Poburko, D., Frieden, M. (2009). Regulation of plasma membrane calcium fluxes by mitochondria. Biochimica et Biophysica Acta 1787, 1383-1394.

39. Deng, X. (2009). Stim and Orai: Dynamic intermembrane coupling to control cellular calcium. J. Biol. Chem. 284, 22501-22505

40. Dhalla, N.S. (1969). Excitation–contraction coupling in heart. I. Comparison of calcium uptake by the sarcoplasmic reticulum and mitochondria of the rat heart. Arch. Int. Physiol. Biochem. 77, 916-934.

41. Dolmetsch, R. E., Pajvani, U., Fife, K., Spotts, J. M., Greenberg, M. E. (2001). Signaling to the nucleus by an L-type calcium channel-calmodulin complex through the MAP kinase pathway. Science 294, 333-339.

42. Dolmetsch, R. E., K., Xu, Lewis, R. S. (1998). Calcium oscillations increase the efficiency and specificity of gene expression. Nature 392, 933-936.

43. Dziadek, M.A., Johnstone L.S. (2007). Biochemical properties and cellular localisation of STIM proteins. Cell Calcium 42, 123-132.

44. Eder, P., Probst D., Rosker C., Poteser, M., , Wolinski, H.S.D., Kohlwein, C., Romanin, C., Groschner, K. (2007). Phospholipase C-dependent control of cardiac calcium homeostasis involves a TRPC3-NCX1 signalling complex, Cardiovascular Research 73, 111-119.

45. Edgell, C.J., McDonald, C.C., Graham, J.B. (1983). Permanent cell line expressing human factor VIII-related antigen established by hybridization. Proc. Natl. Acad. Sci. U S A. 80, 3734-3737.

46. Er, E., Oliver, L., Cartron, P.F., Juin, P., Manon, S., Vallette, F.M. (2006). Mitochondria as the target of the pro-apoptotic protein Bax. Biochem. Biophys. Acta. 1757, 1301-1311.

47. Evtodienko, Y.V. (2000). Sustained oscillations of transmembrane Ca^{2+} fluxes in mitochondria and their possible biological significance. Membr. Cell Biol. 14, 1-17.

48. Fomina, A. F. and Nowycky, M. C. (1999). A current activated on depletion of intracellular Ca^{2+} stores can regulate exocytosis in adrenal chromaffin cells. J. Neurosci. 19, 3711-3722.

49. Feske, S., Gwack, Y., Prakiriya, M., Srikanth, S., Puppel, S. H., Tanasa, B., Hogan, P. G., Lewis, R. S. Daly, M., Rao, A. (2006). A mutation in Orai1 causes immune deficiency by abrogating CRAC channel function. Nature 441, 179-185.

50. Foskett, J.K., White, C., Cheung, K.H., Mak, D.O. (2007). Inositol trisphosphate receptor Ca^{2+} release channels. Physiol. Rev. 87, 593-658.

51. Frederick, R.L., Shaw, J.M. (2007). Moving mitochondria: establishing distribution of an essential organelle. Traffic. 8, 1668-75.

52. Frederick, R.L., McCaffery, J.M., Cunningham, K.W., Okamoto, K., Shaw, J.M. (2004). Yeast Miro GTPase, Gem1p, regulates mitochondrial morphology via a novel pathway. J. Cell Biol. 167, 87-98.

53. Freichel, M., Suh, S.H., Pfeifer, A., Schweig, U., Trost, C., Weissgerber, P., Biel, M., Philipp, S., Freise, D., Droogmans, G., Hofmann, F., Flockerzi, V., Nilius, B. 2001.

Lack of an endothelial store-operated Ca^{2+} current impairs agonist-dependent vasorelaxation in TRP4-/- mice. Nat. Cell Biol. 3, 121–127.

54. Frieden, M., Malli, R., Samardzija, M., Demaurex, N., Graier, W. F. (2002). Subplasmalemmal endoplasmic reticulum controls K_{Ca} channel activity upon stimulation with a moderate histamine concentration in a human umbilical vein endothelial cell line. J. Physiol. 540, 73-84.

55. Frieden, M., James, D., Castelbou, C., Danckaert, A., Martinou, J.C., Demaurex, N. (2004). Ca^{2+} homeostasis during mitochondrial fragmentation and perinuclear clustering induced by hFis1. J. Biol. Chem. 279, 22704-14.

56. Gailly, P. (1998). Ca^{2+} entry in CHO cells, after Ca^{2+} stores depletion, is mediated by arachidonic acid. Cell Calcium 24, 293-304.

57. Ganitkevich, V.Y. (2003). The role of mitochondria in cytoplasmic Ca^{2+} cycling. Experimental Physiology 88, 91-97.

58. Gilabert, J.A., Bkowski, D., Parekh, A.B. (2001). Energized mitochondria increase the dynamic range over which inositol 1,4,5-triphosphate activates store-operated calcium influx. EMBO J. 20, 2672-2679.

59. Girardin N.C., Antigny, F., Frieden, M. 2010. Electrophysiological characterization of store-operated and agonist-induced Ca^{2+} entry pathways in endothelial cell. Pflugers Arch. 460, 109-120.

60. Glitsch, M.D., Bakowski, D., Parekh, A.B. (2002). Store-operated Ca^{2+} entry depends on mitochondrial Ca^{2+} uptake. EMBO J. 21, 6744–6754.

61. Graier, W. F., Sturek, M., Kukovetz, W.R.(1994). Ca^{2+} regulation and endothelial vascular function. Endothelium 1, 223–236.

62. Graier, W.F., Simecek, S., Sturek, M. (1995). Cytochrome P450 mono-oxygenase-regulated signaling of Ca^{2+} entry in human and bovine endothelial cells. J. Physiol. 482, 259-274.

63. Graier, W.F., Paltauf-Doburzynska J., Hill, B.J., Fleischhacker, E., Hoebel, B.G., Kostner, G.M., Sturek, M. (1998). Submaximal stimulation of porcine endothelial cells causes focal Ca^{2+} elevation beneath the cell membrane. J Physiol. 506,109-125.

64. Graier, W.F., Freieden, M. and Malli, R. (2007). Mitochondria and Ca^{2+} signaling: old guests, new functions. European J. of Physiol. 455, 375-396.

65. Grigoriev, I., Gouveia, S.M., van der Vaart, B., Demmers, J., Smyth, J.T., Honnappa, S., Splinter, D., Steinmetz, M.O., Putney, J.W. Jr., Hoogenraad, C.C., Akhmanova, A. (2008). STIM1 is a MT-plus-end-tracking protein involved in remodeling of the ER. Curr. Biol. 18, 177-82.

66. Hadri, L., Pavoine C., Lipskaia, L., Yacoubi, S., Lompre, A. (2006). Transcription of the sarcoplasmic/endoplasmic reticulum Ca^{2+}-ATPase type 3 gene, *ATP2A3*, is regulated by the calcineurin/NFAT pathway in endothelial cells. Biochem. J. 394, 27-33.

67. Hao, L., Rigaud, J.L., Inesi, G. (1994). Ca^{2+}/H^{+} countertransport and electrogenicity in proteoliposomes containing erythrocyte plasma membrane Ca^{2+}-ATPase and exogenous lipids. J. Biol. Chem. 269, 14268-14275.

68. Hardie, R.C. (2007). TRP channels and lipids: from Drosophila to mammalian physiology. J. Physiol. 578, 9-24.

69. Hayashi, T., Rizzuto, R., Hajnoczky, G., Su, T. P. (2009). MAM: more than just a housekeeper. Trends Cell Biol. 19, 81-88.

70. Hayashi, T., Su, T. P. (2007). Sigma-1 receptor chaperones at the ER-mitochondrion interface regulate Ca^{2+} signalling and cell survival. Cell 131, 596-610.

71. Hoebel, B.G., Kostner, G.M., Graier, W.F. (1997). Activation of microsomal cytochrome P450 mono-oxygenase by Ca^{2+} store depletion and its contribution to Ca^{2+} entry in porcine aortic endothelial cells. Br. J. Pharmacol.121, 1579-1588.

72. Hofmann, T., Obukhov, A.G., Schaefer, M., Harteneck, C., Gudermann, T., Schultz, G. (1999). Direct activation of human TRPC6 and TRPC3 channels by diacylglycerol. Nature 397, 259–263.

73. Hogan, P.G., Rao, A. (2007). Dissecting I_{CRAC}, a store-operated calcium current. Trends Biochem. Sci. 32, 235-245.

74. Hoth, M., Penner, R. (1992). Depletion of intracellular calcium stores activates a calcium current in mast cells. Nature 355, 353-356.

75. Hoyt, M.A., Hyman, A.A., Bähler, M. (1997). Motor proteins of the eukaryotic cytoskeleton. Proc. Natl. Acad. Sci. U S A. 94, 12747-8.

76. Ishikawa, J., Ohga, K., Yoshino, T., Takezawa, R., Ichikawa, A., Kubota, H. and Yamada, T. (2003). A pyrazole derivative, YM-58483, potently inhibits store-operated sustained Ca^{2+} influx and IL-2 production in T lymphocytes. J. Immunol. 170, 4441-4449.

77. Jarvis, S.E., Zamponi, G.W. (2001). Interactions between presynaptic Ca^{2+} channels, cytoplasmic messengers and proteins of the synaptic vesicle release complex. Trends Pharmacol. Sci. 22, 519-525.

78. Jiang, Y., Chen, C., Li, Z., Guo, W., Gegner, J. A., Lin, S., Han, J. (1996). Characterization of the structure and function of a new mitogen-activated protein kinase (p38beta). J. Biol. Chem. 271, 17920-17926.

79. Kamouchi, M., Mamin, A., Droogmans, G., Nilius, B. (1999). Nonselective cation channels in endothelial cells derived from human umbilical vein. J Membr. Biol. 169, 29–38.

80. Kim, B. and Matsuka, S. (2008). Cytoplasmic Na^{+}- dependent modulation of mitochondrial Ca^{2+} via electrogenic mitochondrial Na^{+}-Ca^{2+} exchange. J. physiol. 586, 1683-1697.

81. Korzeniowski, M.K., Szanda, G., Balla, T., Spät, A. (2009). Store-operated Ca^{2+} influx and subplasmalemmal mitochondria. Cell Calcium 46, 49-55.

82. Kröner, H. (1986). Ca^{2+} ions, an allosteric activator of calcium uptake in rat liver mitochondria. Arch Biochem. Biophys. 251, 525-535.

83. Kwan, C.Y., Takemura, H., Obie, J.F., Thastrup, O., Putney, J.W. Jr. (1990). Effects of methacholine, thapsigargin and La^{3+} on plasmalemmal and interacellular Ca^{2+} transporter in lacrimal acinar cells. Am. J. Physiol. 258, 1006-1015.

84. Lampe, P.A., Cornbrooks, E.B., Juhasz, A., Johnson, E.M., Franklin, J.L. (1995). Suppression of programmed neuronal death by a thapsigargin-induced Ca^{2+} influx. J. Neurobiol. 26, 205-212.

85. Laude, A. and Simpson, A.W.M. (2009). Compartmentalization signaling: Ca^{2+} compartments, microdomains and the many facets of Ca^{2+} signaling. FEBS Journal 276, 1800-1816.

86. Lemonnier, L., Trebak, M., Lievremont, J.,P., Bird, G.S., Putney, J.W. Jr. (2006). Protection of TRPC7 cation channels from calcium inhibition by closely associated SERCA pumps. FASEB J. 20, 503-505.

87. Lenzen, S., Hickethier, R. and Panten, U. (1986). Interactions between spermine and Mg^{2+} on mitochondrial Ca^{2+} transport. J. Biol. Chem. 261, 16478–16483.

88. Lewis R.S. (2007). The molecular choreography of a store-operated calcium channel. Nature 446, 284-287.

89. Li, N., Zheng, L., Lin, P., Danielpour, D., Pan, Z., Ma, J. (2008). Overexpression of Bax induces down-regulation of store-operated calcium entry in prostate cancer cells. J. Cell Physiol. 216,172-179.

90. Liang, G.H., Kim, J.A., Seol, G.H., Choi, S., Suh, S.H. (2008). The Na^+/Ca^{2+} exchanger inhibitor KB-R7943 activates large-conductance Ca^{2+}-activated K^+ channels in endothelial and vascular smooth muscle cells. Eur. J. Pharmacol. 582, 35-41.

91. Liang, G.H., Park, S., Kim, J.K., Suh, S.H. (2009). Stimulation of large-conductance Ca^{2+}-activated K^+ channels by the Na^+/Ca^{2+} exchanger inhibitor dichlorobenzamil in cultured human umbilical vein endothelial cells and mouse aortic smooth muscle cells.J. Physiol. 60, 43-50.

92. Liao, Y., Erxleben, C., Abramowitz, J., Flockerzi, V., Zhu, M.X., Armstrong, D.L., Birnbaumer L. (2008). Functional interactions among Orai1, TRPCs, and STIM1 suggest a STIM-regulated heteromeric Orai/TRPC model for SOCE/I_{crac} channels. Proc. Natl. Acad. Sci. U S A. 105, 2895-900.

93. Liao, Y., Plummer, N.W., George, M.D., Abramowitz, J., Zhu, M.X., Birnbaumer, L. (2009). A role for Orai in TRPC-mediated Ca^{2+} entry suggests that a TRPC: Orai complex may mediate store and receptor operated Ca^{2+} entry. Proc. Natl. Acad. Sci. U S A. 106, 3202-3206

94. Lin, S., Fagan, K.A., Li, K.X., Shaul, P.W., Cooper, D.M., Rodman, D.M. (2000). Sustained endothelial nitric-oxide synthase activation requires capacitative Ca^{2+} entry. J. Biol. Chem. 275, 17979-17985.

95. Liou, J. (2005). STIM1 is a Ca^{2+} sensor essential for Ca^{2+} store depletion-triggered Ca^{2+} influx. Curr. Biol. 15, 1235-1241.

96. Liou, J., Fivaz, M., Inoue, T., Meyer, T. (2007). Live-cell imaging reveals sequential oligomerization and local plasma membrane targeting of stromal interaction molecule 1 after Ca^{2+} store depletion. Proc. Natl. Acad. Sci. USA. 104, 9301-9306.

97. Litsky, M.L. and Pfeiffer, D.R. (1997). Regulation of the mitochondrial Ca^{2+} uniporter by external adenine nucleotides: the uniporter behaves like a gated channel which is regulated by nucleotides and divalent cations. Biochemistry 36, 7071–7080.

98. Liu, X., Weaver, D., Shirihai, O., Hajnóczky, G. (2009). Mitochondrial 'kiss-and-run': interplay between mitochondrial motility and fusion-fission dynamics. EMBO J. 28, 3074-3089.

99. Liu, X., Hajnóczky, G. (2009). Ca^{2+}-dependent regulation of mitochondrial dynamics by the Miro-Milton complex. Int. J. Biochem. Cell Biol. 41, 1972-1976.

100. Lohmann, S. M., DeCamili, P., Enig, I., Walter, U. (1984). High-affinity binding of the regulatory subunit (RII) of cAMP-dependent protein kinase to microtubule-associated and other cellular proteins. Proc. Natl. Acad. Sci. USA. 81, 6723-6727.

101. Lorene, K. Langeberg, L.K., Scott J.D. (2005). A-kinase-anchoring proteins, J. Cell Sci. 118, 3217-3220.

102. Luik, R.M., Wang. B, Prakriya, M., Wu, M. M., Lewis R.S. (2008). Oligomerization of STIM1 couples ER calcium depletion to CRAC channel activation. Nature 454, 538-42

103. MacAskill, A.F., Brickley, K., Stephenson, F.A., Kittler, J.T. (2009). GTPase dependent recruitment of Grif-1 by Miro1 regulates mitochondrial trafficking in hippocampal neurons. Mol. Cell Neurosci. 40, 301-312.

104. Malli, R., Frieden, M., Osibow, K. and Graier, W.F. (2003a). Mitochondria efficiently buffer subplasmalemmal Ca^{2+} elevation during agonist stimulation. J. Biol. Chem. 278, 10807-10815.

105. Malli, R., Frieden, M., Osibow, K., Zoratti, C., Mayer, M., Demaurex, N., Graier, W.F. (2003b). Sustained Ca^{2+} transfer across mitochondria is essential for mitochondrial Ca^{2+} buffering, store-operated Ca^{2+} entry, and Ca^{2+} store refilling. J. Biol. Chem. 278, 44769-44779.

106. Malli, R., Frieden, M., Trenker, M., Graier, W. F. (2005). The role of mitochondria for Ca^{2+} refilling of the endoplasmic reticulum. J. Biol. Chem. 280, 12114-12122.

107. Malli, R., Naghdi, S., Romanin, C., Graier, W. F. (2008). Cytosolic Ca^{2+} prevents the subplasmalemmal clustering of STIM1: an intrinsic mechanism to avoid Ca^{2+} overload. J. Cell Sci. 121, 3133-3139.

108. McCombs, J.E., Palmer, A.E. (2008). Measuring calcium dynamics in living cells with genetically encodable calcium indicators. Methods 46, 152-9.

109. McElroy, S.P., Drummond, R.M., Gurney, A.M. (2009). Regulation of store-operated Ca^{2+} entry in pulmonary artery smooth muscle cells. Cell Calcium 46, 99-106.

110. Mercer, J.C. et al. (2006). Large store-operated calcium selective currents due to co-expression of Orai1 or Orai2 with the intracellular calcium sensor, Stim1. J. Biol. Chem. 281, 24979–24990.

111. Mitchell, P. (1961). Coupling of phosphorylation to electron and hydrogen transfer by a chemi-osmotic type of mechanism. Nature 191, 144-148.

112. Miyawaki, A. (2003). Visualization of the spatial and temporal dynamics of intracellular signaling. Dev. Cell. Signaling. 4, 295-305.

113. Montalvo, G.B., Artalejo A.R., Gilabert J.A. (2006). ATP from subplasmalemmal mitochondria controls Ca^{2+}- dependent inactivation of CRAC channels, J. Biol. Chem. 281, 35616-35623.

114. Monteith, G.R., Roufogalis, B.D. (1995). The plasma membrane calcium pump – a physiological perspective on its regulation. Cell Calcium 18, 459-470.

115. Montero, M., Alonso, M.T., Carnicero, E., Cuchillo-Ibáñez, I., Albillos, A., García, A.G., García-Sancho, J., Alvarez, J. (2000). Chromaffin-cell stimulation triggers fast millimolar mitochondrial Ca^{2+} transients that modulate secretion. Nat. Cell Biol. 2, 57-61.

116. Montalvo, G.B. Artalejo, A.R., Gilabert. J.A. (2006) ATP from subplasmalemmal mitochondria controls Ca^{2+}-dependent inactivation of CRAC channels. J. Biol. Chem.281, 35616-35623.

117. Montero, M., Lobaton, C.D., Moreno, A., Alvarez, J. (2002). A novel regulatory mechanism of the mitochondrial Ca^{2+} uniporter revealed by the p38 mitogen-activated protein kinase inhibitor SB202190. FASEB J. 16, 1955–1957.

118. Mullins, F.M., Park, C.Y., Dolmetsch, R.E., Lewis, R.S. (2009). STIM1 and calmodulin interact with Orai1 to induce Ca^{2+}-dependent inactivation of CRAC channels. Proc. Natl. Acad. Sci. U S A. 106, 15495-15500.

119. Nagai, T., Sawano, A., Park, E.S., Miyawaki, A. (2001). Circularly permuted green fluorescent proteins engineered to sense Ca^{2+}.Proc. Natl. Acad. Sci. U S A. 98, 3197-202.

120. Nakayama, S., Kretsinger, R.H. (1994). Evolution of the EF-hand family of proteins. Annu. Rev. Biophys. Biomol. Struct. 23, 473-507.

121. Nalefski, E.K., Falke J.J. 1996. The C2 domain calcium-binding motif: structural and functional diversity. Protein Sci. 5, 2375-2390.

122. Neher, E. (1998). Vesicle pools and Ca^{2+} microdomains: new tools for understanding their roles in neurotransmitter release. Neuron 20, 389-99.

123. Nicchitta, C.V., Williamson, J.R. (1984). Spermine, A regulator of mitochondrial calcium cycling. J Biol. Chem. 259, 12978–12983.

124. Nicholls, D.G. (2008). Forty years of Mitchell`s proton circuit: from little grey books to little grey cells, Biochim. Biophys. Acta 1777, 550-556.

125. Nicolau, S.M., de Diego, A.M. , Cortés, L., Egea, J., González, J.C., Mosquera, M., López, M.G., Hernández-Guijo, J.M., García, A.G. (2009). Mitochondrial Na^{+}/Ca^{2+-} exchanger blocker CGP 37157 protects against chromaffin cell death elicited by veratridine. J. Pharmacol. Exp. Ther. 330, 844-854.

126. Nilius, B., Schwartz, G., Oike, M., Droogmans, G. (1993). Histamine-activated., non-selective cation currents and Ca^{2+} transients in endothelial cells from human umbilical vein. Pflugers Arc. 424, 285-293.

127. Nilius, B. (2003). From TRPs to SOCs, CCEs, and CRACs: consensus and controversies. Cell Calcium 33, 293-298.

128. Nilius, B., Owsianik, G., Voets, T., Peters J.A. (2007). Transient receptor potential cation channels in disease. Physiol. Rev. 87, 165-217.

129. Oceandym, D., Cartwright, E.J., Emerson, M., Prehar, S., Baudoin, F.M., Zi, M., et al. 2007. Neuronal nitric oxide synthase signalling in the heart is regulated by the sarcolemmal calcium pump 4b. Circulation 115, 483-492.

130. Oh-hora, M. (2009). Calcium signaling in the development and function of T-lineage cells. Immunol. Rev. 231, 210-224.

131. Orci, L., Ravazzola, M., Le Coadic, M., Shen, W.W., Demaurex, N., Cosson, P. (2009). From the cover: STIM1-induced precortical and cortical subdomains of the endoplasmic reticulum. Proc. Natl. Acad. Sci. U.S.A. 106, 19358-19362.

132. O'Rourke, B., Blatter, L. (2009). Mitochondrial Ca^{2+} uptake: Tortoise or hare?. Journal of Molecular and Cellular Cardiology 46, 767-774.

133. Palmer, A.E., Jin, C., Reece, J. C., Tsien, R. Y. (2003). Bcl-2-mediated alterations in endoplasmic reticulum Ca^{2+} analyzed with an improved genetically encoded fluorescent sensor. Proc. Natl. Acad. Sci. USA. 101, 17404-17409.

134. Palmi, M., Youmbi, G.T., Fusi, F., Sgaragli, G.P., Dixon, H.B., Frosini, M and Tipton, K.F. (1999). Potentiation of mitochondrial Ca^{2+} sequestration by taurine. Biochem. Pharmacol. 58, 1123–1131.

135. Paltauf-Doburzynska, J., Posch, K., Paltauf G., Graier, W. F. (1998). Stealth ryanodine-sensitive Ca^{2+} release contributes to activity of capacitative Ca^{2+} entry and nitric oxide synthase in bovine endothelial cells. J. Physiol. 513, 369-379.

136. Paltauf-Doburzynska, J., Freiden M., Spitaler, M., Graier W. F. (2000). Histamine-induced Ca^{2+} oscillations in a human endothelial cell line depend on transmembrane ion flux, ryanodine receptors and endoplasmic reticulum Ca^{2+}-ATPase. J. Physiol. 524,701-713.

137. Palty, R., Silverman, W. F., Hershfinkel, M., Caporale, T., Sensi, S.L., Parnis, J., Nolte, C., Fishman, D., Shaoshan-Barmatz, Hermann, S., Khananshvili, D., sekler, I. (2010). NCLX is an essential component of mitochondrial Na^{+}/Ca^{2+} exchange.Proc. Natl. Acad. Sci. USA.107, 436-441.

138. Pandol, S.J., and Schoeffield-Payne, M.S. (1990). Cyclic GMP mediates the agonist-stimulated increase in plasma membrane calcium entry in the pancreatic acinar cell, J. Biol. Chem. 265, 12846-12853.

139. Parekh, A.B. (1998). Slow feedback inhibition of calcium release-activated calcium current by calcium entry. J. Biol. Chem. 273, 14925-14932.

140. Parekh, A.B., and Putney, J.W., Jr. (2005). Store operated Ca^{2+} channels. Physiol. Rev. 85, 757-810.

141. Parekh, A.B. (2008). Ca^{2+} microdomains near plasma membrane Ca^{2+} channels: impact on cell function. Physiol. 586, 3043-3054.

142. Parekh, A.B. (2008). Mitochondrial regulation of store-operated CRAC channels. Cell Calcium 44, 6-13.

143. Park, C.Y., Hoover, P.J., Mullins, F.M., Bachhawat, P., Covington, E.D., Raunser ,S., Walz, T., Garcia, K.C., Dolmetsch, R.E., Lewis, R.S. (2009). STIM1 clusters and activates CRAC channels via direct binding of a cytosolic domain to Orai1. Cell 136, 876-890.

144. Park M.K., Ashby, M.C., Erdemli, G., Petersen, O.H., Tepikin, A.V. (2001). Perinuclear, perigranular and sub-plasmalemmal mitochondria have distinct functions in the regulation of cellular calcium transport. EMBO J. 20, 1863-74.

145. Patterson, R.L., Van Rossum, D.L., Gill, D.L. (1999). Store-operated Ca^{2+} entry: evidence for a secretion-like coupling model. Cell 98, 487-499.

146. Peinelt, C., et al. (2006). Amplification of CRAC current by STIM1 and CRACM1 (Orai1). Nat. Cell Biol. 8, 771-773.

147. Penna, A., Demuro, A., Yeromin, A.V., Zhang, S.L., Safrina, O., Parker, I., Cahalan, M.D. (2008). The CRAC channel consists of a tetramer formed by Stim-induced dimerization of Orai dimers. Nature 456, 116-120.

148. Perez-Reyes, E. (2003). Molecular physiology of low-voltage-activated t-type calcium channels. Physiol. Rev. 83, 117-161.

149. Pfeiffer, D.R., Gunther, T.E., Eliiseev, R., Broekemeier, K.M., Gunther, K.K. (2001). Release of Ca^{2+} from mitochondria via the saturable mechanisms and the permeability transition. IUBMB Life 52, 205-212.

150. Prakriya, M., Feske, S., Gwack, Y., Srikanth, S., Rao, A., Hogan, P.G. (2006). Orai1 is an essential pore subunit of the CRAC channel. Nature 443, 230-233.

151. Prasad, V., Okunade, G.W., Miller, M.L., Shull, G.E. (2004). Phenotypes of SERCA and PMCA knockout mice. Biochem. Biophys. Res. Commun. 322, 1192-1203.

152. Putney, J.W., Jr. (1986). A model for receptor regulated Ca^{2+} entry. Cell Calcium 7, 1-12.

153. Putney J.W. Jr. (2001). Pharmacology of capacitative calcium entry. Mol. Interventaions 1, 84-94.

154. Putney, J.W. Jr., Broad, L.M., Braun, F., Lievremont, J. and Bird, G.S. (2001). Mechanisms of capacitative calcium entry. Journal of Cell Science114, 2223-2229

155. Putney, J.W. Jr. (2009). Capacitative calcium entry: from concept to molecules. Immunol. Rev. 231, 10-22.

156. Quintana, A., Schwarz, E.C., Schwindling, C., Lipp, P., Kaestner, L., Hoth, M. (2006). Sustained activity of calcium release-activated calcium channels requires translocation of mitochondria to the plasma membrane. J. Biol. Chem. 281, 40302-40309.

157. Randriamampita, C., Tsien, R.Y. (1993). Emptying of intracellular Ca^{2+} stores releases a novel small messenger that stimulates Ca^{2+} influx. Nature 364, 809-814.

158. Rapizzi, E., Pinton, P., Szabadkai, G., Wieckowski, M. R., Vandecasteele, G., Baird, G., Tuft, R.A., Fogarty, K.E., Rizzuto, R. (2002). Recombinant expression of the voltage-dependent anion channel enhances the transfer of Ca^{2+} microdomains to mitochondria. J. Cell Biol. 159, 613-624.

159. Rizzuto, R., Brini, M., Pizzo, P., Murgia, M., Pozzan, T. (1995). Chimeric green fluorescent protein as a tool for visualizing subcellular organelles in living cells. Curr. Biol. 5, 635-642.

160. Rizzuto, R., Bernardi, P., Pozzan, T. (2000). Mitochondria as all-round players of the calcium game. J. Physiol. 529, 37-47.

161. Rizzuto, R., Pozzan, T. (2006). Microdomains of intracellular Ca^{2+}: molecular determinants and functional consequences. Physiol. Rev. 86, 369-408.

162. Rong, Y.P., Bultynck, G., Aromolaran, A.S., Zhong, F., Parys, J.B., De Smedt, H., Mignery, G.A., Roderick, H.L., Bootman, M.D., Distelhorst, C.W. (2009). The BH_4 domain of Bcl-2 inhibits ER calcium release and apoptosis by binding the regulatory and coupling domain of the IP_3 receptor. Proc. Natl. Acad. Sci. U S A. 106, 14397-14402.

163. Roos, J., et al. (2005). STIM, an essential and conserved component of Ca^{2+} store-operated Ca^{2+} channel function. J. Cell Biol. 169, 435-445.

164. Rudolf, R., Mongillo, M., Rizzuto, R., Pozzan, T. (2003). Looking forward to seeing calcium, Nat. Rev. Mol. Cell Biol. 4, 579-86.

165. Rzigalinski, B.A., Willoughby, K.A., Hoffman, S.W., Falck, J.R., Ellis, E.F. (1999). Calcium influx factor, further evidence it is 5,6-epoxyeicosatrienoic acid, J. Biol. Chem. 274, 175-185.

166. Sampieri, A., Zepeda, A., Asanov, A., Vaca, L. (2009). Visualizing the store-operated channel complex assembly in real time: identification of SERCA2 as a new member. Cell Calcium 45, 439-46.

167. Saotome, M., Safiulina, D., Szabadkai, G., Das, S., Fransson, A., Aspenstrom, P., Rizzuto, R., Hajnóczky, G. (2008). Bidirectional Ca^{2+}-dependent control of mitochondrial dynamics by the Miro GTPase. Proc. Natl. Acad. Sci. U S A. 105, 20728-20733.

168. Schwarz, M., Andrade-Navarro, M.A., Gross, A. (2007). Mitochondrial carriers and pores: Key regulators of the mitochondrial apoptotic program? Apoptosis 12, 869-876.

169. Sedova, M., Blatter, L.A. (1999). Dynamic regulation of $[Ca^{2+}]_i$ by plasma membrane Ca^{2+}-ATPase and Na^+/Ca^{2+} exchange during capacitative Ca^{2+} entry in bovine vascular endothelial cells. Cell Calcium 25, 333-343.

170. Sencer, S., Papineni, R.V., Halling, D.B., Pate, P., Krol, J., Zhang, J.Z., Hamilton, S.L. (2001). Coupling of RYR1 and L-type Calcium Channels via Calmodulin Binding Domains. J. Biol. Chem. 276, 38237-38241.

171. Schuh, K., Uldrijan, S., Telkamp, M., Rothlein, N., Neyses, L. (2001). The plasmamebrane calmodulin-dependent calcium pump: a major regulator of nitric oxide synthase I.J. Biol. Chem. 278, 41264-41252.

172. Schuh, K., Uldrijan, S., Gambaryan, S., Roethlein, N., Neyses, L. (2003). Interaction of plasma membrane Ca^{2+} pump 4b/Cl with the Ca^{2+}/calmodulin-dependent membrane –associated kinase CASK. J. Biol. Chem. 78, 9778-9783.

173. Shukla, S., Sumaria, C.S., Pradeepkumar, P.I. (2010). Exploring Chemical Modifications for siRNA Therapeutics: A Structural and Functional Outlook. ChemMedChem. 5, 328-349.

174. Shuttleworth, T.J. (2009). Arachidonic acid, ARC channels, and Orai proteins. Cell Calcium. 45, 602-610.

175. Smani, T., Patel, T., Bolotina, V.M. (2008). Complex regulation of store-operated Ca^{2+} entry pathway by PKC-epsilon in vascular SMCs. Am. J. Physiol. Cell Physiol. 294, 1499-508.

176. Smets, I., Caplanusi, A., Despa, S., Molnar, Z., Radu, M., Vandenven, M., Ameloot, M., Steels, P. (2004). Ca^{2+} uptake in mitochondria occurs via the reverse action of the Na^{+}/Ca^{2+} exchanger in metabolically inhibited MDCK cells. Am. J. Physiol. Renal., Physiol. 286, F798-794.

177. Smyth, J.T., DeHaven, W.I., Bird, G.S., Putney J.W. Jr. (2007). Role of the microtubule cytoskeleton in the function of the store-operated Ca^{2+} channel activator STIM1. J. Cell Sci. 120, 3762-71.

178. Smyth, J.T., Dehaven, W.I., Bird, G.S., Putney, J.W. Jr. (2008). Ca^{2+}-store-dependent and -independent reversal of Stim1 localization and function. J. Cell Sci. 121, 762-772.

179. Smyth, J.T., Petranka, J.G., Boyles, R.R., DeHaven, W.I., Fukushima, M., Johnson, K.L., Williams, J.G., Putney, J.W. Jr. (2009). Phosphorylation of STIM1 underlies suppression of store-operated calcium entry during mitosis. Nat. Cell Biol. 11, 1465-1472.

180. Soboloff, J., Spassova, M.A., Tang, X.D., Hewavitharana, T., Xu, W., Gill, D.L. (2006). Orai1 and STIM reconstitute store-operated calcium channel function, J. Biol. Chem. 281, 20661-20665.

181. Soboloff, J., Spassova, M.A., Dziadek, M.A., Gill, D.L. (2006b). Calcium signals mediated by STIM and Orai proteins-a new paradigm in inter-organelle communication, Biochim. Biophys. Acta 1763, 1161–1168.

182. Soboloff, J., Spassova, M., Hewavitharana, T., He, L.P., Luncsford, P., Xu, W., Venkatachalam, K., van Rossum, D., Patterson, R.L., Gill, D.L. (2007). TRPC channels: integrators of multiple cellular signals. Handb. Exp. Pharmacol. 179, 575-591.

183. Sours-Brothers, S., Ding, M., Graham, S., Ma, R. (2009). Interaction between TRPC1/TRPC4 assembly and STIM1 contributes to store-operated Ca^{2+} entry in mesangial cells. Exp. Biol. Med. 234, 673-82.

184. Stephenson, F.A., Cousins, S.L., Kenny, A.V. (2008). Assembly and forward trafficking of NMDA receptors. Mol. Membr. Biol. 25, 311-320.

185. Swillens, S., Dupont, G., Combettes, L., Champeil, P. (1999). From calcium blips to calcium puffs: Theoretical analysis of the requirements for interchannel communication, Proc. Natl. Acad. Sci. U S A. 96, 13750-13755.

186. Szabadkai, G., Bianchi, K., Várnai, P., De Stefani, D., Wieckowski, M. R., Cavagna, D., Nagy, A. I., Balla, T., Rizzuto, R.(2006). Chaperone-mediated coupling of endoplasmic reticulum and mitochondrial Ca^{2+} channels. J Cell Biol. 175, 901-911.

187. Targos, B., Barańska, J. and Pomorsk P. (2005). Store-operated calcium entry in physiology and pathology of mammalian cells. Acta Biochem. Pol. 52, 397-409.

188. Tatt, L., Morley, G. M., Chopra, R., Khwaja, A. (2003). The Src-selective kinase inhibitor PP1 also inhibits Kit and Bcr-Abl tyrosine kinases. J. Biol. Chem. 278, 4847-4853.

189. Thomas, D., Hanley, M.R. (1995). Evaluation of calcium influx factors from stimulated Jurkat T-lymphocytes by microinjection into Xenopus oocytes, J. Biol. Chem. 270, 6429-6432.

190. Thompson, J.L., Mignen, O., Shuttleworth, T.J. (2009). The Orai1 severe combined immune deficiency mutation and calcium release-activated Ca^{2+} channel function in the heterozygous condition. J. Biol. Chem. 284, 6620-6626.

191. Tinel, H., Cancela, J.M., Mogami, H., Gerasimenko, J.V., Gerasimenko, O.V., Tepikin, A.V., Petersen, O.H. (1999). Active mitochondria surrounding the pancreatic

acinar granule region prevent spreading of inositol trisphosphate-evoked local cytosolic (Ca^{2+}) signals. EMBO J. 18, 4999-5008.

192. Toullec, D., Pianetti, P., Coste, H., Bellevergue, P., Grand-Perret, T., Ajakane, M., Baudet, V., Boissin, P., Boursier, E., Loriolle, F., Duhamel, L., Charon, D., Kirilovsky J. (1991). The bisindolylmaleimide GF 109203X is a potent and selective inhibitor of protein kinase C. J. Biol. Chem. 266, 15771-15781.

193. Trenker, M., Malli, R., Fertschai, I., Levak-Frank, S. and Graier W.F. (2007). Uncoupling proteins 2 and 3 are fundamental for mitochondrial Ca^{2+} uniport. Nat. Cell Biol. 9, 445-52.

194. Trenker, M., Fertschai, I., Malli, R., Graier, W.F. (2008). UCP2/3 – Likely to be fundamental for mitochondrial Ca^{2+} uniport. Nat. Cell. Biol. 10, 1237-1240.

195. Tsien, R.Y. (1980). New calcium indicators and buffers with high selectivity against magnesium and protons: design, synthesis, and properties of prototype structures. Biochemistry 19, 2396-2404.

196. Varadi, A., Cirulli, V., Rutter, G.A. (2004). Mitochondrial localization as a determinant of capacitative Ca^{2+} entry in HeLa cells. Cell Calcium 36, 499-508.

197. Vriens J., Watanabe H., Janssens A., Droogmans G., Voets T., Nilius B. (2004). Cell swelling, heat, and chemical agonists use distinct pathways for the activation of the cation channel TRPV4. Proc. Natl. Acad. Sci U S A. 101, 396-401.

198. Vig, M., Beck, A., Billingsley, J. M., Lis, A., Paryaz, S., Peinelt, C., Koomoa, D.L., Soboloff, J., Gill, D.L ., Fleig, A., Kinet, J. P., Penner, R. (2006). CRACM1 is a plasma membrane protein essential for store-operated Ca^{2+} entry. Science 312, 1220-1223.

199. Villalobos, C., Nuñez L., Montero, M., García, A.G., Alonso, M.T. Chamero, P., Alvarez, J., García-Sancho J. (2002). Redistribution of Ca^{2+} among cytosol and organella during stimulation of bovine chromaffin cells. FASEB J. 16, 343-353.

200. Wan, T.C., Zabe, M., Dean, W.L. (2003). Plasma membrane Ca^{2+}-ATPase isoform 4b is phosphorylated on tyrosine 1176 in activated human platelets. Thromb. Haemost. 89, 122-131.

201. Wang, X., Schwarz, T.L. (2009). The mechanism of Ca^{2+} -dependent regulation of kinesin-mediated mitochondrial motility. Cell 136, 163-74.

202. Watanabe, H., Vriens, J., Prenen J, Droogmans G, Voets T, Nilius B.(2003). Anandamide and arachidonic acid use epoxyeicosatrienoic acids to activate TRPV4 channels. Nature 424, 434-438.

203. Weiss, G. B. (1974). Cellular pharmacology of lanthanum. Ann. Rev. Pharmacol. 14, 343-354.

204. Williams, R. T., Manji, S. S., Parker, N. J., Hancock, M. S., Van Stekelenburg, L., Eid, J. P., Senior, P. V., Kazenwadel, J. S., Shandala, T., Siant, R., Smith, P. J., Dziadek M. A. (2001). Identification and characterization of the STIM (stromal interaction molecule) gene family: coding for a novel class of transmembrane proteins.

205. Willoughby, D., Wachten, S., Masada, N., Cooper, DM. (2010). Direct demonstration of discrete Ca^{2+} microdomains associated with different isoforms of adenylyl cyclase. J. Cell Sci. 123, 107-117.

206. Worley, PF., Zeng, W., Huang, GN., Yuan, J.P., Kim JY., Lee, MG., Muallem, S.(2007). TRPC channels as STIM1-regulated store-operated channels. Cell Calcium 42, 205-211.

188. Wu, M. M., Buchanan, J., Luik, R. M., Lewis, R. S. (2006). Ca^{2+} store depletion causes STIM1 to accumulate in ER regions closely associated with the plasma membrane. J. Cell Biol. 174, 803–813.

207. Xu, X., Star, R.A., Tortorici, G., Muallem, S. (1994). Depletion of intracellular Ca^{2+} stores activates nitric-oxide synthase to generate cGMP and regulate Ca^{2+} influx, J. Biol. Chem. 269, 12645-12653.

208. Yeromin, AV., Zhang, SL., Jiang, W., Yu, Y., Safrina, O., Cahalan, MD. (2006). Molecular identification of the CRAC channel by altered ion selectivity in a mutant of Orai. Nature 443, 226-229.

209. Yi, M., Weaver, D., Hajnóczky, G. (2004). Control of mitochondrial motility and distribution by the calcium signal: a homeostatic circuit. J. Cell Biol. 167, 661-72.

210. Young, K. W., Bootman, M. D., Channing D. R., Lipp, P., Maycox, P. R., Meakin, J., Challiss, R. A., Nahorski, S. R. (2000). Lysophosphatidic acid-induced Ca^{2+} mobilization requires intracellular sphingosine 1-phosphate production. Potential involvement of endogenous EDG-4 receptors. J. Biol. Chem. 275, 38532-38539.

211. Yuan, J. P., Kiselyov, K., Shin, D. M., Chen, J., Shcheynikov, N., Kang, S. H., Dehoff, M. H., Schwarz, M. K., Seeburg, P. H., Muallem, S., Worley, P. F. (2003). Homer

binds TRPC family channels and is required for gating of TRPC1 by IP_3 receptors. Cell 114, 777-789.

212. Yuan, J. P., Zeng, W., Huang, G. N., Worley, P. F., Muallem, S. (2007). STIM1 heteromultimerizes TRPC channels to determine their function as store-operated channels. Nat. Cell Biol. 9, 636-45.

213. Zhang, S. L., Yu, Y., Roos, J., Kozak, J. A., Deerinck, T. J., Ellisman, M. H., Stauderman, K. A., Cahalan, MD. (2005). STIM1 is a Ca^{2+} sensor that activates CRAC channels and migrates from the Ca^{2+} store to the plasma membrane. Nature 437, 902-905.

214. Zhang, S. L., Yeromin, A. V., Zhang, X. H., Yu, Y., Safrina, O., Penna, A., Roos, J., Stauderman, K. A., Cahalan, M. D. (2006). Genome-wide RNAi screen of Ca^{2+} influx identifies genes that regulate Ca^{2+} release-activated Ca^{2+} channel activity. Proc. Natl. Acad. Sci. USA. 103**,** 9357-9362.

215. Zhang, Y., Chen, Y. H., Bangaru, S. D., He, L., Abele, K., Tanabe, S., Kozasa, T., Yang, J. (2008). Origin of the voltage dependence of G-protein regulation of P/Q-type Ca^{2+} channels. J. Neurosci. 28,14176-14188.

216. Zheng, L., Stathopulos, P. B., Guang-Yao L, Ikura, M. (2008). Biophysical characterization of the EF-hand and SAM domain containing Ca^{2+} sensory region of STIM1 and STIM2. Biochem. Biophysic. Res. Comm. 365, 240-246.

217. Zweifach, A., Lewis, R. S. (1995a). Rapid inactivation of depletion-activated calcium current (I_{CRAC}) due to local calcium feedback. J. Gen. Physiol. 105, 209-226.

218. Zweifach, A., Lewis, R. S. (1995b). Slow calcium-dependent inactivation of depletion-activated calcium current. Store -dependent and -independent mechanisms. J. Biol. Chem. 270, 14445-14451.

6. Publications